

**DESIGN AND PERFORMANCE EVALUATION OF DIFFERENT  
POWER PAD TOPOLOGIES FOR ELECTRIC VEHICLES  
WIRELESS CHARGING SYSTEMS**

By

Muhammad Sifatul Alam Chowdhury

A thesis submitted to the

School of Graduate Studies

in partial fulfillment of the requirements for the degree of

Master of Engineering

Faculty of Engineering and Applied Science

Memorial University of Newfoundland

October 2019

St. John's

Newfoundland and Labrador

Canada

## **Abstract**

Range limitations and charging of electric vehicles (EVs) are major concerns in the modern electrified transportation systems. In this thesis, design and performance analysis of three power pads considered for EV's wireless charging systems are carried out. In particular, a comparative performance analysis is conducted for circular and double D (DD) power pads, and a new power pad named DDC power pad is designed by combining these two power pads. Wireless charging systems of EV's are developed, mainly based on the inductive power transfer (IPT) system where the power is transferred through electromagnetic induction. A systematic approach to power pad design is presented in detail and the Society of Automotive Engineers (SAE) recommended practice J2954 is followed for designing the physical dimension of these power pads. To this end, Finite Element Analysis (FEA) tool ANSYS Maxwell 3D is used for simulation. Extensive simulation studies are carried out to verify the efficiency of the proposed DDC power pad. It is found that the proposed DDC power pad offers significantly improved performance compared to the existing circular and DD power pads under various misaligned positions.

## **Acknowledgements**

The author would like to convey his earnest gratitude and respect to his supervisor Dr. Xiaodong Liang for her encouragement, guidance and constructive feedback throughout the development of this thesis.

The author deeply appreciates the financial support of the Natural Science and Engineering Research Council (NSERC) and the Graduate Fellowship from Memorial University of Newfoundland. Without their support, this work would not have been possible.

The author would like to thank Memorial University of Newfoundland for all kinds of support for this research.

Finally, the author would like to give special thanks to his family members, for their unconditional love and mental supports.

# Table of Contents

<b>Abstract</b> .....	ii
<b>Acknowledgement</b> .....	iii
<b>List of Tables</b> .....	viii
<b>List of Figures</b> .....	ix
<b>List of Abbreviations</b> .....	xiv
<b>List of symbols</b> .....	xv
<b>Chapter 1</b> .....	1
<b>Introduction</b> .....	1
1.1 Background .....	1
1.2 Thesis Outline .....	3
References .....	7
<b>Chapter 2</b> .....	9
<b>Literature Review</b> .....	9
<b>Emerging Wireless Charging Systems for Electric Vehicles – Achieving High Power Transfer Efficiency: A Review</b> .....	15
2.1 Introduction .....	17
2.2 Fundamental principle of EV wireless charging .....	21
2.3 Wireless Charging with a Short Air-Gap .....	25
2.3.1 Coupled Magnetic Resonance system.....	25

2.3.2 Capacitive Power Transfer system.....	28
2.3.3 Inductive Power Transfer system.....	32
2.3.3.1 Stationary IPT system.....	33
2.3.3.2 Dynamic IPT system.....	35
2.3.3.3 Online Electric Vehicle (OLEV).....	41
2.3.3.4 Permanent Magnet Power Transfer (PMPT).....	44
2.4 EV Wireless Charging with a Large Air-Gap.....	47
2.5 EV Comparison between different topologies.....	51
2.6 Conclusion .....	52
References .....	54
<b>Chapter 3 .....</b>	<b>68</b>
<b>Comparative Characteristic Analysis of Circular and Double D Power Pads for Electric Vehicle Wireless Charging Systems.....</b>	<b>68</b>
3.1 Introduction .....	70
3.2 Performance Evaluation Procedure.....	72
3.3 Modeling and Simulation of power Pads.....	75
3.4. Conclusions.....	82
References .....	83
<b>Chapter 4 .....</b>	<b>85</b>

<b>Design of a Ferrite-Less Power Pad for Wireless Charging Systems of Electric Vehicles.....</b>	<b>85</b>
4.1 Introduction .....	87
4.2 Design of the Proposed Power Pad.....	88
4.3 Simulation Results.....	93
4.3.1 Vertical Misalignment.....	93
4.3.2 Vertical and Horizontal Misalignment .....	96
4.4 Comparison with Other Power Pads.....	99
4.5 Conclusion .....	101
References .....	103
<b>Chapter 5 .....</b>	<b>105</b>
<b>Power Transfer Efficiency Evaluation of Different Power Pads for Electric Vehicle's Wireless Charging Systems.....</b>	<b>105</b>
5.1 Introduction .....	107
5.2 Power Transfer Efficiency Evaluation Methodology.....	108
5.3 Efficiency Analysis of Power Pads.....	111
5.3.1 Circular Power Pads.....	111
5.3.2 DD Power Pads.....	113
5.3.3 DDC Power Pads .....	115

5.4 Comparison of the Three Types of Power Pads.....	118
5.5 Conclusion .....	119
References .....	120
<b>Chapter 6</b> .....	<b>122</b>
<b>Conclusion</b> .....	<b>122</b>
6.1 Summary.....	122
6.2 Future Works .....	125
<b>List of Publications</b> .....	<b>126</b>

## **List of Tables**

Table 2. 1: General characteristics of different power pads available for EV wireless Charging...	40
Table 2. 2: Summary of Online Electric Vehicle (OLEV).....	45
Table 2. 3: Comparison of different EV wireless charging systems.....	51

## List of Figures

Figure 2.1: Different power pad structures.....	13
Figure 2.2: General classification of EV wireless charging systems.....	20
Figure 2.3: EV wireless charging system: (a) general block diagram [22]; (b) schematic diagram of a two-coil wireless power transfer system [21] .....	21
Figure 2.4: A typical circuit configuration for an EV wireless charging system [25].....	22
Figure 2.5: Power transfer efficiency considering different quality factor [21].....	25
Figure 2.6: The equivalent circuit of a CMR system [27].....	26
Figure 2.7: Calculated and measured load power vs. load resistance [28].....	27
Figure 2.8: Schematic diagram of a typical CPT system [40].....	28
Figure 2.9: A modified CPT system with extra inductors and capacitors [39].....	30
Figure 2.10: Schematic diagram of an IPT-CPT combined topology [41].....	30
Figure 2.11: Measured efficiency vs. output power of different circuit topologies considering different levels of misalignments [41]: (a) an IPT-CPT combined topology; (b) a CPT topology; (c) an IPT topology.....	32
Figure 2.12: Measured efficiency vs. output power for a CPT topology considering different levels of misalignments [42].....	32
Figure 2.13: A stationary IPT system [13]: a) circuit configuration, b) equivalent circuit.....	34
Figure 2.14: Experimental currents $I_{DC}$ and $I_L$ vs. $V_{DC}$ for a stationary IPT system at the aligned condition [13].....	35
Figure 2.15: A general schematic diagram of dynamic charging system for electric vehicles [2]..	37
Figure 2.16: Power transfer between the coils [2][46].....	38
Figure 2.17: A schematic diagram of a proposed dynamic IPT system [13].....	38

Figure 2.18: The proposed dynamic IPT system [13]: (a) equivalent circuit; (b) the definition of the air-gap..... 39

Figure 2.19: Power transfer in the proposed dynamic IPT system [13]: (a) traveling distance of the vehicle-side coil; (b) waveforms of input and output currents..... 39

Figure 2.20: Variation of the coupling co-efficient  $k$  vs. misalignments between transmitting and receiving coils for different power pads: (a) simulation results [48]; (b) experimental results [49].....41

Figure 2.21: General system configuration for an OLEV system [52]..... 42

Figure 2.22: Power transfer efficiency vs. output power for a dual type system [51].....43

Figure 2.23: Power transfer efficiency with loosely coupled coils [55]..... 44

Figure 2.24: Power flow of a typical PMPT system [65]..... 46

Figure 2.25: Calculated (solid line) and experimental (+) results for efficiency at receiving end with different load resistance [65]..... 46

Figure 2.26: EV wireless charging through MPT [70]..... 48

Figure 2.27: Beam efficiency obtained for far and near field using  $\tau$  parameter [71].....49

Figure 2.28: MPT efficiency obtained for different distances [75].....51

Figure 3.1: General classification of power pads..... 71

Figure 3.2: Physical dimensions recommended in SAE J2954 for power pads: (a) DD, (b) Circular [11]..... 73

Figure 3.3: Power pad models designed by ANSYS Maxwell 3D using specifications in SAE J2954: (a) DD, (b) Circular..... 74

Figure 3.4: Flow chart of performance evaluation procedure for power pads..... 75

Figure 3.5: Variation of coupling coefficient vs vertical misalignment between VA and GA for DD and circular power pads..... 76

Figure 3.6: Variation of mutual inductance vs vertical misalignment between VA and GA for DD and circular power pads..... 77

Figure 3.7: Variation of coupling coefficient when both vertical and horizontal misalignment are applied to DD power pads..... 78

Figure 3.8: Parameters variations (3D plots) for DD power pads at the vertical misalignment of 150 mm: (a) magnetic field intensity (H), (b) magnetic flux density (B), (c) magnetic flux lines.. .....79

Figure 3.9: Variation of coupling coefficient when both vertical and horizontal misalignment are applied to circular power pads..... 80

Figure 3.10: Parameters variations (3D plots) for circular power pads at the vertical misalignment of 150 mm: (a) magnetic field intensity (H), (b) magnetic flux density (B), (c) magnetic flux lines..... 81

Figure 4.1: Physical dimensions recommended in SAE J2954 for power pads: (a) DD, (b) Circular [4].....89

Figure 4.2: The proposed power pad designed using ANSYS Maxwell 3D..... 90

Figure 4.3: A comprehensive evaluation procedure for a power pad design.....91

Figure 4.4: Different stages of the proposed power pad design using software: (a) create a circular power pad model; (b) create a DD power pad model; (c) create a proposed power pad model; (d) create both transmitting and receiving ends of power pads..... 92

Figure 4.5: Coupling coefficient  $k$  vs. vertical misalignment between power pads..... 94

Figure 4.6: Mutual inductance vs. vertical misalignment between power pads.....	94
Figure 4.7: Simulation results at 150 mm vertical misalignment: (a) magnetic field intensity H; (b) magnetic flux density B; (c) magnetic flux lines.....	96
Figure 4.8: Coupling coefficient vs. vertical misalignments for different horizontal misalignments.....	97
Figure 4.9: Mutual inductance vs. vertical misalignments for different horizontal misalignments.....	97
Figure 4.10: Simulation results when both horizontal and vertical misalignments between the power pads are 150 mm: (a) magnetic field intensity H; (b) magnetic flux density B; (c) magnetic flux lines.....	98
Figure 4.11: The proposed power pad compared to circular and DD power pads: (a) coupling coefficient vs. vertical misalignment; (b) mutual inductance vs. vertical misalignment; (c) coupling coefficient vs. horizontal misalignment (the vertical misalignment is equal to 15 mm).....	101
Figure 5.1: Power pad designed using ANSYS Maxwell 3D: (a) Circular power pads; (b) DD power pads; (c) DDC power pads.....	109
Figure 5.2: The proposed power transfer efficiency evaluation method for power pads.....	110
Figure 5.3: The magnetic field intensity for circular power pads at 150 mm vertical misalignment.....	111
Figure 5.4: The power transfer efficiency vs. the inverter operating frequency for different vertical misalignments (circular power pads).....	112
Figure 5.5: The power transfer efficiency vs. the inverter operating frequency for different horizontal misalignments (circular power pads).....	113

Figure 5.6: The magnetic field intensity for DD power pads at 150 mm vertical misalignment...	114
Figure 5.7: The power transfer efficiency vs. the inverter operating frequency for different vertical misalignments (DD power pads).....	115
Figure 5.8: The power transfer efficiency vs. the inverter operating frequency for different horizontal misalignments (DD power pads).....	115
Figure 5.9: The magnetic field intensity for DDC power pads at 150 mm vertical misalignment.....	116
Figure 5.10: The power transfer efficiency vs. the inverter operating frequency for different vertical misalignments (DDC power pads).....	117
Figure 5.11: The power transfer efficiency vs. the inverter operating frequency for different horizontal misalignments (DDC power pads).....	117
Figure 5.12: Comparison of power transfer efficiencies among circular, DD and DDC power pads: (a) vertical misalignments; (b) horizontal misalignment.....	118

## List of Abbreviations

AC	Alternating current
EV	Electric vehicle
HEV	Hybrid electric vehicle
IPT	Inductive power transfer
OLEV	Online electric vehicle
BP	Bipolar pad
DC	Direct current
DDP	Double-D power pad
DDQP	Double-D quadrature power pad
SAE	Society of automotive engineers
WPT	Wireless power transfer
DWC	Dynamic wireless charging
CPT	Capacitive power transfer
PFC	Power factor correction
V2G	Vehicle to Grid
PEV	Plug-In Electric Vehicle
EVSE	Electric Vehicle Supply Equipment
PHEV	Plug-In Hybrid Electric Vehicle

## List of symbols

$\kappa$	Coupling coefficient
$\eta$	Power transfer efficiency
$\mu_0$	Permeability
$\mu_r$	Relative permeability
$B$	magnetic flux density
$H$	Magnetic field intensity
$M$	Mutual inductance
$\dot{I}_1$	RMS current in the primary
$\dot{I}_2$	RMS current in the secondary
$\dot{U}_{21}$	Induced voltage in the primary coil
$\dot{U}_{12}$	Induced voltage in the secondary coil
$S_{12}$	Exchanged apparent power from the primary coil to the secondary coil
$S_{21}$	Exchanged apparent power from the secondary coil to the primary coil
$L_1$	Self-inductance of the primary
$L_2$	Self-inductance of the secondary
$R_{Le}$	Load resistance
$R_2$	Winding resistance of secondary coil
$Q_1$	Quality factor of primary
$Q_2$	Quality factor of secondary
$Q_c$	coupled quality factor
$\omega_s$	Source angular frequency
$L_{mTo}$	Unit magnetizing inductance of the transmitter coil

# Chapter 1

## Introduction

### 1.1 Background

Electric vehicles (EV) are gaining rapid acceptance by consumers due to their minimal emissions to the environment. Conventional vehicles powered by fossil fuels contribute to a major portion of global environmental pollution. The transportation sector is considered a major consumer of energy all over the world. For instance, it consumed 28% of total energy in the USA in 2014 [1]. To reduce the dependency on fossil fuels, EVs are introduced where electricity is used as the fuel. By using efficient power electronic devices and electric propulsion systems, EVs can exhibit better performance than conventional fossil fuel powered vehicles [2]- [4]. Different types of EVs are introduced based on energy storage capacity and propulsion systems. Although various EV charging methods are employed, charging the vehicle remains a challenging research area. Plug-in charging system is widely used for charging electric vehicles; however, wireless charging systems bear the potential to become tomorrow's norm for EV charging systems.

The concept of wireless power transfer (WPT) was introduced by Tesla in 1891 [2]. The wireless charging system for EVs is the extended format of wireless power transfer technology. Initially, the wireless power transfer technology was developed based on capacitive coupling methods. However, the modern EV wireless charging system is mostly developed based on Inductive Power Transfer (IPT) technology. Various limitations of plug-in charging systems boosted the research on EV wireless charging system development. Some of the limitations of EV plug-in charging

system can be summarized as: a) complex system architecture and operational procedure; b) installation cost especially for residential use; and c) operational safety issues. To make the EV charging more convenient and flexible, wireless charging systems are now being considered as a key research area in the field of electrified transportation [5].

Using wireless charging systems, an EV can be charged either in stationary mode or when the vehicle is in motion and the overall battery capacity of the vehicle can be reduced by 20 % [6]. In case of EV wireless charging systems, high frequency AC power is generated in the transmitting side. This high frequency AC power transmitted to the receiving side is based on the principle of electromagnetic induction between power pads. Generally, a set of power pads (containing one power pad on the transmitting side and another power pad on the receiving side) is used for the stationary wireless charging, whereas multiple power pads are combined in a single system for EV's dynamic wireless charging. Power pads play the key role to transfer power efficiently to the vehicle. Proper design of power pads ensures efficient power transfer to the vehicle as well as reducing the overall system complexity.

As the modern EV wireless charging system is mainly based on Inductive Power Transfer (IPT), it is expected that power pads should exhibit a higher value of coupling coefficient. Performance of power pads in different misaligned positions greatly influences the overall power transfer efficiency of the entire charging system. Different types of power pads have been introduced in research, including the circular power pad, Double D power pad and Double D Quadrature (DDQ) power pad [2]. Circular power pads are widely used in EV wireless charging system due to their design flexibility and reduced leakage flux [7]. However, performance of the circular power pad greatly fluctuates under misalignment conditions. To overcome the limitations of the circular

power pad, DD power pad is introduced in the research which exhibits advantages of both the circular power pad and flux pipe topology. Combination of two different power pad topologies apparently results in a higher value of coupling coefficient. A higher value of coupling coefficient ensures a higher rate of power transfer efficiency with minimum system complexity. DD power pads exhibit better performance compared to circular power pads in misaligned positions, especially under vertical misalignment. Besides these two major types of power pad, bipolar/tripolar power pads are also developed to improve the overall power transfer efficiency for various misaligned positions [8]. In this thesis, the main focus is to design and develop power pads for efficient power transfer to EVs.

## **1.2 Thesis Outline**

The outline of this dissertation is as follows:

### **Chapter 1**

In Chapter 1, the motivation of the research topic is introduced and the objectives of the research are identified.

### **Chapter 2**

In Chapter 2, a literature review for the research is conducted to design and develop power pads for efficient power transfer to EVs under various conditions. The circular and DD power pads are two major power pad topologies considered for the EV wireless charging systems and their performances in different misalignment conditions are investigated in this thesis. A performance comparison between circular and DD power pads is carried out. In this chapter, firstly literatures

are reviewed to introduce the EV wireless charging systems, which can be either stationary charging or dynamic charging systems. The fundamental principle of EV wireless charging systems is explained. Secondly, literature review of different EV wireless charging systems and state of the art power pad topologies for EV wireless charging is presented. This portion of the review facilitates better understanding of the EV conductive charging system, wireless charging system and state of the art power pad topologies for the EV wireless charging systems. This chapter consists of one manuscript, which is published in the proceedings of the following conferences: *2018 IEEE Industry Application Society Annual Meeting in Portland, Oregon, USA* [10].

### **Chapter 3**

In Chapter 3, a performance comparison between circular and DD power pads is carried out. In this chapter, a comparative characteristic analysis of circular and DD power pads for EV wireless charging systems is performed. The Society of Automotive Engineers (SAE) recommended practice J2954 [9] is followed for designing the physical dimension of these power pads. Finite Element Analysis tool ANSYS Maxwell 3D is used for simulation. Parameters such as the coupling coefficient and mutual inductance are evaluated for each type of power pads by applying vertical and horizontal misalignments. It is found that DD power pads exhibit promising characteristics for EV wireless charging systems. The research work undertaken in this chapter is consistent with the overall objectives of this thesis, as it contributes to the advancement of power pad design for a compact and efficient wireless charging system for EVs. This chapter has been published in the proceedings of *2019 IEEE Canadian Conference of Electrical and Computer Engineering (CCECE) in Edmonton, AB, Canada* [11].

## **Chapter 4**

In Chapter 4, a new power pad structure named DDC power pad is proposed by combining DD and circular power pads to further improve performance. In this chapter, several performance analyses are carried out to compare the performance of the proposed DDC power pads with existing circular and DD power pads. Physical models of circular and DD power pads are first built by using specifications in SAE J2954; these models are then combined to form the proposed DDC power pad. The design and simulation of the proposed DDC power pads are carried out using the Finite Element Analysis simulation software, ANSYS Maxwell 3D. Simulation results indicate that the proposed DDC power pads show improved performance compared to circular and DD power pads. This chapter has been published in the proceedings of 2019 *IEEE Canadian Conference of Electrical and Computer Engineering (CCECE) in Edmonton, AB, Canada* [12].

## **Chapter 5**

In Chapter 5, three power pads (circular, DD, and DDC) are evaluated for power transfer efficiency in wireless charging systems with respect to various vertical and horizontal misalignments. In this chapter, Circular and DD power pads are designed following SAE Recommended Practice J2954 and using the software ANSYS Maxwell 3D. The power transfer efficiency among the three types of power pads is compared. The new DDC power pad has 14.48% and 18.03% improved performance compared to the circular power pad at 150mm vertical misalignment and 115mm horizontal misalignment, respectively. This chapter has been published in the proceedings of 2019 *Canadian Conference of Electrical and Computer Engineering (CCECE) in Edmonton, AB, Canada* [13].

## **Chapter 6**

In Chapter 6, the research outcomes are summarized. Potential future work is addressed.

Several articles have been published based on the work carried out under this research; one is published in the proceedings of 2018 IEEE Industry Application Society (IAS) Annual Meeting, another three are published in the proceedings of 2019 Canadian Conference on Electrical and Computer Engineering (CCECE).

## References

- [1] D. Patil, J. Miller, B. Fahimi, P. T. Balsara, and V. Galigerkere, "A Coil Detection System for Dynamic Wireless Charging of Electric Vehicle," (Early access) *IEEE Transactions on Transportation Electrification*, pp. 1–1, 2019.
- [2] A. Ahmad, M. S. Alam, and R. Chabaan, "A comprehensive review of wireless charging technologies for electric vehicles," *IEEE Trans. Transportation Electrification*, Vol. 4, No. 1, pp. 38 – 63, 2018.
- [3] J. Dai and D. C. Ludois, "A survey of wireless power transfer and a critical comparison of inductive and capacitive coupling for small gap applications," *IEEE Trans. Power Electron.*, vol. 30, no. 11, pp. 6017–6029, Nov. 2015.
- [4] J. M. Miller, O. C. Onar, and M. Chinthavali, "Primary-side power flow control of wireless power transfer for electric vehicle charging," *IEEE Trans. Emerg. Sel. Topics Power Electron.*, vol. 3, no. 1, pp. 147–162, Mar. 2015.
- [5] T. Fujita, T. Yasuda, and H. Akagi, "A dynamic wireless power transfer system applicable to a stationary system," *IEEE Trans. Industry Applications*, Vol. 53, No. 4, pp. 3748-3757, 2017.
- [6] S. Li and C. C. Mi, "Wireless power transfer for electric vehicle applications," *IEEE journal of emerging and selected topics in power electronics*, Vol. 3, No. 1, pp. 4-17, 2015.
- [7] M. Budhia, J. T. Boys, G. A. Covic, and C.-Y. Huang, "Development of a single-sided flux magnetic coupler for electric vehicle IPT charging systems," *IEEE Trans. Ind. Electron.*, vol. 60, no. 1, pp. 318-328, January 2013.
- [8] S. Kim, G. A. Covic, and J. T. Boys, "Tripolar pad for inductive power transfer systems for EV charging," *IEEE Trans. Power Electron*, vol. 32, no. 7, pp. 5045-5057, July 2017.

- [9] SAE Recommended Practice J2954, “Wireless power transfer for light-duty plug-in/electric vehicles and alignment methodology,” November 2017.
- [10] Xiaodong Liang, and Muhammad Sifatul Alam Chowdhury\*, "Emerging Wireless Charging Systems for Electric Vehicles – Achieving High Power Transfer Efficiency: A Review", Proceedings of 2018 IEEE Industry Applications Society (IAS) Annual Meeting, pp. 1-14, Portland, OR, USA, September 23 - 27, 2018.
- [11] Muhammad Sifatul Alam Chowdhury\*, and Xiaodong Liang, "Comparative Characteristic Analysis of Circular and Double D Power Pads for Electric Vehicle Wireless Charging Systems," Proceedings of IEEE Canadian Conference of Electrical and Computer Engineering (CCECE) 2019, Edmonton, AB, Canada, May 5-8, 2019.
- [12] Muhammad Sifatul Alam Chowdhury\*, and Xiaodong Liang, "Design of a Ferrite-Less Power Pad for Wireless Charging Systems of Electric Vehicles," Proceedings of IEEE Canadian Conference of Electrical and Computer Engineering (CCECE) 2019, Edmonton, AB, Canada, May 5-8, 2019.
- [13] Muhammad Sifatul Alam Chowdhury\*, and Xiaodong Liang, "Power Transfer Efficiency Evaluation of Different Power Pads for Electric Vehicle’s Wireless Charging Systems", Proceedings of IEEE Canadian Conference of Electrical and Computer Engineering (CCECE) 2019, Edmonton, AB, Canada, May 5-8, 2019.

## Chapter 2

### Literature Review

In wireless charging systems, there is no physical connection between a vehicle and a charger. Tesla introduced the concept of WPT in 1891 based on capacitive coupling [1]. Besides this, William C. Brown developed rectenna (rectifying antenna) to transfer power for a longer distance through microwaves in 1960 [2]. Nowadays, EV charging through an IPT system receives a plethora of research attention, although charging can also be done through capacitive power transfer (CPT), LASER, Microwave, etc. The Lawrence Berkeley National Laboratory performed the very first IPT based EV dynamic wireless charger demonstration in 1977 [3]. In the 1990s, the University of Auckland demonstrated an IPT vehicle using rectangular power pad [4]. The advantages of wireless charging systems include: a) it provides compact, flexible and safe EV charging without direct human interaction; b) the overall cost of charging is significantly reduced compared to conventional conductive charging; c) the architecture of the charging system is simple, which makes it very convenient for residential use with minimal maintenance required [5]; and d) dynamic WPT technology enables the vehicle to charge while moving, and reduces the range limitation of EVs.

The wireless charging systems can be either dynamic or stationary. The dynamic wireless charging technology enables a vehicle to be charged while cruising; a vehicle must be parked when using the stationary wireless charging technology. EV dynamic wireless charging system development research is led by the Korean Advanced Institute of Science and Technology (KAIST), but the concept of highway charging was first reported in [6].

In wireless charging systems, power pads are placed on both the ground and vehicle sides. The ground side arrangement is known as the ground assembly (GA) or transmitting side, while the vehicle side arrangement is known as the vehicle assembly (VA) or receiving side. The AC power from the grid is firstly converted into DC power; the DC power is then converted into high frequency AC power. The high frequency AC current supplied to the primary transmitting power pad creates a magnetic field, and the magnetic field induces a voltage in the secondary receiving power pad. The time-varying magnetic field generated by high-frequency AC currents in the transmitting power pad is linked to the power pad installed in the vehicle. In case of dynamic wireless charging, the speed of the vehicle greatly affects the overall power transferred to the vehicle. Depending on the vehicle speed, the power transfer efficiency can be dropped to 50% compared with the stationary wireless charging [7]. It is required that power pads should exhibit a high value of coupling coefficient ( $k$ ) and the capability to transfer power in different misaligned positions [8]. Depending on the charging system configuration and the misalignment distance between the power pads, the  $k$  value varies. For a typical 85 kHz system, the  $k$  value may range between 0.1 to 0.4, and a lower  $k$  value due to large misalignment distances can be improved by using ferrite bars.

EV wireless charging systems can be classified into two major streams based on the distance between transmitting and receiving ends: 1) charging with a short air-gap distance (near field); and 2) charging with a long air-gap distance (far field). A short air-gap configuration is also known as a near field power transfer system, where the transmitter and receiver remain in close proximity. Generally, the air-gap ranges up to 40 cm [9]. Among various WPT technologies, the Coupled Magnetic Resonance (CMR) system is promising because it enables power transfer in a longer

distance with high efficiency. A CPT system uses the electric field to transfer AC power, and the power can be transferred through obstacles, such as metal barriers, without significant losses [10]. In an IPT system, the power is transferred through power pads; losses in the coils account for 30-50% overall losses of the system [11]. EV wireless charging through a large air-gap is known as far field topology, which includes two major types: 1) power transfer through microwave; and 2) power transfer through LASER [12].

Power pads are important parts of the EV wireless charging system, as the link between power grids and vehicles is established through power pads. Power rails are generally used for roadway powered vehicles, and these power pads are only energized when an EV is passing over it. However, their complex system configuration and maintenance cost is still an unsolved issue when used in dynamic wireless charging systems. Various polarized and non-polarized power pads are introduced to overcome the limitations of power rails which can be used for both dynamic and stationary wireless charging of EVs. Using polarized power pads, the magnetic flux can be generated both in vertical and horizontal directions whereas non-polarized power pads can only generate the magnetic flux in the vertical direction [13]. Examples of non-polarized power pads are circular and square power pads; DD and Double D Quadrature (DDQ) are examples of the polarized power pad.

Circular power pads are widely used for stationary wireless charging system design, due to their reduced leakage flux and compact design [14]. Due to design flexibility, circular power pads can be easily deployed for both grid side and vehicle sides. However, their performance fluctuates with the increment of the air-gap. DD power pads combine the advantage of both circular power pad and flux pipe topology, and thus result in a higher value of coupling coefficient than circular power

pads [15][16]. Due to the width of a DD power pad, it exhibits higher tolerance in misalignment conditions. As DD power pads result in very low leakage flux, the overall power transfer efficiency does not fluctuate much by adding shielding [15]. For the same size of power pads, the flux path height of DD power pads is almost double compared to circular power pads, which significantly improves the overall power transfer efficiency of the system [17].

Bipolar/tripolar power pads are being developed by combining two or three coils together, which results in better performance in misaligned positions [16][18]. These coils can be energized individually, and the independent control technique can be applied. Bipolar power pad exhibits a higher value of coupling coefficient, resulting in higher power transfer efficiency, and it requires 25-30% less copper to construct compared to DDQ power pads [19]. Tripolar power pads are prepared by combining three coils which requires a separate inverter for each decoupled coil [20]. However, the complex system architecture makes these power pads unattractive. DDQ power pads are designed by adding a quadrature coil to DD power pads, resulting in excellent misalignment tolerance. For a similar size of the power pad structure, DDQ power pads result in a much larger charging zone which makes this power pad a protentional choice for the EV dynamic wireless charging system [21]. However, the size of DDQ power pads is still an issue, as combining two different topologies increases the overall dimension of the power pad. Different power pad structures considered for EV wireless charging are presented in figure 2.1.

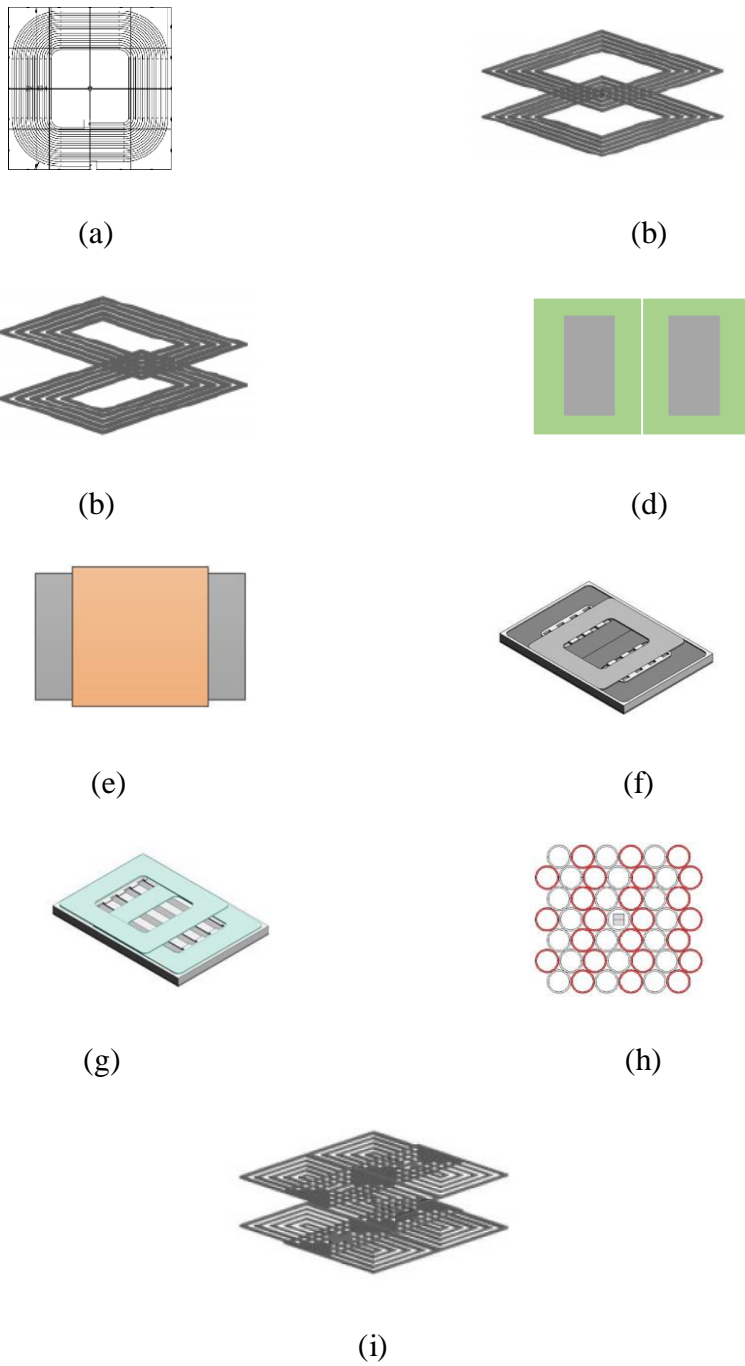


Figure 2.1: Different power pad structures: a) Circular [22] b) Square[22] c) Rectangular[22] d) Double D (DD) [23] e) Solenoid [23] f) Double D Quadrature (DDQ) [23] g) Multi coil h) Multi coil homogeneous [4] i) Four squares [22].

In this thesis, a performance analysis of various power pad structures is carried out and several enhancements are proposed to improve power transfer efficiency. In this chapter, the literature review is mainly focused on different power pads and their application in the electric vehicle wireless charging system. Moreover, literature related to advanced control approaches to improve the overall power transfer efficiency is also discussed. This is an important concern in modern consumer-friendly electrified transportation system.

# **Emerging Wireless Charging Systems for Electric Vehicles – Achieving High Power Transfer Efficiency: A Review**

Xiaodong Liang, *Senior Member, IEEE* and Muhammad Sifatul Alam Chowdhury, *Student  
Member, IEEE.*

Faculty of Engineering and Applied Science, Memorial University of Newfoundland, St.  
John's, Newfoundland, Canada.

A version of this work has been published in the proceeding of 2018 IEEE Industry Application Society Annual Meeting in Portland, Oregon, USA. The co-author of this manuscript Muhammad Sifatul Alam Chowdhury participated in this work under the supervision of Dr. Xiaodong Liang. Sifat performed literature review and wrote some content of the paper. Dr. Liang provided continuous technical guidance, wrote some content of the paper, and modified the final version of the paper. In this chapter, the manuscript is presented with altered figure numbers, table numbers, section numbers and reference formats in order to match the thesis formatting guidelines set out by Memorial University of Newfoundland.

**Abstract-** Electric vehicles (EVs) are increasingly purchased worldwide, however, several issues, such as the limited driving range, battery deterioration, unavailability of charging stations etc, present barriers for advancement of EVs. To overcome the range anxiety of EVs, it's crucial to develop its advanced charging infrastructure. In this paper, a literature review is conducted on EV wireless charging systems with the focus on achieving high power transfer efficiency. A general classification of wireless charging techniques is firstly presented; various state-of-the-art wireless charging techniques reported in the literature are summarized and compared.

**Keywords-** Capacitive power transfer, coupled magnetic resonance, electric vehicle, inductive power transfer, wireless charging.

## 2.1 Introduction

In the first nine months of 2017, sales of electric vehicles (EVs) in Canada increased by 56% compared to 2016, and 41 models of EVs (15 models of battery EVs, and 26 models of plug-in hybrid EVs) were available in Canadian automobile market [24]. Given this promising future of EVs, more research effort is required to develop advanced technologies for EV applications. EV charging systems remain to be a challenging research area [25][26][27].

To transfer power to EVs through charging systems, two methods can be implemented: a) conductive charging, and b) wireless charging. The creation of EVs can be traced back to 1800 when several small-scale prototypes of EVs were investigated by different research groups, and William Morrison in the US introduced an EV capable of accommodating six passengers [28]. EVs with different capacity, range and charging systems were introduced during past decades. A fast conductive charger for small traction batteries was developed in 1993 [29]. At present, a conductive fast charger can charge a vehicle up to 80% within 15 minutes [25]. A direct physical connection is established between an EV and the power supply in order to charge a vehicle using a conductive charger. AC-DC rectifiers are generally employed to charge EV battery from AC power source.

Conductive chargers are generally classified into two major categories: a) onboard charger, and b) offboard charger [25]. Circuit configuration, charging capacity, and charging time largely depend on the type of chargers employed for vehicles. Over decades of continuous efforts from researchers and engineers, conductive charging became a mature technology, and different conductive charging topologies have already been in use [26]. In conventional conductive charging

technology, boost converters are used in EV chargers for power factor correction (PFC). Different converter topologies are reviewed in [30]-[32]. Three charging levels are employed for EV conductive charging. A Level 1 system is equipped with a 120 V AC power for a single-phase onboard EV charger to provide up to 1.9 kW power to the vehicle [31]. A Level 2 system is equipped with a 240 V AC power for both single-phase and three-phase onboard chargers to provide up to 19.2 kW power to the vehicle [33]. For fast charging, a Level 3 system is equipped with a 208-600 V AC power for three phase off-board chargers, it can charge a vehicle within an hour with an expected power level of 100 kW [34].

However, there are limitations related to the conductive charging system [35]: 1) Operational safety is always highly required as vehicles need to get connected manually with the charging system; 2) By following the standard J1772 for EV conductive charging system from Society of Automotive Engineers (SAE) [33], system architectures are complicated especially for residential charging systems; 3) Electricity cost per mile is higher than EV dynamic wireless charging. These limitations are considered as burdens for future smart transportation. To overcome them, wireless charging is presently deemed as a key research area for EVs [36].

Tesla introduced the concept of wireless power transfer (WPT) in 1891 based on capacitive coupling [1]. For wireless charging, there is no physical connection between a vehicle and a charger. EV wireless chargers generally employ coupling plates known as a transmitting end (at roadside) and a receiving end (at vehicle side). Nowadays, EV charging through an inductive power transfer (IPT) system receives huge research attraction, although the charging can also be done through the capacitive power transfer (CPT), LASER, Microwave etc. Lawrence Berkeley National Laboratory made the very first IPT based EV dynamic wireless charger demonstration in

1977 [3]. Wireless charging systems can be either dynamic or stationary. The dynamic wireless charging technology enables a vehicle to be charged while cruising; a vehicle must be parked when using the stationary wireless charging technology. The advantages of wireless charging systems include: 1) it provides compact, flexible and safe EV charging without direct human interaction; 2) The overall cost of charging is significantly reduced compared to conventional conductive charging; 3) The architecture of the charging system is simple, which makes it very convenient for residential use with the minimum maintenance required [37]; 4) Dynamic WPT technology enables the vehicle charging while moving, and reduces the range limitation of EVs; 5) Vehicle to Grid (V2G) operation using wireless charging can reduce the overall battery capacity of EVs by 20% [38][41].

Based on the literature review, EV wireless charging system is classified into two major streams based on the distance between the transmitting and the receiving ends: 1) charging with a short air-gap distance (near field); 2) charging with a long air-gap distance (far field). A general classification of EV wireless charging system is presented in Figure 2.2.

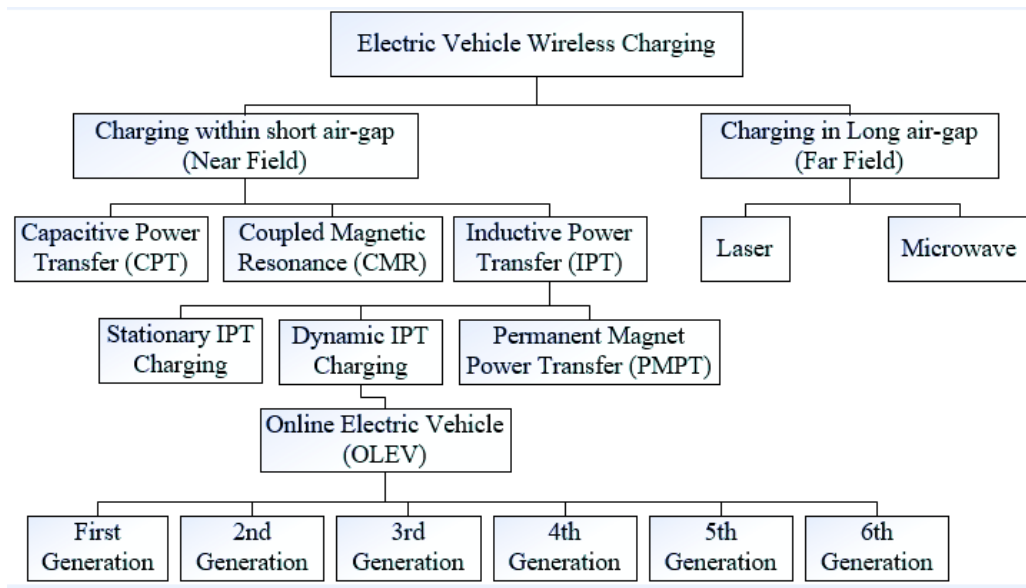


Figure 2.2: General classification of EV wireless charging systems.

To achieve efficient power transfer, the coil installed in the vehicle should be compact, and the system should have the ability to transfer power when subjected to considerable misalignment. The efficiency for various charging coils considering misalignment has been extensively researched [39][21][40]. The purpose of this paper is to provide a summary of the state-of-art technologies for EV wireless charging systems with a particular focus on achieving high power transfer efficiency.

The paper is arranged as follows: in Section 2.2, the fundamental principle of EV wireless charging is introduced; topologies used for charging the vehicle with a short air-gap between transmitting and receiving ends are presented in Section 2.3; topologies available to transfer power through a long air-gap are reviewed in Section 2.4; comparative discussion between different wireless topologies are provided in Section 2.5; conclusions are drawn in Section 2.6.

## 2.2 Fundamental principle of EV wireless charging

Wireless charging systems are based on the WPT technology. The general block diagram and schematic diagram for a two-coil WPT system is illustrated in Figure 2.3 (a). A typical circuit configuration is shown in Figure 2.4.

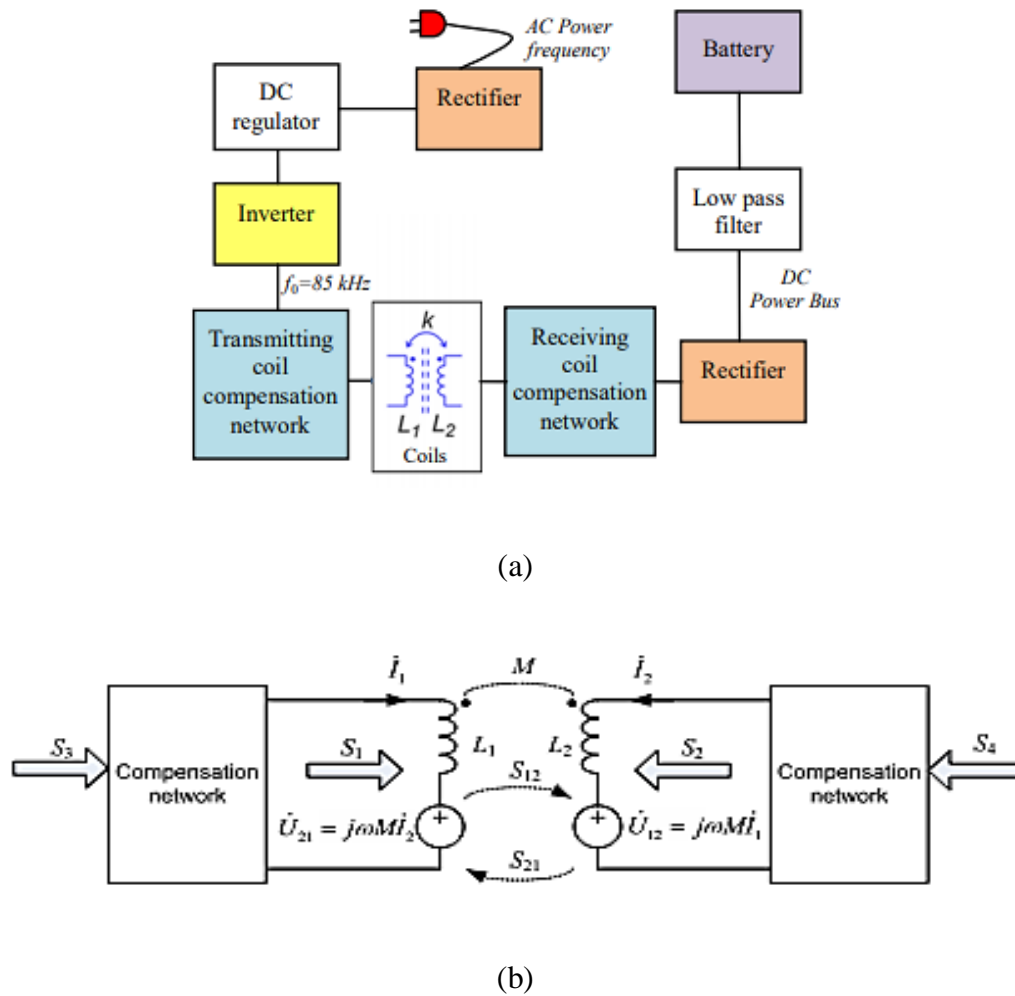


Figure 2.3: EV wireless charging system: (a) general block diagram [42]; (b) schematic diagram of a two-coil wireless power transfer system [41].

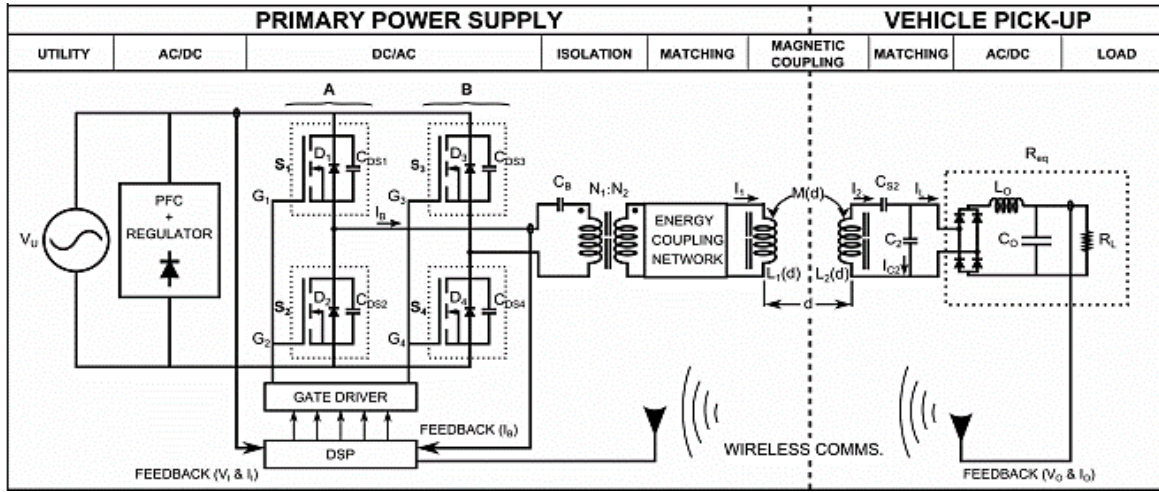


Figure 2.4: A typical circuit configuration for an EV wireless charging system [45].

The AC power from the grid is firstly converted into DC power, the DC power is then converted into high frequency AC power. The high frequency AC current supplied to the primary transmitting coil creates a magnetic field, and the magnetic field induces a voltage in the secondary receiving coil. The system efficiency using this technology can be increased by resonating. The complex power exchanged between the two coils can be calculated by [41]

$$\begin{aligned}\dot{S}_{12} &= -\dot{U}_{12}I_2^* = -j\omega MI_1I_2^* \\ &= \omega MI_1I_2 \sin\varphi_{12} - j\omega MI_1I_2 \cos\varphi_{12}\end{aligned}\quad (1)$$

$$\begin{aligned}\dot{S}_{21} &= -\dot{U}_{21}I_1^* = -j\omega MI_2I_1^* \\ &= -\omega MI_1I_2 \sin\varphi_{12} - j\omega MI_1I_2 \cos\varphi_{12}\end{aligned}\quad (2)$$

Where,  $I_1$  are  $I_2$  are the rms current in the primary and secondary coil, respectively;  $\dot{U}_{21}$  is the induced voltage in the primary coil by the current in the secondary coil;  $\dot{U}_{12}$  are the induced voltage in the secondary coil by the current in the primary coil;  $S_{12}$  is the exchanged apparent power from

the primary coil to the secondary coil;  $S_{21}$  is the exchanged apparent power from the secondary coil to the primary coil;  $\varphi_{12}$  is the phase angle difference between  $\dot{I}_1$  and  $\dot{I}_2$ ; and  $M$  is mutual inductance of the two coils.

The transferred active power from the primary coil to the secondary coil can be determined by [41]

$$P_{12} = \omega M I_1 I_2 \sin \varphi_{12} \quad (3)$$

The total complex power (when  $\varphi_{12} = 90^\circ$ ) is [21]:

$$\begin{aligned} S &= \dot{S}_1 + \dot{S}_2 = j\omega L_1 \dot{I}_1 \dot{I}_1^* + j\omega M \dot{I}_2 \dot{I}_1^* + j\omega L_2 \dot{I}_2 \dot{I}_2^* + j\omega M \dot{I}_1 \dot{I}_2^* \\ &= j\omega (L_1 \dot{I}_1 \dot{I}_1^* + M \dot{I}_2 \dot{I}_1^* + L_2 \dot{I}_2 \dot{I}_2^* + M \dot{I}_1 \dot{I}_2^*) \\ &= j\omega (L_1 I_1^2 + L_2 I_2^2 + 2M I_1 I_2 \cos \varphi_{12}) \end{aligned} \quad (4)$$

Where,  $L_1$  and  $L_2$  are the self-inductance of the primary transmitting and secondary receiving coil, respectively;  $S_1$  and  $S_2$  are apparent power associated with the primary and secondary coil, respectively. From Eq. (4), the reactive power going through the coils can be expressed by [41]

$$\begin{aligned} Q &= \omega (L_1 I_1^2 + L_2 I_2^2 + 2M I_1 I_2 \cos \varphi_{12}) \\ &= \omega L_1 I_1^2 + \omega L_2 I_2^2 + 2\omega M I_1 I_2 \cos \varphi_{12} \end{aligned} \quad (5)$$

The ratio between reactive and active power for the two-coil system can be determined as follows [41]:

$$f(\varphi_{12}) = \left| \frac{\omega M I_1 I_2 \sin \varphi_{12}}{\omega L_1 I_1^2 + \omega L_2 I_2^2 + 2\omega M I_1 I_2 \cos \varphi_{12}} \right| \quad (6)$$

To obtain a greater efficiency,  $f(\varphi_{12})$  should be the maximum. By solving Eqs. (7) and (8), the maximum value of  $f(\varphi_{12})$  can be obtained.

$$\frac{\partial}{\partial \varphi_{12}} f(\varphi_{12}) = 0, \quad (7)$$

$$\frac{\partial^2}{\partial^2 \varphi_{12}} f(\varphi_{12}) < 0 \quad (8)$$

The efficiency can then be expressed as follows [41]:

$$\eta(a) = \frac{1}{\frac{a+\frac{1}{a}+2}{k^2 Q_1 Q_2} + \frac{1}{a} + 1} \quad (9)$$

where  $a$  is the ratio of equivalent load resistance ( $R_{Le}$ ) and winding resistance of secondary coil ( $R_2$ ),  $k$  is the coupling co-efficient between the two coils,  $Q_1$  and  $Q_2$  are quality factor of primary and secondary coil, respectively. The maximum efficiency can be obtained through the following equations:

$$\frac{\partial}{\partial a} \eta(a) = 0 \quad (10)$$

$$\frac{\partial^2}{\partial^2 a} \eta(a) < 0 \quad (11)$$

The maximum efficiency can be expressed by [41]

$$\eta_{max} = \frac{k^2 Q_1 Q_2}{(1 + \sqrt{k^2 Q_1 Q_2})^2} \quad (12)$$

The relationship between the maximum efficiency, quality factors and the coupling coefficient  $k$  is shown in Figure 2.5 [41]. As an example, if quality factors of both coils are maintained to be 300,  $k$  between the coils is equal to 0.2, a maximum power transfer efficiency of 96.7% can be

achieved. In [43][44], the maximum efficiency is derived based on different types of compensation networks.

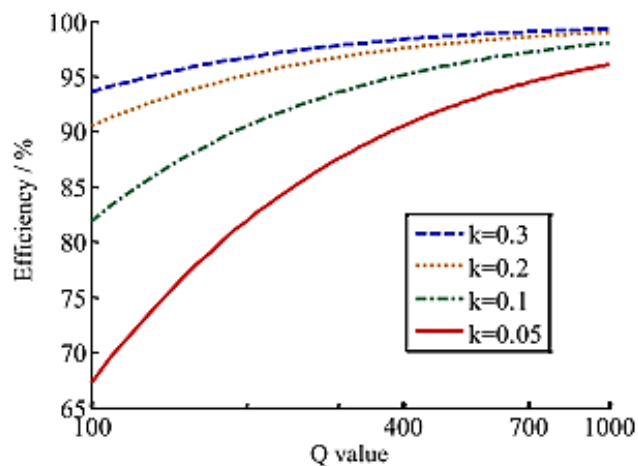


Figure 2.5: Power transfer efficiency considering different quality factor [41]

## 2.3 Wireless Charging with a Short Air-Gap

One major drawback of a WPT system is that the power transfer efficiency is reduced significantly with the increment of the air-gap distance between the transmitter and receiver. In this section, several EV wireless charging topologies employed with a short air-gap are provided. A short air-gap configuration is also known as a near field power transfer system, where the transmitter and receiver remain in close proximity. Generally, the air-gap ranges up to 40 cm [9].

### 2.3.1 Coupled Magnetic Resonance system

Among various WPT technologies, the Coupled Magnetic Resonance (CMR) system is promising because it enables power transfer in a longer distance with a high efficiency. In a CMR system, power transfer to the vehicle is achieved through three magnetic couplings: 1) from power

source coil to transmitter coil, 2) from transmitter coil to receiver coil, and 3) from receiver coil to load coil. The equivalent circuit of a CMR system is shown in Figure 2.6. Although a CMR system exhibits high power transfer efficiency, multiple couplings make the system complex to implement [9][46]. The maximum load power  $P_{L,m}$  and the maximum efficiency  $\eta_{max}$  for the CMR system in Figure 2.6 can be expressed by [47],

$$P_{L,m} = \frac{Q_c^2 \times v_T^2}{n_0 r_0 \sqrt{1 + Q_c^2 \times (1 + Q_c^2)^2}} \quad (13)$$

$$\eta_{max} \equiv \frac{n_0^2 \times \omega_s^2 \times L_{mT}^2}{(r_0 + \sqrt{r_0^2 + n_0^2 \times \omega_s^2 \times L_{mT}^2})^2} \quad (14)$$

Where,  $Q_c \equiv \frac{\omega_s L_{mT}}{r_T}$  is defined as the coupled quality factor,  $V_T$  is the output voltage of the transmitter coil,  $n_0$  is the number of turn for transmitting and receiving coils,  $r_0$  is the unit internal resistance,  $\omega_s$  is the source angular frequency,  $r_T$  is the sum of internal resistance of the transmitter coil,  $L_{mT}$  is the magnetizing inductance of the transmitter coil, and  $L_{mT0}$  is the unit magnetizing inductance of the transmitter coil.

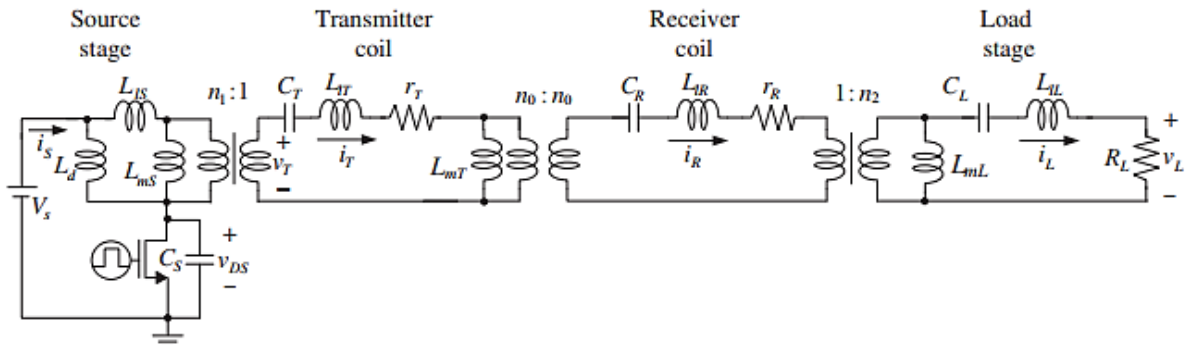


Figure 2.6: The equivalent circuit of a CMR system [46].

To analyze the efficiency of a CMR system with variations of the air-gap distance, an experimental result is reported in [47], where an 80.2% efficiency is achieved at a 13 cm distance. Figure 2.7 shows a comparison between the calculated and measured load power through an experiment for different load resistance  $R_L$  ranging from  $10\ \Omega$  to  $500\ \Omega$  for the system in Figure 2.6. The difference between the calculated and measured values is due to core losses of the impedance transformer [47]. Reference [48] exhibits a similar result.

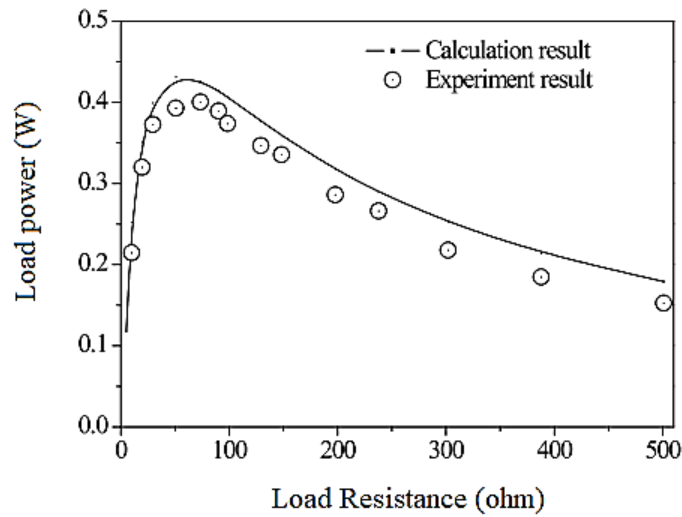


Figure 2.7: Calculated and measured load power vs. load resistance [47].

With the development of Inductive Power Transfer (IPT) system, power transfer through the CMR technology is no longer considered the best solution. Reference [49] reported an IPT system with a long range power transfer mechanism that successfully transferred 1403 W power for a 3 m distance; while a CMR system only transferred 60 W power for a 2.1 m distance [50]. The IPT system as a dominant WPT research area will be introduced in Section 2.3.3.

To improve the efficiency of a CMR system, an impedance matching method is proposed in [51]. A theoretical model of a CMR system is proposed and validated by experimental results in [52], where a tuning matching circuit is proposed to improve the efficiency of the CMR system. Besides this, several CMR topologies for efficient power transfer to EV are discussed in [53]-[55]. To implement CMR system as a regular EV charging system, more experiments should be further conducted to enhance the overall power transfer efficiency.

### 2.3.2 Capacitive Power Transfer system

A capacitive power transfer (CPT) system uses electric field to transfer ac power, and the power can be transferred through obstacles, such as metal barriers, without significant losses [10][56]. Figure 2.8 shows a schematic diagram of a typical CPT system [58]. Because capacitor plates are coupled loosely in the CPT system and the coupling capacitance is small, the overall power transfer efficiency is greatly reduced [10]. The CPT topology uses metal plates, such as aluminum plates, to form a capacitor. Because aluminum plates have better conductivity at a lower cost, it results in a reduced installation cost compared to the IPT technology.

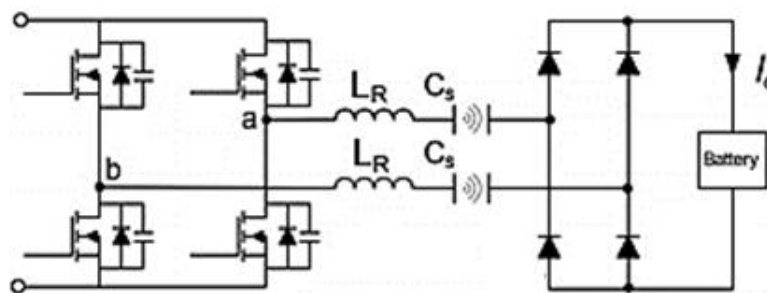


Figure 2.8: Schematic diagram of a typical CPT system [58].

To improve the performance, extra capacitors can be added to the system. For example, a modified CPT topology using two capacitors and two inductors externally on each side of the coupling capacitor is proposed in [57] (Figure 2.9), this system achieved a 90.8% efficiency by transferring 2.4 kW of power with a 150 mm air-gap between the transmitting and receiving ends. With the increment of the air-gap from 150 mm to 300 mm, the efficiency is slightly reduced to 89.1% with 1.6 kW power transferred.

A combined circuit topology with both IPT and CPT technologies is proved to be a success. As shown in Figure 2.10, an inductive-capacitive power transfer system for EV application is proposed in [59]. The input side is a MOSFET inverter, which produces the voltage excitation; the output side is a diode rectifier, which produces DC power to recharge the battery. The proposed system is validated by a 3 kW experimental setup. Experimental results showing the relationship of the measured efficiency with the output power and misalignment between transmitting and receiving ends is demonstrated in Figure 2.11 (a). Without any misalignment, a 94.45% power transfer efficiency can be achieved with 2.84 kW maximum power transferred. A 100 mm misalignment only slightly reduces the efficiency, but 150 mm or 200 mm misalignment can result in a significant drop of the efficiency. The efficiency is 91.49% with 1.35 kW output power for a 200 mm misalignment. The efficiency decay due to misalignments of the proposed IPT-CPT topology is comparatively lower than an IPT or a CPT topology.

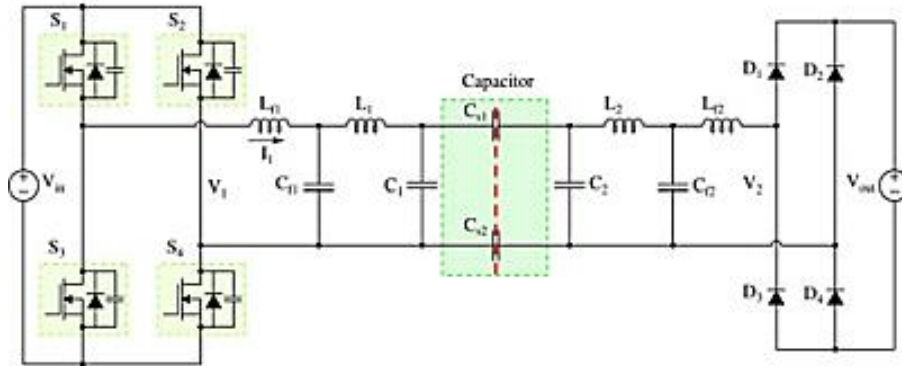


Figure 2.9: A modified CPT system with extra inductors and capacitors [57].

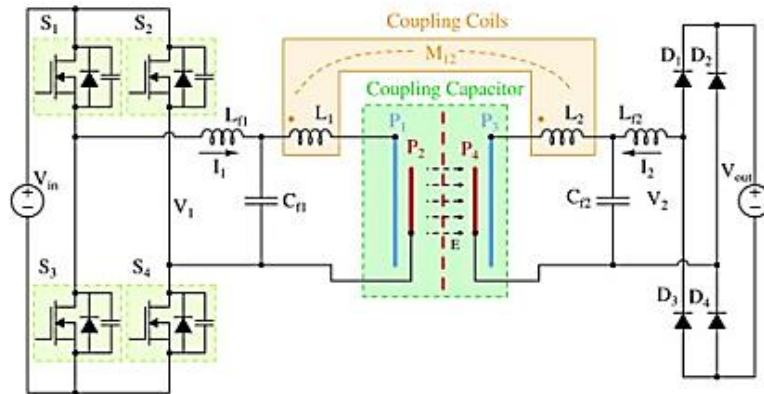
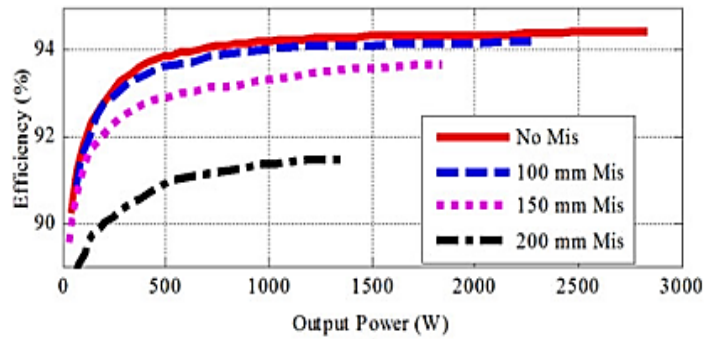


Figure 2.10: Schematic diagram of an IPT-CPT combined topology [59].

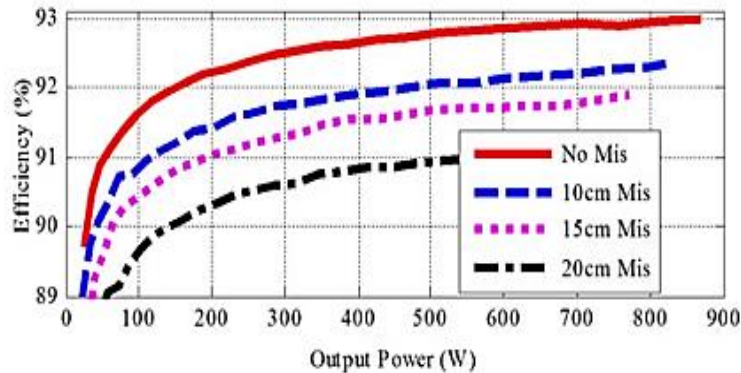
Figure 2.11 (b) is a CPT only topology. Without a misalignment, the maximum output power is 0.86 kW with a 93.04% power transfer efficiency; with a 200 mm misalignment, the maximum output power is reduced to 0.69 kW with a 91.18% power transfer efficiency [59]. A CPT system proposed in [60] has a lower efficiency of 85.87% for a 150 mm misalignment, and 84.68% for a 300 mm misalignment as shown in Figure 2.12.

Figure 2.11 (c) is an IPT only topology. Without a misalignment, the maximum output power is 1.95 kW with a 94.89% power transfer efficiency; with a 200 mm misalignment, the maximum output power is significantly reduced to 0.75 kW with a 91.68% power transfer efficiency [59].

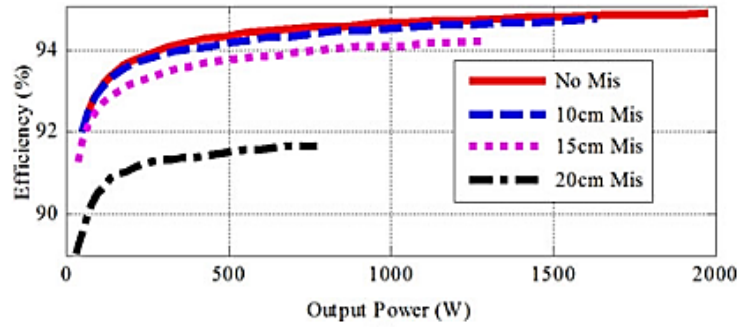
To summarize, the combined IPT-CPT topology renders a better output power efficiency compared to a single CPT or IPT topology, and it also performs well in the case of handling large misalignments between transmitting and receiving ends. To transfer a large amount of power, a combined advanced IPT-CPT topology can be developed as a future research direction.



(a)



(b)



(c)

Figure 2.11: Measured efficiency vs. output power of different circuit topologies considering different levels of misalignments [59]: (a) an IPT-CPT combined topology; (b) a CPT topology; (c) an IPT topology.

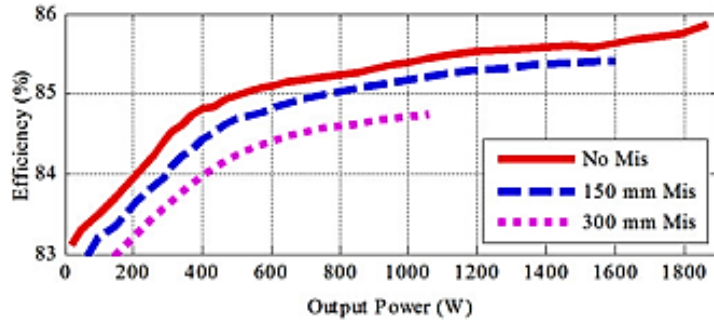


Figure 2.12: Measured efficiency vs. output power for a CPT topology considering different levels of misalignments [60].

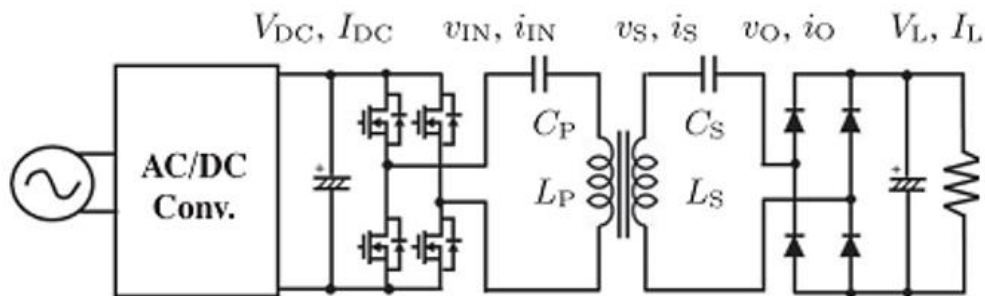
### 2.3.3 Inductive Power Transfer system

The fundamental principle of the IPT system relies on Faradays and Ampere's laws. An EV can be charged in three different modes through an IPT system: stationary static charging, dynamic charging, and quasi-dynamic charging. In an IPT system, the power can be delivered to EVs at an

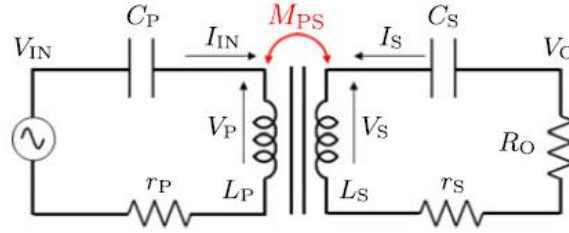
approximate rate of 5-50 kW [61]. By deploying this technology in the highway, the range anxiety of EVs can be reduced greatly. A proper sized power pad needs to be installed in the highway and vehicles. In an IPT system, the power is transferred through coils, losses in the coils account for 30-50% overall losses of the system [11]. The recommended practice for EV wireless charging by Society of Automotive Engineers (SAE) has defined three power classes for WPT technology: 1) WPT 1, the power level is up to 3.7 kW; 2) WPT 2, the power level is up to 7.7 kW; and 3) WPT 3, the power level is up to 11 kW [62].

### 2.3.3.1 Stationary IPT system

Stationary IPT system is generally employed for transferring power up to 50 kW. Figure 2.13 shows the system configuration and equivalent circuit of a stationary IPT system. A rectifier is connected with utility grids to generate DC power, the DC input voltage and current,  $V_{DC}$  and  $I_{DC}$ , further feeds into a full bridge inverter and generate high frequency AC power (85 kHz in this system), the high frequency AC input voltage and current,  $V_{IN}$  and  $I_{IN}$  is then fed into the primary coil. A rectifier is also employed on the secondary side to store the transferred energy.  $C_P$  and  $C_S$  are primary and secondary resonant capacitors, respectively.



(a)



(b)

Figure 2.13: A stationary IPT system [36]: a) circuit configuration, b) equivalent circuit.

The back electromotive force (EMF) for both primary and secondary sides can be expressed as follows [36]:

$$V_P = -j\omega M_{PS}I_S + j\omega L_P I_{IN} \quad (15)$$

$$V_S = j\omega M_{PS}I_{IN} + j\omega L_S I_S \quad (16)$$

Where  $L_P$  and  $L_S$  are the self-inductance of road and vehicle side coil, respectively;  $M_{PS}$  is the mutual-inductance between the two coils;  $\omega$  is the angular frequency;  $I_{IN}$  is the input high frequency AC current fed into the primary coil; and  $I_S$  is the current on the secondary coil. Based on the circuit configuration in Figure 2.12, we have

$$V_{IN} = V_P + \frac{I_{IN}}{j\omega C_P} \quad (17)$$

$$V_S = V_O + \frac{I_S}{j\omega C_S} \quad (18)$$

In [36], experiments for this stationary IPT system are conducted. In the system, the air gap is 135 mm, the coils have an overall power capacity of 3 kW, and the input DC voltage varies between 30 V and 263 V. Figure 2.14 demonstrates the relationship of the input DC current IDC

and load current  $I_L$  vs. the input DC voltage when considering different load resistance  $R_L$ . It appears that the two currents have a linear relationship with the input DC voltage. The system exhibits 91.4% power transfer efficiency with a maximum output power of 2.5 kW when the input DC voltage is 263 V and the load resistance is 20 ohms.

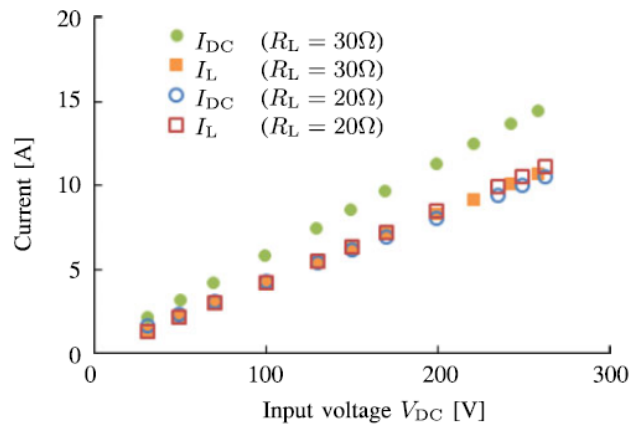


Figure 2.14: Experimental currents  $I_{DC}$  and  $I_L$  vs.  $V_{DC}$  for a stationary IPT system at the aligned condition [36].

### 2.3.3.2 Dynamic IPT system

The concept of dynamic charging system was introduced in 1978, which enables the vehicle storing energy while moving. Reference [26] reports that most electric vehicles can achieve a range of 300 miles if 1% of the highway network supports dynamic charging. Korean Advanced Institute of Science Technology (KAIST) played a lead role in the field of EV dynamic wireless charging, and solved many fundamental issues, such as continuous transfer of power from the road surface to vehicles, and electromagnetic field analysis. Figure 2.15 shows a general schematic diagram of an EV dynamic charging system. In such a system, the coil installed under road surface is known

as power rail or track coil, the coil installed on a vehicle is known as pickup coil, Re-charging the battery is achieved through magnetic coupling between the two coils [25].

Power transfer to vehicles largely depends on proper alignments of track and pickup coils. A perfect power transfer is the result of a perfect alignment matching between the two coils, which is a factor of the vehicle speed. Figure 2.16 shows power transfer between two track coils and one moving pickup coil [25][7]. The overlap between the roadside track coil and the moving pickup coil is represented by diagonal lines in this figure. It can be observed that power transfer to the vehicle is 100% when the pickup coil is perfectly aligned with the track coil, and power transfer is drastically reduced when the pickup coil positioned in the middle of two track coils [25].

A dynamic IPT system consisting of several stationary ground-side (primary) coils and a moving vehicle-side (secondary) coil is proposed in [36] (Figure 2.17). A common vehicle-side coil is used in this system for both dynamic and stationary situations. An AC-DC converter unit supplies power to several parallel-connected inverter units, and an inverter unit will start operation by the assistant of sensing devices when a vehicle approaches ground-side coil units connected to the inverter. The equivalent circuit of the dynamic IPT system is shown in Figure 2.17(a), which is similar to Figure 2.13 except more coils involved. Figure 2.18(b) shows the definition of an air-gap. The power transfer of the proposed IPT system is tested through experiments as shown in Figure 2.19 with a vehicle speed of 1000 mm/s. Variations of the peak-to-peak input and output currents,  $I_{DC}$  and  $I_L$ , are 30% and 10%, respectively.

To ensure stable power transfer to the vehicle, different types of coil configuration (power pad) are investigated for both track and pickup coils, such as circular coil, flux pipe, solenoid coil,

double D (DD) coil, Tripolar power pad etc. Reference [63] reports a DD coil, which combines advantages of both a circular coil and a flux pipe power pad. A review is carried out on different power pads of EV wireless charging system in [8], and general characteristics of different power pads are summarized in Table 2.1 [8].

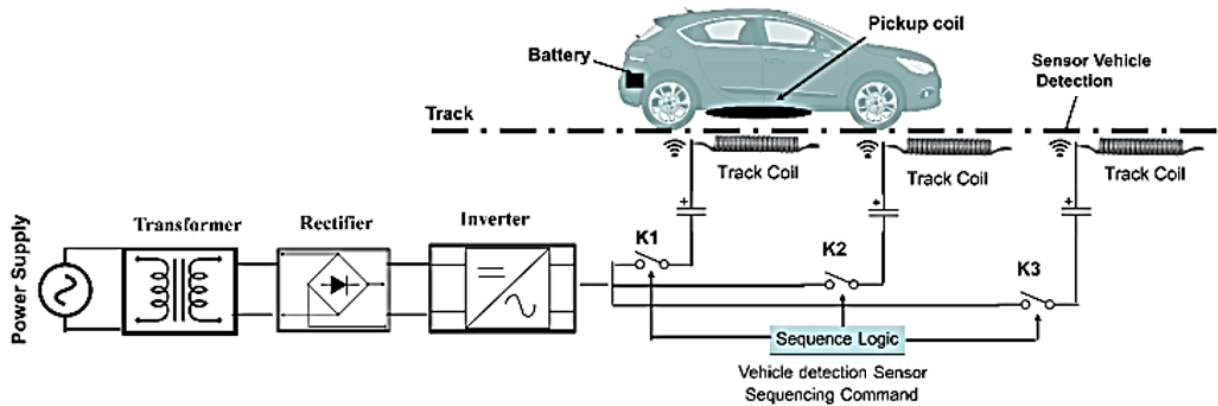


Figure 2.15: A general schematic diagram of dynamic charging system for electric vehicles [25].

Circular coils [65][66] are the most commonly used power pad for EV wireless charging systems, they generally produce the single-sided magnetic flux, which results in reduced amount of leakage flux and a better power transfer efficiency. Current density of circular coils should be less than 5 A/mm<sup>2</sup> for the optimum thermal characteristics [65]. On the other hand, solenoid coils are smaller, lighter, and more tolerant of misalignment in a medium or large air gap [36]. Solenoid coils are chosen in [36] due to two reasons: 1) superior performance in misalignment compared to circular coils; 2) mutual inductance between ground-side coils and the vehicle-side coil would be zero if circular coils are used, which will result in zero power feeding [36].

Reference [63] proposes an EV charging system based on an overlapped DD coil for low speed applications, this system exhibits better power transfer efficiency varying between 88.3% and 90.4%. A current control method for the track coil is proposed and the efficiency is determined based on mutual inductance between track and pickup coils.

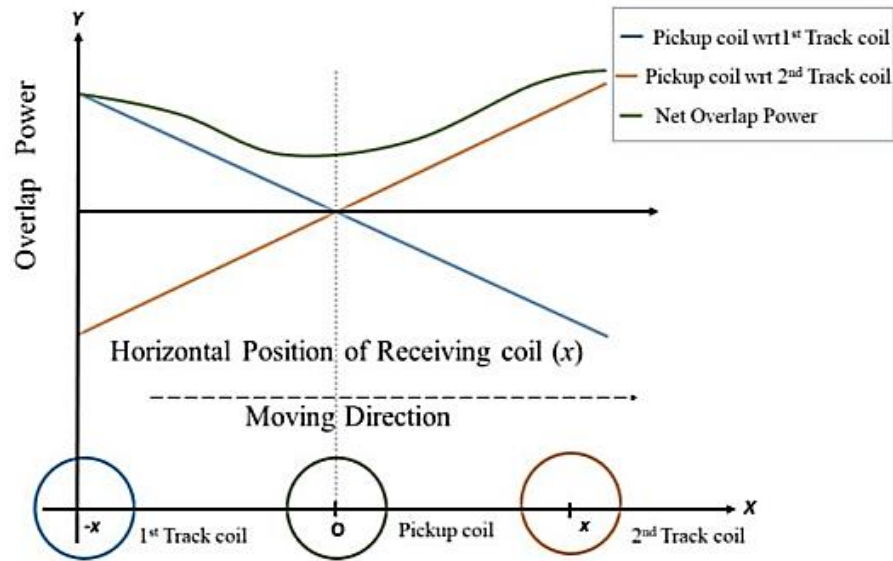


Figure 2.16: Power transfer between the coils [25][7].

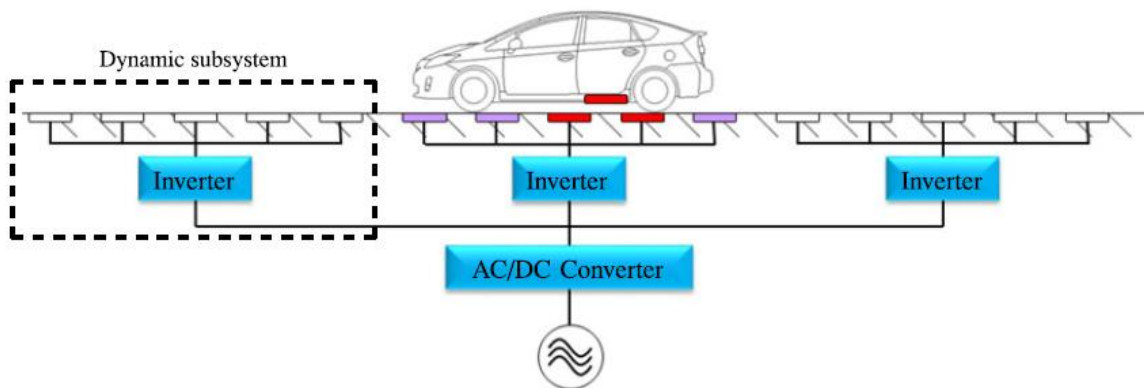
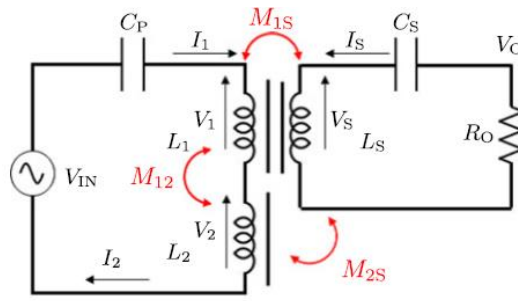
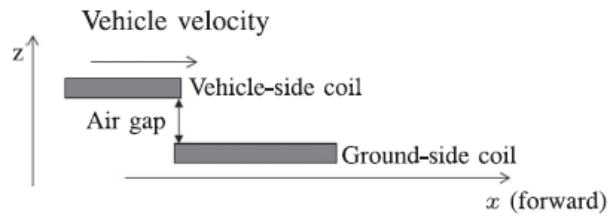


Figure 2.17: A schematic diagram of a proposed dynamic IPT system [36].

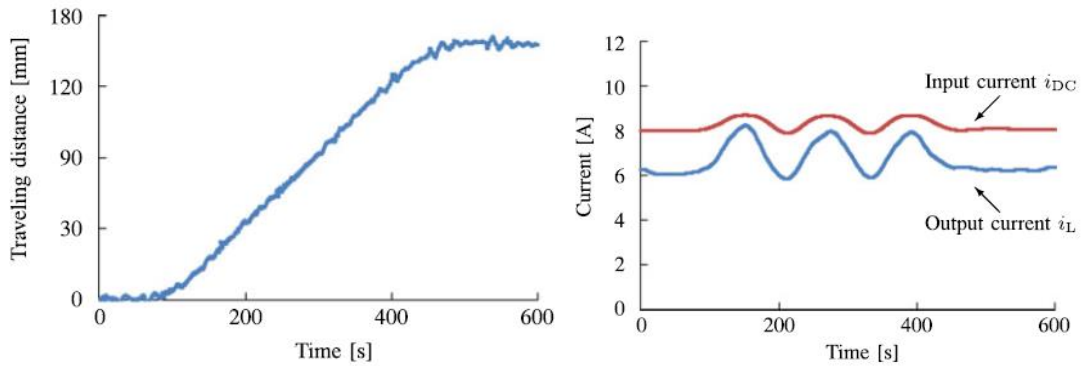


(a)



(b)

Figure 2.18: The proposed dynamic IPT system [36]: (a) equivalent circuit; (b) the definition of the air-gap.



(a)

(b)

Figure 2.19: Power transfer in the proposed dynamic IPT system [36]: (a) traveling distance of the vehicle-side coil; (b) waveforms of input and output currents.

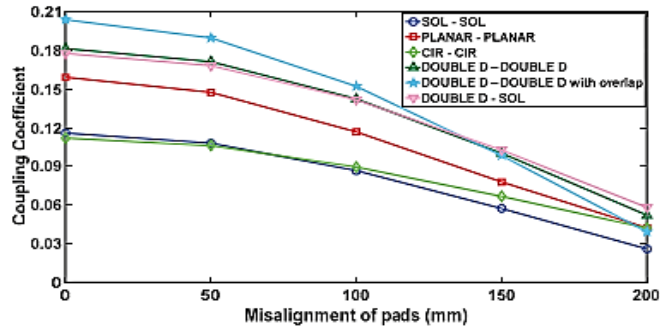
Table 2.1: General characteristics of different power pads available for EV wireless Charging

[8]

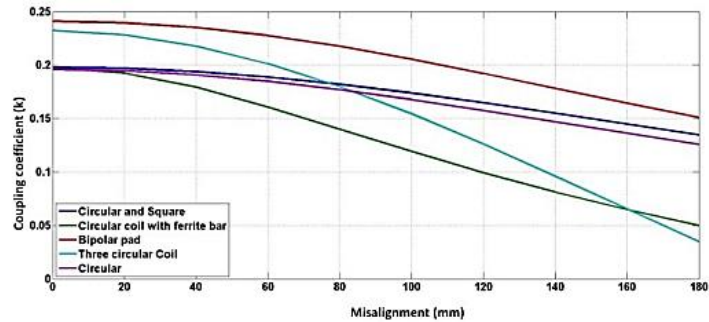
	Circular Coil	DD Coil	DD-Q Coil	Bipolar Coil	Tripolar Coil	Flux Pipe
Misalignment characteristics	Poor	Poor	Good	Moderate	Very good	Moderate
Coupling co-efficient	Low	High	High	High	High	Medium
EMF exposure	High	Low	Low	Low	Low	Low
Magnetic flux Occurring	Only on one side	On both sides	On both sides	Only on one side	Only on one side	On both sides
Shielding results impact on coupling co-efficient	Very low	High	High	High	Very low	High

The coupling co-efficient  $k$  is a critical factor for WPT system design [64][8]. Reference [64] reports the variation of  $k$  for different power pads considered. The rate of output power transfer depends on  $k$ . A greater value of misalignment between transmitting (road side) and receiving (vehicle side) coils results in a reduced output power transfer with a decaying  $k$  value. A simulation is carried out in [64] for the misalignment ranging from 0 – 200 mm between transmitting and receiving coils. Figure 2.20(a) shows the simulated variation of  $k$  vs. misalignment between coils considering different types of power pads. The result indicates that the double D-double D coils with overlap have the highest coupling co-efficient ( $k = 0.2038$ ) for a perfect alignment, however,  $k$  is only 0.113 for circular-circular coils. Although circular coil has the lowest coupling coefficient, circular and plain rectangular coils do show a relatively small variation of  $k$  with respect to different misaligned distances, such as 50 mm, 150 mm and 200 mm, compared to other combinations. The overlapped DD coils, on the other hand, has a relatively larger variations of  $k$

for different misalignments. Through comparison, it is found that that overlapped DD coils are more suitable for EV wireless charging systems [64]. Reference [8] presents experimental results for different power pads as shown in Figure 2.20(b).



(a)



(b)

Figure 2.20: Variation of the coupling co-efficient  $k$  vs. misalignments between transmitting and receiving coils for different power pads: (a) simulation results [64]; (b) experimental results [8].

### 2.3.3.3 Online Electric Vehicle (OLEV)

To reduce the range anxiety of EVs, charging while the vehicle is moving is a vital solution. On-line Electric Vehicle (OLEV) is one type of dynamic IPT system, it was developed by Korean

Advanced Institute of Science and Technology (KAIST), initially introduced in order to transfer large amount of power to vehicles [67]. Energy storage of the OLEV can be recharged whether the vehicle is moving or stopped. Similar to other dynamic IPT design concepts, the entire OLEV system can be divided into two sides: 1) stationary (road) side, and 2) moving (vehicle) side. The stationary side is installed under the road surface, generally consisting of electric power lines, rectifiers and inverters, where the inverter converts the 60 Hz supplied grid power into 260 A AC current with a 20 kHz frequency; the moving side is installed on the vehicle, generally consisting of a pick-up module, an energy storage system, rectifiers, motors and regulators [67]. Figure 2.21 shows a general system configuration for an OLEV system.

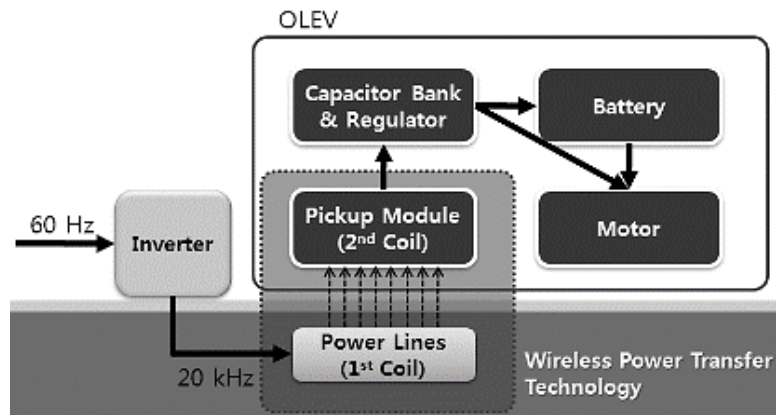


Figure 2.21: General system configuration for an OLEV system [67].

Both mono and dual types of OLEV systems are discussed in the literature. It is concluded in [65] that: 1) the mono type system with one magnetic flux loop exhibits better output power characteristics during the system misalignment than the dual type system; 2) the dual type system, however, provides higher output power with a larger coupling-coefficient  $k$  than the mono type. Reference [66] also indicates a similar result showing a larger coupling-coefficient  $k$  for a dual

type system. Figure 2.22 shows the power transfer efficiency of a dual type system as a function of output power for different distances between the power line and pickup module [66]. In [68], an OLEV system with a 26 cm air gap has an 80% power transfer efficiency. The maximum of 81.7% power transfer efficiency with 79.5 kW transferred power is achieved by this system.

Reference [69] reports an OLEV system with an 8 cm air gap between transmitting and receiving ends, it has a 60% efficiency. To enhance the efficiency of power transfer for the system configuration with a large air gap, different topologies with loosely coupled coils for IPT are discussed in [50][70][71]. Figure 2.23 shows the calculated and experimental results of power transfer efficiency using the loosely coupled coils. To improve power transfer to vehicles, an efficient pickup method is suggested in [72], efficient resonant inverters are proposed in [73], and voltage control methods on the vehicle side is investigated in [74][75]. Different OLEV technologies are summarized in Table 2.2 [76]-[79].

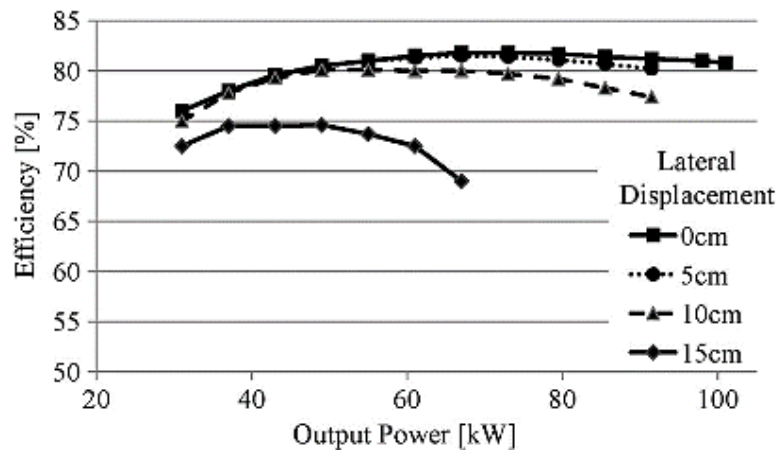


Figure 2.22: Power transfer efficiency vs. output power for a dual type system [65].

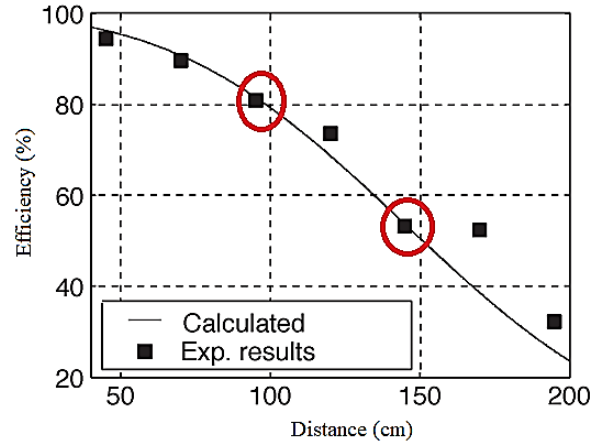


Figure 2.23: Power transfer efficiency with loosely coupled coils [70].

### 2.3.3.4 Permanent Magnet Power Transfer (PMPT)

The EV wireless charging through permanent magnet coupling is another variation of IPT technology although significant differences between their working principles are observed. Reference [80] proposes a PMPT system, where electrical power is converted into mechanical power using permanent magnet similar to a motor. Using magnetic interaction, a torque is induced on the permanent magnet of the receiving end, which results in a synchronous rotation of the permanent magnet of both transmitting and receiving ends. The power is transferred through the air-gap. Rotating permanent magnet of the receiver results in the changing of the magnetic flux, and thus, the mechanical power is converted back to electrical power similar to a generator. Figure 2.24 shows a general power flow inside a PMPT system.

Figure 2.25 shows the power transfer efficiency on the receiving end of a PMPT system vs. load resistance ranging from 0 ohm to 500 ohm. The efficiency is measured using different

frequencies ranging from 30 Hz to 100 Hz. It is found that the calculated efficiency values closely follow experimental results in this figure [80].

Due to complex system architecture and maintenance issue, and low power transfer efficiency, the PMPT system is not considered feasible for EV wireless charging system at the current state. However, it is concluded in [81] that: a) A PMPT system with over 90% efficiency can be considered as an attractive topology for EV wireless charging; b) The system efficiency can be increased by strengthening the electrodynamic coupling; c) the mechanical system with higher coupling characteristics are feasible.

Table 2.2: Summary of Online Electric Vehicle (OLEV) [76] - [79]

Generations for OLEV	General Characteristics
First Generation	<ul style="list-style-type: none"> <li>- Used E-shape core for both roadside and vehicle side systems.</li> <li>- Power transfer efficiency is 80% with a 1 cm air gap and 10 mG EMF.</li> <li>- Experimented using a golf cart with the switching frequency of 20 kHz.</li> <li>- Total length of the power rail was 40 m.</li> </ul>
Second Generation	<ul style="list-style-type: none"> <li>- Used U-shape core for roadside system and I-shape core for vehicle side system.</li> <li>- Power transfer efficiency is 72% with a 17 cm air gap and a 51 mG EMF.</li> <li>- Experimented using a bus that successfully transferred 60 kW power.</li> <li>- Total length of the power rail was 240 m.</li> </ul>
Third Generation	<ul style="list-style-type: none"> <li>- Used W-shape core for roadside system and I-shape core for vehicle side system.</li> <li>- Power transfer efficiency is 71% with a 17 cm air gap considering a SUV.</li> <li>- Power transfer efficiency is 83% with a 20 cm air gap considering a bus.</li> <li>- Total width of the power rail was 80 cm.</li> </ul>
Fourth Generation	<ul style="list-style-type: none"> <li>- Used I-shape core for both roadside and vehicle side systems.</li> <li>- Power transfer efficiency is 80% with a 20 cm air gap and a 10 mG EMF.</li> <li>- Experimented using a bus that successfully transferred 27 kW power.</li> </ul>

	<ul style="list-style-type: none"> <li>- Reduced 20% installation cost compared to the third generation OLEV [79].</li> </ul>
Fifth Generation	<ul style="list-style-type: none"> <li>- Used S-shape core for roadside system and flat pick-up for vehicle side system.</li> <li>- Power transfer efficiency is 91% with a 20 cm air gap (The efficiency does not include inverters).</li> <li>- Experimented in a lab with successfully transferring 22 kW power.</li> <li>- Width of the roadside power supply rail is reduced 2 times comparing to the fourth generation OLEV</li> </ul>
Sixth Generation	<ul style="list-style-type: none"> <li>- Proposed a system without any core for the roadside and rectangular pickup coil in the vehicle side</li> <li>- Installation cost can be significantly reduced as the proposed system requires less protective system</li> <li>- The self and mutual inductance are half of conventional system, which ensures better lateral tolerance.</li> </ul>

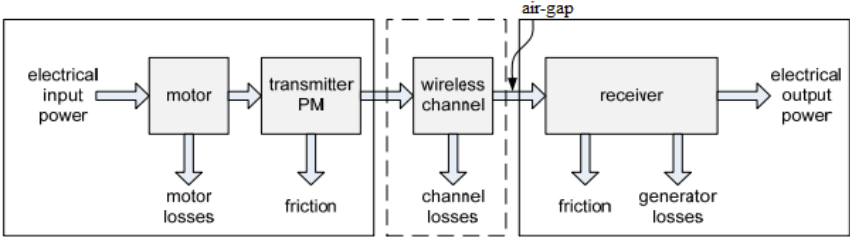


Figure 2.24: Power flow of a typical PMPT system [80].

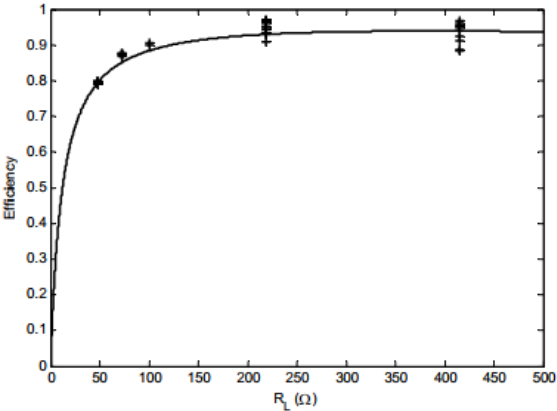


Figure 2.25: Calculated (solid line) and experimental (+) results for efficiency at receiving end with different load resistance [80].

## 2.4 EV Wireless Charging with a Large Air-Gap

EV wireless charging through a large air-gap is known as far field topology. It can be classified into two major classes: 1) power transfer through microwave; and 2) power transfer through LASER [25]. These technologies are briefly discussed because they are very new for vehicular applications. Currently, they are only at the experimental stage.

Microwave power transfer (MPT) system uses transmitting and receiving antennas for EV charging. Power transfer is done by microwave beam, which is emitted from the transmitting antenna. The receiving antenna is installed in the vehicle, known as rectenna (rectifying antenna), it captures the emitted microwave beam from the transmitting antenna [82]. The captured microwave beam is further converted into DC power and supplied to the energy storage of EVs. Aperture Coupled Micro Strip Patch Antenna (ACMPA) is installed on the vehicle side to receive transmitting power from transmitting antenna due to its dimensional flexibility and economic feasibility. Fundamental principle and design consideration for transmitting and receiving antennas of a MPT system are broadly discussed in [83][84]. Generally speaking, the power transfer efficiency of a MPT system is not attractive for EV wireless charging compared to other resonant WPT systems, however, the efficiency can be improved by designing proper antennas. Power transfer through a MPT system in earlier designs uses the frequency 2.45 GHz, it has been recognized that the implementation of a higher frequency enables the technology to transfer power for a longer distance. Figure 2.26 represents a general schematic of EV wireless charging through MPT [85].

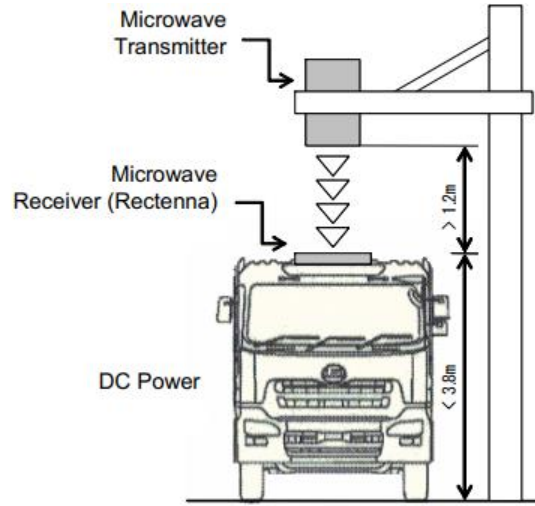


Figure 2.26: EV wireless charging through MPT [85].

Friis transmitting equation can be employed for determining the microwave beam efficiency considering a large air-gap as follows [86]:

$$P_r = \frac{\lambda^2 G_r G_t}{(4\pi D)^2} = \frac{A_r A_t}{(\lambda D)^2} P_t \quad (19)$$

The efficiency can then be calculated by

$$\eta = \frac{P_r}{P_t} \quad (20)$$

Where  $D$  is the distance between rectenna and transmitting antenna,  $\lambda$  is the wavelength,  $P_t$  is the power transmitted through the transmitting antenna,  $P_r$  is the power received on the vehicle side,  $G_r$  is the gain of receiving antenna,  $G_t$  is the overall gain of the transmitting antenna,  $A_r$  and  $A_t$  are the receiving antenna and transmitting antenna aperture area, respectively.

For a near field MPT operation, Friis equation is not feasible. Instead of using Friis equation,  $\tau$  parameter is used to calculate microwave beam efficiency, which can be expressed as follows [86]:

$$\tau = \frac{A_r A_t}{(\lambda D)^2} \quad (21)$$

Microwave beam efficiency obtained by using the  $\tau$  parameter for both far field and near field is illustrated in Figure 2.27, where the left blue curve indicates the efficiency for far field, and the right green curve indicates the efficiency for near field. Microwave beam efficiency increases with the increase of  $\tau$ . Theoretically, the efficiency can reach 100% when the value of  $\tau$  exceeds 2.5.

A MPT system for EV wireless charging is proposed in [85], where power transfer is done using magnetron and slot antenna in a short 10 cm air-gap. Experiment results show a near 67% efficiency. The efficiency increases to 76% by redesigning the antennas on both transmitting and receiving ends [85]. Comparing with modern wireless EV charging technologies, this outcome is not promising for a short air-gap EV wireless charging system.

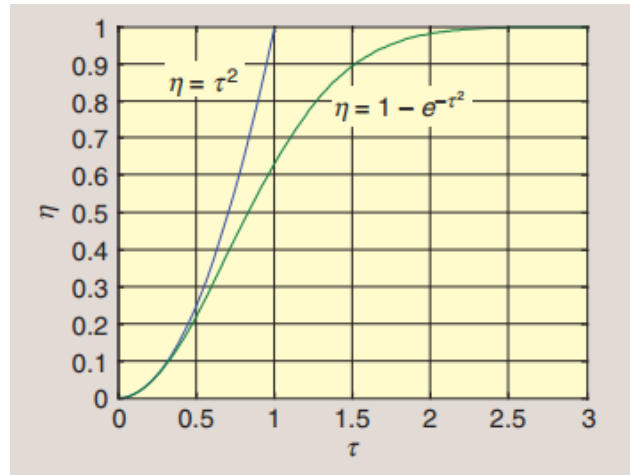


Figure 2.27: Beam efficiency obtained for far and near field using  $\tau$  parameter [86].

Reference [87] proposes an MPT system with the rectenna placed on the roof of the vehicle. The system with a 6 m air-gap between transmitting and receiving antennas was tested through experiments for transferring 10 kW power using a 2.45 GHz frequency. The system has a

maximum of 79.1% microwave efficiency, which is significantly attractive with such a large air-gap. In [88], five different antennas are investigated, which can be used on the roof of a vehicle.

Reference [89] reports an efficiency of 50.5% using the frequency of 2.45 GHz. An efficiency of more than 80% is reported in [90] using a frequency of 5.85 GHz as shown in Figure 2.28. Depending on the fundamental frequency, transmitting and receiving antennas for both roadside and vehicle side are redesigned, and high power transfer efficiency of 90% can be obtained for a 5 m distance [90].

The MPT for EV wireless charging can overcome limitations of conventional chargers. Major advantages of the MPT technology are summarized as follows [91]:

- EVs can be charged either in motion or parked using the same MPT system.
- The MPT can transfer power through a large air-gap between transmitting and receiving ends.
- Beam steering technology enables the MPT to charge multiple vehicles from the same transmitting antenna.
- Financially, the MPT technology is very attractive for large scale deployment.

Due to complex system architectures, low efficiency and high precaution requirement, EV wireless charging through the LASER technology has not yet been proved feasible. The research in this area is going on in the field, but the large scale deployment of the LASER technology for EV wireless charging is not expected to be realized in the near future.

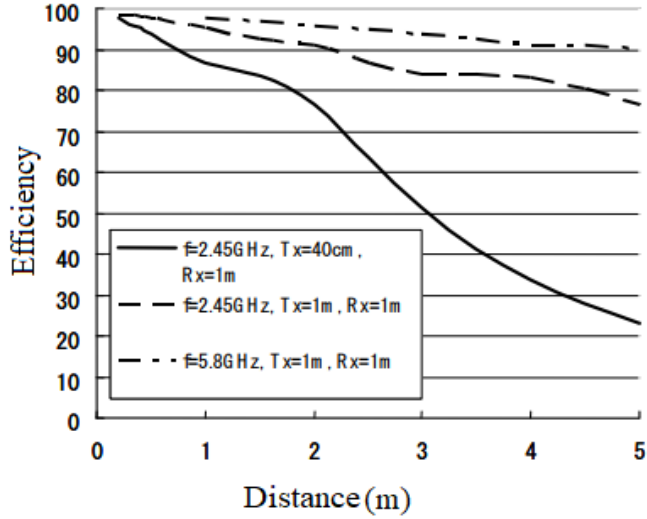


Figure 2.28: MPT efficiency obtained for different distances [90].

## 2.5 EV Comparison between different topologies

EVs with improved power electronic devices might play an important role in our future transportation system. A general comparison between several EV wireless charging topologies are summarized in Table 2.3.

Table 2.3: Comparison of different EV wireless charging systems [58][92][93]

System characteristics	Short Air-Gap (Near Field)			Long Air-Gap (Far Field)
	Capacitive Power Transfer (CPT)	Inductive Power Transfer (IPT)	Coupled Magnetic Resonance (CMR)	Microwave Power Transfer (MPT)
Frequency range	1 kHz to 20 MHz	20 kHz to 200 kHz	1 kHz to 38 MHz	1 MHz to 30 MHz
Power transfer efficiency	Low	Moderate	Low	Moderate
Maximum efficiency reported	Over 93% for 15 cm [34]	Over 94% for 15 cm [34]	Over 80% for 13 cm [21]	Over 90% for 1 Km [26]
Applicable power level	Low	High	High	Low/Medium

Transmitting and receiving apparatus	Electrodes	Coils	Coils	Rectifying antennas
EMI	Moderate	Moderate	Low	Moderate
System architecture	Moderate	Moderate	Complex	Moderate
Typical charging distance	Limited to a few cm.	Limited to a few cm.	Limited to a few m.	Limited to a few km.
Installation cost	Cheap	Moderately expensive	Moderately expensive	Moderately expensive

## 2.6 Conclusion

In this paper, EV wireless charging systems are classified based on the air-gap length between transmitting and receiving ends. Various EV wireless charging techniques reported in the literature are reviewed. The principle of each technique is introduced, various topologies associated with each technique are summarized and compared with a particular focus on power transfer efficiency. For a sustainable electrified transportation system, dynamic wireless charging system should be developed for a greater output power efficiency during misalignments with a reduced installation cost. Enabling the vehicle to grid (V2G) technology and the development of dynamic wireless charging will open a new era of electrified transportation system with reduced battery capacity and increased vehicle driving range.

The recommended future research directions include:

- 1) More coupler (power pad) configurations with higher power transfer efficiency and better misalignment characteristics should be investigated.
- 2) Bi-directional operation of wireless charging system should be advanced to make it technically and commercially feasible.

3) Smart charging system is desired with secure and reliable sensing devices and communication network.

Research on electromagnetic effect on human body should be carried out for safe operation of EV wireless charging.

## References

- [1] J. Dai and D. C. Ludois, "A Survey of Wireless Power Transfer and a Critical Comparison of Inductive and Capacitive Coupling for Small Gap Applications," *IEEE Trans. Power Electronics*, Vol. 30, No. 11, pp. 6017–6029, 2015.
- [2] A. Bomber and L. Rosa, "Wireless power transmission: an obscure history, possibly a bright future," *Physics*, vol. 464, pp. 1-15, 2006.
- [3] M. Bojarski, E. Asa, K. Colak, and D. Czarkowski, "Analysis and Control of Multiphase Inductively Coupled Resonant Converter for Wireless Electric Vehicle Charger Applications," *IEEE Trans. Transportation Electrification*, Vol. 3, No. 2, pp. 312–320, 2017.
- [4] C. Liu, C. Jiang, and C. Qiu, "Overview of coil designs for wireless charging of electric vehicle," in *2017 IEEE PELS Workshop on Emerging Technologies: Wireless Power Transfer (WoW)*, 2017, pp. 1-6.
- [5] A. A. S. Mohamed, C. R. Lashway, and O. Mohammed, "Modeling and Feasibility Analysis of Quasi-Dynamic WPT System for EV Applications," *IEEE Trans. Transportation Electrification*, Vol. 3, No. 2, pp. 343–353, 2017.
- [6] J. Bolger, F. Kirsten, and L. Ng, "Inductive power coupling for an electric highway system," in *28th IEEE vehicular technology conference*, 1978, pp. 137-144.

- [7] J. M. Miller, P. T. Jones, J.-M. Li, and O. C. Onar, "ORNL experience and challenges facing dynamic wireless power charging of EV's," *IEEE Circuits Syst. Mag.*, vol. 15, no. 2, pp. 40–53, May 2015.
- [8] D. Patil, M. K. McDonough, J. M. Miller, B. Fahimi, and P. T. Balsara, "Wireless Power Transfer for Vehicular Applications: Overview and Challenges," *IEEE Transactions on Transportation Electrification*, vol. 4, no.1, pp. 3-37, March 2018.
- [9] A. Umenei, "Understanding low frequency non-radiative power transfer,"[https://www.wirelesspowerconsortium.com/data/downloadables/6/8/9/understanding-low-frequency-non-radiative-power-transfer-8\\_8\\_11.pdf](https://www.wirelesspowerconsortium.com/data/downloadables/6/8/9/understanding-low-frequency-non-radiative-power-transfer-8_8_11.pdf).
- [10] C. Liu, A. P. Hu, G. A. Covic, and N.-K. C. Nair, "Comparative study of CCPT systems with two different inductor tuning positions," *IEEE Trans. Power Electronics*, Vol. 27, No. 1, pp. 294-306, 2012.
- [11] F. Y. Lin, G. A. Covic, and J. T. Boys, "Leakage flux control of mismatched IPT systems," *IEEE Trans. Transportation Electrification*, Vol. 3, No. 2, pp. 474-487, 2017.
- [12] A. Ahmad, M. S. Alam, and R. Chabaan, "A comprehensive review of wireless charging technologies for electric vehicles," *IEEE Trans. Transportation Electrification*, Vol. 4, No. 1, pp. 38 – 63, 2018.
- [13] A. Zaheer, H. Hao, G. A. Covic, and D. Kacprzak, "Investigation of multiple decoupled coil primary pad topologies in lumped IPT systems for interoperable electric vehicle charging," *IEEE Trans. on Power Electronics*, vol. 30, no. 4, pp. 1937–1955, 2015.

- [14] M. Budhia, G. A. Covic, and J. T. Boys, "Design and optimization of circular magnetic structures for lumped inductive power transfer systems," *IEEE Trans. Power Electron.*, vol. 26, no. 11, pp. 3096-3108, November 2011.
- [15] M. Budhia, J. T. Boys, G. A. Covic, and C.-Y. Huang, "Development of a single-sided flux magnetic coupler for electric vehicle IPT charging systems," *IEEE Trans. Ind. Electron.*, vol. 60, no. 1, pp. 318-328, January 2013.
- [16] A. Zaheer, G. A. Covic, and D. Kacprzak, "A bipolar pad in a 10-kHz 300-W distributed IPT system for AGV applications," *IEEE Trans. Ind. Electron.*, vol. 61, no. 7, pp. 3288-3301, July 2014.
- [17] N. Rasekh and M. Mirsalim, "Analysis of a compact and efficient DDQ pad integrated to the LCC compensation topology for IPT," in *2018 9th Annual Power Electronics, Drives Systems and Technologies Conference (PEDSTC)*, 2018, pp. 26-29.
- [18] S. Kim, G. A. Covic, and J. T. Boys, "Tripolar pad for inductive power transfer systems for EV charging," *IEEE Trans. Power Electron.*, vol. 32, no. 7, pp. 5045-5057, July 2017.
- [19] G. A. Covic, M. L. G. Kissin, D. Kacprzak, N. Clausen, and H. Hao, "A bipolar primary pad topology for EV stationary charging and highway power by inductive coupling," in *Proc. IEEE Energy Convers. Congr. Expo.*, Phoenix, AZ, USA, Sep. 2011, pp. 1832-1838.
- [20] S. Kim, G. A. Covic, and J. T. Boys, "Tripolar pad for inductive power transfer systems for EV charging," *IEEE Trans. Power Electron.*, vol. 32, no. 7, pp. 5045-5057, Jul. 2017.

- [21] Z. Zhang, H. Pang, C. H. Lee, X. Xu, X. Wei, and J. Wang, "Comparative analysis and optimization of dynamic charging coils for roadway-powered electric vehicles," *IEEE Trans. Magnetics*, Vol. 53, No. 11, pp. 1-6, 2017.
- [22] K. Knaisch, M. Springmann, and P. Gratzfeld, "Comparison of coil topologies for inductive power transfer under the influence of ferrite and aluminum," in *2016 Eleventh International Conference on Ecological Vehicles and Renewable Energies (EVER)*, 2016, pp. 1-9.
- [23] SAE Recommended Practice J2954, "Wireless power transfer for light-duty plug-in/electric vehicles and alignment methodology," November 2017.
- [24] "Recent update of Canadian automotive market", obtained from: <https://www.fleetcarma.com/electric-vehicle-sales-in-canada-q3-2017/> [March 2, 2018].
- [25] A. Ahmad, M. S. Alam, and R. Chabaan, "A comprehensive review of wireless charging technologies for electric vehicles," *IEEE Trans. Transportation Electrification*, Vol. 4, No. 1, pp. 38 – 63, 2018.
- [26] S. Lukic and Z. Pantic, "Cutting the cord: Static and dynamic inductive wireless charging of electric vehicles," *IEEE Electrification Magazine*, Vol. 1, No. 1, pp. 57-64, 2013.
- [27] F. Ahmad, M. S. Alam, and M. Asaad, "Developments in xEVs charging infrastructure and energy management system for smart microgrids including xEVs," *Sustainable Cities and Society*, Vol. 35, pp. 552–564, 2017.

- [28] "History of EV development", accessed at: <https://www.energy.gov/articles/history-electric-car> [July 12, 2018].
- [29] J. Nor, "Art of charging electric vehicle batteries," *Proceedings of WESCON 93*, pp. 521-525, 1993.
- [30] B. Singh, B. N. Singh, A. Chandra, K. Al-Haddad, A. Pandey, and D. P. Kothari, "A review of single-phase improved power quality AC-DC converters," *IEEE Trans. Industrial Electronics*, Vol. 50, No. 5, pp. 962-981, 2003.
- [31] S. S. Williamson, A. K. Rathore, and F. Musavi, "Industrial electronics for electric transportation: Current state-of-the-art and future challenges," *IEEE Trans. Industrial Electronics*, Vol. 62, No. 5, pp. 3021-3032, 2015.
- [32] B. Singh, S. Gairola, B. N. Singh, A. Chandra, and K. Al-Haddad, "Multipulse AC-DC converters for improving power quality: a review," *IEEE Trans. Power Electronics*, Vol. 23, No. 1, pp. 260-281, 2008.
- [33] B. Singh, S. Gairola, B. N. Singh, A. Chandra, and K. Al-Haddad, "Multipulse AC-DC converters for improving power quality: a review," *IEEE Trans. Power Electronics*, Vol. 23, No. 1, pp. 260-281, 2008.
- [34] M. Yilmaz and P. T. Krein, "Review of battery charger topologies, charging power levels, and infrastructure for plug-in electric and hybrid vehicles," *IEEE Trans. Power Electronics*, Vol. 28, No. 5, pp. 2151-2169, 2013.

- [35] P. Bansal, "Charging of electric vehicles: technology and policy implications," *Journal of Science Policy & Governance*, Vol. 6, No. 1, pp. 1-20, 2015.
- [36] T. Fujita, T. Yasuda, and H. Akagi, "A dynamic wireless power transfer system applicable to a stationary system," *IEEE Trans. Industry Applications*, Vol. 53, No. 4, pp. 3748-3757, 2017.
- [37] A. A. S. Mohamed, C. R. Lashway, and O. Mohammed, "Modeling and Feasibility Analysis of Quasi-Dynamic WPT System for EV Applications," *IEEE Trans. Transportation Electrification*, Vol. 3, No. 2, pp. 343–353, 2017.
- [38] P. Javanbakht, S. Mohagheghi, B. Parkhideh, S. Dutta, R. Chattopadhyay, and S. Bhattacharya, "Vehicle-to-grid scheme based on inductive power transfer for advanced distribution automation," *2013 IEEE Energy Conversion Congress and Exposition*, pp. 3250 – 3257, 2013.
- [39] X. Zhang, Z. Yuan, Q. Yang, Y. Li, J. Zhu, and Y. Li, "Coil design and efficiency analysis for dynamic wireless charging system for electric vehicles," *IEEE Trans. Magnetics*, Vol. 52, No. 7, pp. 1-4, 2016.
- [40] Y. Gao, C. Duan, A. A. Oliveira, A. Ginart, K. B. Farley, and Z. T. H. Tse, "3-D Coil Positioning Based on Magnetic Sensing for Wireless EV Charging," *IEEE Trans. Transportation Electrification*, Vol. 3, No. 3, pp. 578-588, 2017.
- [41] S. Li and C. C. Mi, "Wireless power transfer for electric vehicle applications," *IEEE journal of emerging and selected topics in power electronics*, Vol. 3, No. 1, pp. 4-17, 2015.

- [42] T. Campi, S. Cruciani, V. De Santis, F. Maradei, and M. Feliziani, "EMC and EMF safety issues in wireless charging system for an electric vehicle (EV)," in *Electrical and Electronic Technologies for Automotive, 2017 International Conference of*, pp. 1-4, 2017.
- [43] Y. Zhang, Z. Zhao, and K. Chen, "Frequency decrease analysis of resonant wireless power transfer," *IEEE Trans. Power Electronics*, Vol. 29, No. 3, pp. 1058-1063, 2014.
- [44] A. Kamineni, G. A. Covic, and J. T. Boys, "Analysis of coplanar intermediate coil structures in inductive power transfer systems," *IEEE Trans. Power Electronics*, Vol. 30, No. 11, pp. 6141-6154, 2015.
- [45] B. Esteban, M. Sid-Ahmed, and N. C. Kar, "A comparative study of power supply architectures in wireless EV charging systems," *IEEE Trans. Power Electronics*, Vol. 30, No. 11, pp. 6408-6422, 2015.
- [46] C. T. Rim and C. Mi, "Review of Coupled Magnetic Resonance System (CMRS)," Chapter 23, *Wireless Power Transfer for Electric Vehicles and Mobile Devices First Edition*, 2 June 2017.
- [47] B. H. Choi, E. S. Lee, J. Huh, and C. T. Rim, "Lumped impedance transformers for compact and robust coupled magnetic resonance systems," *IEEE Trans. Power Electronics*, Vol. 30, No. 11, pp. 6046-6056, 2015.
- [48] J. Huh, W. Lee, S. Choi, G.-H. Cho, and C.-T. Rim, "Explicit static circuit model of coupled magnetic resonance system," *2011 IEEE 8th International Conference on Power Electronics and ECCE Asia (ICPE & ECCE)*, pp. 2233-2240, 2011.

- [49] C. Park, S. Lee, G.-H. Cho, and C. T. Rim, "Innovative 5-m-off-distance inductive power transfer systems with optimally shaped dipole coils," *IEEE Trans. Power Electronics*, Vol. 30, No. 2, pp. 817-827, 2015.
- [50] A. Kurs, A. Karalis, R. Moffatt, J. D. Joannopoulos, P. Fisher, and M. Soljačić, "Wireless power transfer via strongly coupled magnetic resonances," *Science*, Vol. 317, No. 5834, pp. 83-86, 2007.
- [51] C.-S. Wang, O. H. Stielau, and G. A. Covic, "Design considerations for a contactless electric vehicle battery charger," *IEEE Trans. Industrial Electronics*, Vol. 52, No. 5, pp. 1308-1314, 2005.
- [52] A. P. Sample, D. T. Meyer, and J. R. Smith, "Analysis, experimental results, and range adaptation of magnetically coupled resonators for wireless power transfer," *IEEE Trans. Industrial Electronics*, Vol. 58, No. 2, pp. 544-554, 2011.
- [53] E. M. Thomas, J. D. Heebl, C. Pfeiffer, and A. Grbic, "A power link study of wireless non-radiative power transfer systems using resonant shielded loops," *IEEE Trans. Circuits and Systems I: Regular Papers*, Vol. 59, No. 9, pp. 2125-2136, 2012.
- [54] M. Kiani and M. Ghovanloo, "The circuit theory behind coupled-mode magnetic resonance-based wireless power transmission," *IEEE Trans. Circuits and Systems I: Regular Papers*, Vol. 59, No. 9, pp. 2065-2074, 2012.

- [55] B. L. Cannon, J. F. Hoburg, D. D. Stancil, and S. C. Goldstein, "Magnetic resonant coupling as a potential means for wireless power transfer to multiple small receivers," *IEEE Trans. Power Electronics*, Vol. 24, No. 7, pp. 1819-1825, 2009.
- [56] J. Dai and D. C. Ludois, "Single active switch power electronics for kilowatt scale capacitive power transfer," *IEEE Journal of Emerging and Selected Topics in Power Electronics*, Vol. 3, No. 1, pp. 315-323, 2015.
- [57] F. Lu, H. Zhang, H. Hofmann, and C. Mi, "A double-sided LCLC-compensated capacitive power transfer system for electric vehicle charging," *IEEE Trans. Power Electronics*, Vol. 30, No. 11, pp. 6011-6014, 2015.
- [58] F. Musavi and W. Eberle, "Overview of wireless power transfer technologies for electric vehicle battery charging," *IET Power Electronics*, Vol. 7, No. 1, pp. 60-66, 2014.
- [59] F. Lu, H. Zhang, H. Hofmann, and C. C. Mi, "An inductive and capacitive combined system with LC-compensated topology," *IEEE Trans. Power Electronics*, Vol. 31, No. 12, pp. 8471-8482, 2016.
- [60] H. Zhang, F. Lu, H. Hofmann, W. Liu, and C. C. Mi, "A four-plate compact capacitive coupler design and LCL-compensated topology for capacitive power transfer in electric vehicle charging application," *IEEE Trans. Power Electronics*, Vol. 31, No. 12, pp. 8541-8551, 2016.
- [61] G. R. Nagendra, G. A. Covic, and J. T. Boys, "Sizing of Inductive Power Pads for Dynamic Charging of EVs on IPT Highways," *IEEE Trans. Transportation Electrification*, Vol. 3, No. 2, pp. 405-417, 2017.

- [62] "SAE Electric Vehicle Inductive Coupling Recommended Practice", accessed at: [https://www.sae.org/standards/content/j2954\\_201711/](https://www.sae.org/standards/content/j2954_201711/) [July 12, 2018].
- [63] Y. Liu, R. Mai, D. Liu, Y. Li, and Z. He, "Efficiency optimization for wireless dynamic charging system with overlapped DD coil arrays," *IEEE Trans. Power Electronics*, Vol. 33, No. 4, pp. 2832-2846, 2018.
- [64] H. Movagharnejad and A. Mertens, "Design optimization of various contactless power transformer topologies for wireless charging of electric vehicles," *2016 18th European Conference on Power Electronics and Applications (EPE'16 ECCE Europe)*, pp. 1-10, 2016.
- [65] J. Shin, B. Song, S. Lee, S. Shin, Y. Kim, G. Jung, *et al.*, "Contactless power transfer systems for on-line electric vehicle (OLEV)," *2012 IEEE International Electric Vehicle Conference (IEVC)*, pp. 1-4, 2012.
- [66] J. Kim, J. Kim, S. Kong, H. Kim, I.-S. Suh, N. P. Suh, *et al.*, "Coil design and shielding methods for a magnetic resonant wireless power transfer system," *Proceedings of the IEEE*, Vol. 101, No. 6, pp. 1332-1342, 2013.
- [67] S. Ahn, and J. Kim. "Magnetic field design for high efficient and low EMF wireless power transfer in on-line electric vehicle." *Proceedings of the 5th European Conference on Antennas and Propagation (EUCAP)*, pp. 3979 – 3982, 2011.
- [68] J. Shin, S. Shin, Y. Kim, S. Ahn, S. Lee, G. Jung, *et al.*, "Design and implementation of shaped magnetic-resonance-based wireless power transfer system for roadway-powered moving electric vehicles," *IEEE Trans. Industrial Electronics*, Vol. 61, No. 3, pp. 1179-1192, 2014

- [69] "Roadway powered electric vehicle project track construction and testing program phase 3D", Partners Advanced Transit Highways (PATH), Berkeley, CA, USA. [Online]. Available: <http://www.path.berkeley.edu>.
- [70] C.-J. Chen, T.-H. Chu, C.-L. Lin, and Z.-C. Jou, "A study of loosely coupled coils for wireless power transfer," *IEEE Trans. Circuits and Systems II: Express Briefs*, Vol. 57, No. 7, pp. 536-540, 2010.
- [71] C.-S. Wang, G. A. Covic, and O. H. Stielau, "Power transfer capability and bifurcation phenomena of loosely coupled inductive power transfer systems," *IEEE Trans. Industrial Electronics*, Vol. 51, No. 1, pp. 148-157, 2004.
- [72] M. L. Kissin, G. A. Covic, and J. T. Boys, "Steady-state flat-pickup loading effects in polyphase inductive power transfer systems," *IEEE Trans. Industrial Electronics*, Vol. 58, No. 6, pp. 2274-2282, 2011.
- [73] C.-S. Wang, G. A. Covic, and O. H. Stielau, "Investigating an LCL load resonant inverter for inductive power transfer applications," *IEEE Trans. Power Electronics*, Vol. 19, No. 4, pp. 995-1002, 2004.
- [74] H. H. Wu, G. A. Covic, J. T. Boys, and D. J. Robertson, "A series-tuned inductive-power-transfer pickup with a controllable AC-voltage output," *IEEE Trans. Power Electronics*, Vol. 26, No.1, pp. 98-109, 2011.
- [75] H. H. Wu, J. T. Boys, and G. A. Covic, "An AC processing pickup for IPT systems," *IEEE Trans. Power Electronics*, Vol. 25, No. 5, pp. 1275-1284, 2010.

- [76] J. Huh, S. W. Lee, W. Y. Lee, G. H. Cho, and C. T. Rim, "Narrow-width inductive power transfer system for online electrical vehicles," *IEEE Trans. Power Electronics*, Vol. 26, No. 12, pp. 3666-3679, 2011.
- [77] S. Choi, B. Gu, S. Jeong, and C. T. Rim, "Ultra-slim S-type inductive power transfer system for road powered electric vehicles," *International Electric Vehicle Technology Conference and Automotive Power Electronics in Japan (EVTeC and APE Japan)*, 2014.
- [78] A. Zaheer, D. Kacprzak, and G. A. Covic, "A bipolar receiver pad in a lumped IPT system for electric vehicle charging applications," *IEEE Energy Conversion Congress and Exposition (ECCE)*, pp. 283-290, 2012.
- [79] C. C. Mi, G. Buja, S. Y. Choi, and C. T. Rim, "Modern advances in wireless power transfer systems for roadway powered electric vehicles," *IEEE Trans. Industrial Electronics*, Vol. 63, No. 10, pp. 6533-6545, 2016.
- [80] W. Li, "High efficiency wireless power transmission at low frequency using permanent magnet coupling," Master of Applied Science, University of British Columbia, 2009.
- [81] J. O. Mur-Miranda, S. Cheng, and D. P. Arnold, "Improving the efficiency of electrodynamic wireless power transmission," *2013 7th European Conference on Antennas and Propagation (EuCAP)*, pp. 2848-2852, 2013.
- [82] M. S. Hossain and A. Barua, "Charging electric vehicles via microwave energy transmission and analysis of advanced energy storage system," *2013 International Conference on Informatics, Electronics & Vision (ICIEV)*, pp. 1-6, 2013.

- [83] A. Massa, G. Oliveri, F. Viani, and P. Rocca, "Array designs for long-distance wireless power transmission: State-of-the-art and innovative solutions," *Proceedings of the IEEE*, Vol. 101, No. 6, pp. 1464-1481, 2013.
- [84] J. S. Ho, S. Kim, and A. S. Poon, "Midfield wireless powering for implantable systems," *Proceedings of the IEEE*, Vol. 101, No. 6, pp. 1369-1378, 2013.
- [85] N. Shinohara, Y. Kubo, and H. Tonomura, "Wireless charging for electric vehicle with microwaves," *2013 3rd International Electric Drives Production Conference (EDPC)*, pp. 1-4, 2013.
- [86] N. Shinohara, "Power without wires," *IEEE Microwave Magazine*, Vol. 12, No. 7, pp. S64-S73, 2011.
- [87] N. Shinohara, Y. Kubo, and H. Tonomura, "Mid-distance wireless power transmission for electric truck via microwaves," *Proceedings of 2013 URSI International Symposium on Electromagnetic Theory (EMTS)*, pp. 841-843, 2013.
- [88] Y. Kubo, N. Shinohara, and T. Mitani, "Development of a kW class microwave wireless power supply system to a vehicle roof," *2012 IEEE MTT-S International Microwave Workshop Series on Innovative Wireless Power Transmission: Technologies, Systems, and Applications (IMWS)*, pp. 205-208, 2012.
- [89] W. C. Brown, "Adapting microwave techniques to help solve future energy problems," *IEEE Trans. Microwave Theory and Techniques*, Vol. 21, No. 12, pp. 753-763, 1973.

- [90] N. Shinohara, "Beam efficiency of wireless power transmission via radio waves from short range to long range," *Journal of electromagnetic engineering and science*, Vol. 10, No. 4, pp. 224-230, 2010.
- [91] H. Toromura, Y. Huang, S. Koyama, J. Miyakoshi, and N. Shinohara, "Biological effects of high-power microwave power transfer for electric vehicle," *2016 IEEE Wireless Power Transfer Conference (WPTC)*, pp. 1-3, 2016.
- [92] D. Kishan and P. S. R. Nayak, "Wireless power transfer technologies for electric vehicle battery charging - A state of the art," *2016 International Conference on Signal Processing, Communication, Power and Embedded System (SCOPEs)*, pp. 2069-2073, 2016.
- [93] Q. Liu, J. Wu, P. Xia, S. Zhao, W. Chen, Y. Yang, *et al.*, "Charging unplugged: Will distributed laser charging for mobile wireless power transfer work?" *IEEE Vehicular Technology Magazine*, Vol. 11, No. 4, pp. 36-45, 2016

## Chapter 3

# Comparative Characteristic Analysis of Circular and Double D Power Pads for Electric Vehicle Wireless Charging Systems

Muhammad Sifatul Alam Chowdhury, *Student Member, IEEE*, Xiaodong Liang, *Senior Member, IEEE*

Faculty of Engineering and Applied Science, Memorial University of Newfoundland, St. John's, Newfoundland, Canada.

A version of this chapter has been published in the proceedings of 2019 Canadian Conference of Electrical and Computer Engineering (CCECE). Muhammad Sifatul Alam Chowdhury developed this work under the supervision of Dr. Xiaodong Liang. Sifat's contributions to this paper are listed as follows:

- Performed literature review required for the background information.
- Developed all the codes and performed analysis in ANSYS Maxwell.
- Analyzed the results.
- Wrote the paper.

Dr. Xiaodong Liang provided continuous technical guidance, checked the results, reviewed the manuscript, provided important suggestions to accomplish the work, and modified final version of the manuscript. In this chapter, the manuscript is presented with altered figure numbers, table

numbers and reference formats in order to match the thesis formatting guidelines set out by Memorial University of Newfoundland.

**Abstract-** To provide safe and flexible power transfer to electric vehicles (EVs), wireless charging systems have been introduced. By improving the overall system efficiency of wireless charging systems for EVs, the range anxiety of EVs can be significantly reduced. In this paper, a comparative characteristic analysis is carried out between circular and double D (DD) power pads for EV wireless charging systems. The Society of Automotive Engineers (SAE) recommended practice J2954 is followed for designing physical dimension of these power pads. Finite Element Analysis (FEA) tool ANSYS Maxwell 3D is used for simulation. Parameters such as coupling coefficient and mutual inductance are evaluated for each type of power pads by applying vertical and horizontal misalignment. It is found that DD power pads exhibit promising characteristics for EV wireless charging systems.

**Keywords-** Electric vehicles, Finite Element Analysis (FEA), power pad, wireless charging system.

### 3.1 Introduction

Electric vehicles (EVs) are increasingly emerged in many countries due to their technical and environmental advancement than conventional vehicles [1]-[3]. Most commercially available EVs in the market such as hybrid electric vehicle (HEV) and Plug-in Electric Vehicle (PHEV) are using plug-in charging system to recharge EV's in-house battery. To overcome drawbacks of conventional charging system, wireless charging system for EVs was introduced. Numerous advantages of wireless charging systems for the system design, power transfer efficiency, and system complexity are reported in [4]-[6]. To design advanced wireless charging systems, extensive research was conducted by academia and industry in designing power electronic devices and power pads. Power pads are key components for EV wireless charging systems. Different types of power pads including circular, rectangular, double D (DD) power pads are investigated to obtain the optimum power transfer efficiency [7]-[9]. Circular power pads are commonly used, but DD power pads is believed to transfer power with better misalignment characteristics [10].

In wireless charging systems, power pads are placed on both ground and vehicle sides. The ground side arrangement is known as ground assembly (GA) or transmitting side; while the vehicle side arrangement is known as vehicle assembly (VA) or receiving side. The time-varying magnetic field generated by high-frequency AC currents in the transmitting power pad is linked to the power pad installed in the vehicle.

It is required that power pads should exhibit a high value of coupling coefficient ( $k$ ) (the  $k$  values range between 0 and 1) and the capability to transfer power in different misaligned positions [10]. Depending on the charging system configuration and the misalignment distance between the

power pads, the  $k$  value varies. For a typical 85 kHz system, the  $k$  value may range between 0.1 to 0.4, and a lower  $k$  value due to large misalignment distances can be improved by using ferrite bars. A general classification of power pads considered for EV's wireless charging systems is presented in Figure 3.1.

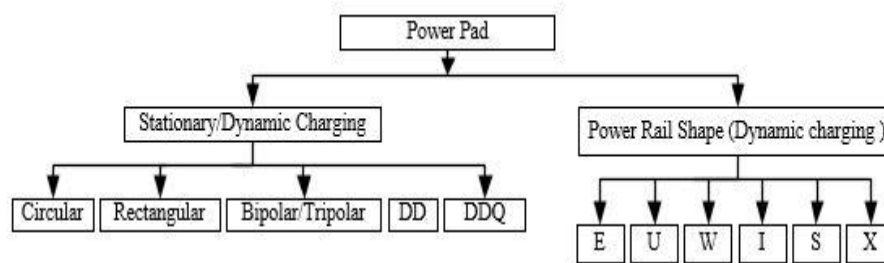


Figure 3.1: General classification of power pads.

Circular power pads are widely used for EV wireless charging system design due to its reduced leakage flux and compact design [11], but their performance fluctuates with the increment of air-gap. DD power pads combine the advantage of both circular power pad and flux pipe topology, and thus, result in a higher value of coupling coefficient than circular power pads [12][13]. Bipolar/tripolar power pads are prepared by combining two or three coils together, which exhibit better performance in misaligned positions [13][14]. However, the complex system architecture makes these power pads unattractive. Double D quadrature (DDQ) power pads are prepared by adding a quadrature coil with DD power pads, resulting in the excellent misalignment tolerance. However, the size of DDQ power pad is still an issue as combining two different topologies increase the overall dimension of the power pad. Power rails are generally used for roadway powered vehicle, and these power pads are only energized when an EV is passing over it. However,

the complex system configuration and maintenance cost is still an unsolved issue for them when used in dynamic wireless charging systems.

SAE J2954 provides guidelines mainly focusing on the circular power pad topology, but DD power pads are also mentioned as a potential technology. Therefore, in this paper a comparative characteristic analysis is carried out between circular and DD power pads. Both types of power pads are designed based on the system specification recommended in the Society of Automotive Engineers (SAE) recommended practice J2954 [15].

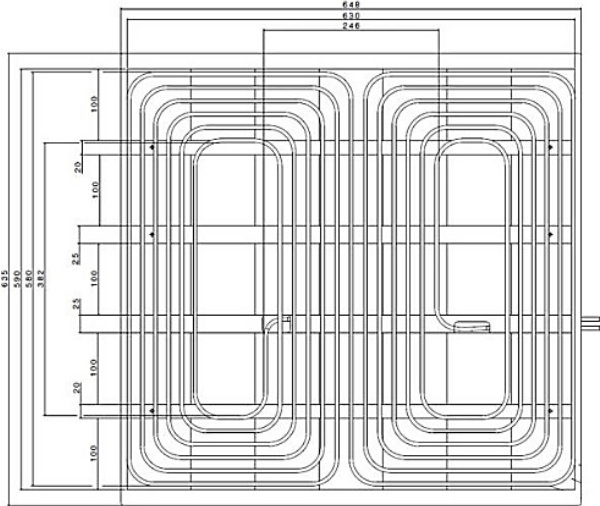
The paper is arranged as follows: A brief discussion on different types of power pads is provided in introduction. A performance evaluation procedure is proposed in Section 3.2. Sections 3.3 represents modeling and simulation results of DD and circular power pads. A conclusion is drawn based on the simulation result in Section 3.4.

### **3.2 Performance Evaluation Procedure**

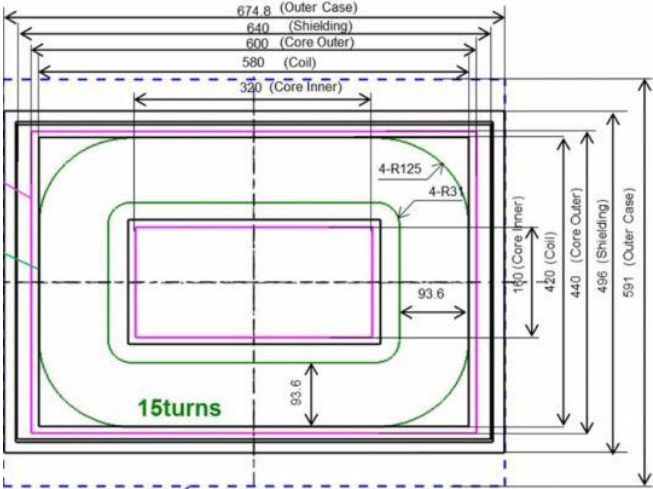
In this section, circular and DD power pads are designed using Finite Element Analysis (FEA) simulation software, ANSYS Maxwell 3D, based on physical dimensions recommended in SAE J2954. Figure 3.2 shows the recommended dimensions for these power pads in SAE J2954. Figure 3.3 shows the final power pad models in ANSYS Maxwell 3D.

To evaluate the performance of power pads, an evaluation procedure is proposed in Figure 3.4. Firstly, the power pad geometry is selected and designed through ANSYS Maxwell 3D. Secondly, the characteristic analysis of a type of power pads is done without applying any misalignment between the transmitting and receiving sides. Thirdly, apply both vertical and horizontal displacements. The simulation results are then validated by comparing the design criteria that are

commonly used in the literature. The coupling coefficient  $k$  varies between 0 and 1, a higher value indicates good coupling and transfer efficiency of the wireless charging system [16].

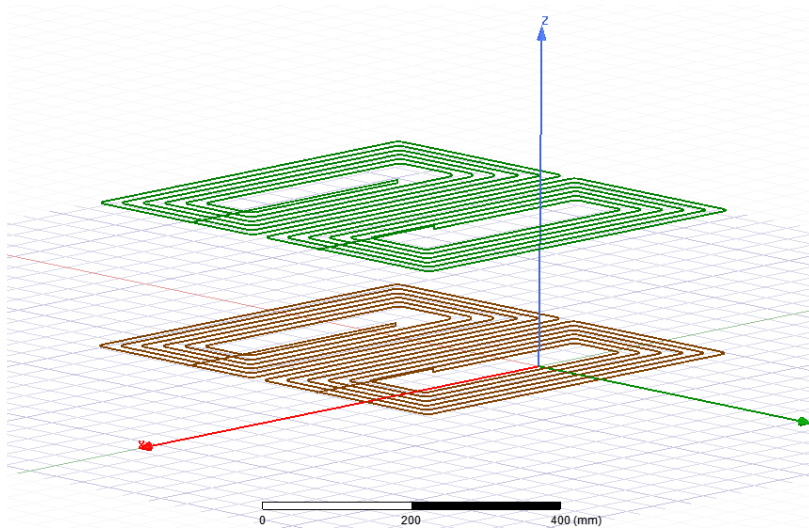


(a)

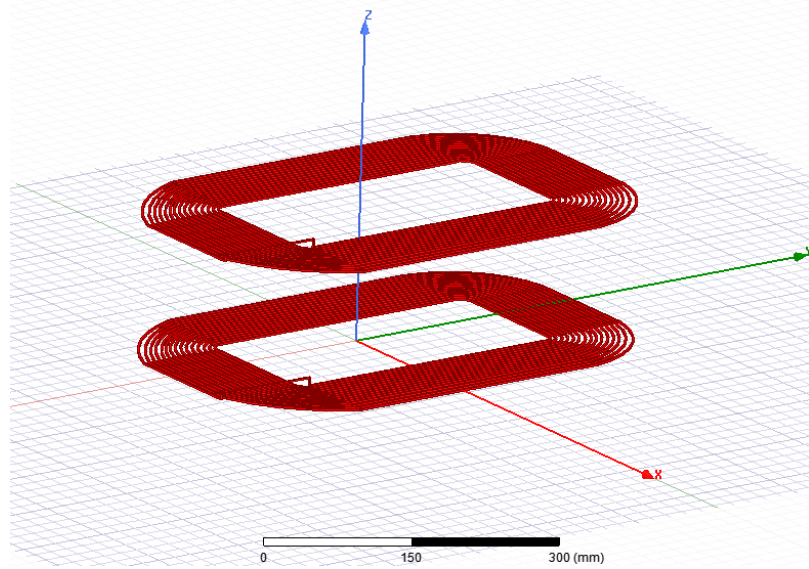


(b)

Figure 3.2: Physical dimensions recommended in SAE J2954 for power pads: (a) DD, (b) Circular [11].



(a)



(b)

Figure 3.3: Power pad models designed by ANSYS Maxwell 3D using specifications in SAE

J2954: (a) DD, (b) Circular.

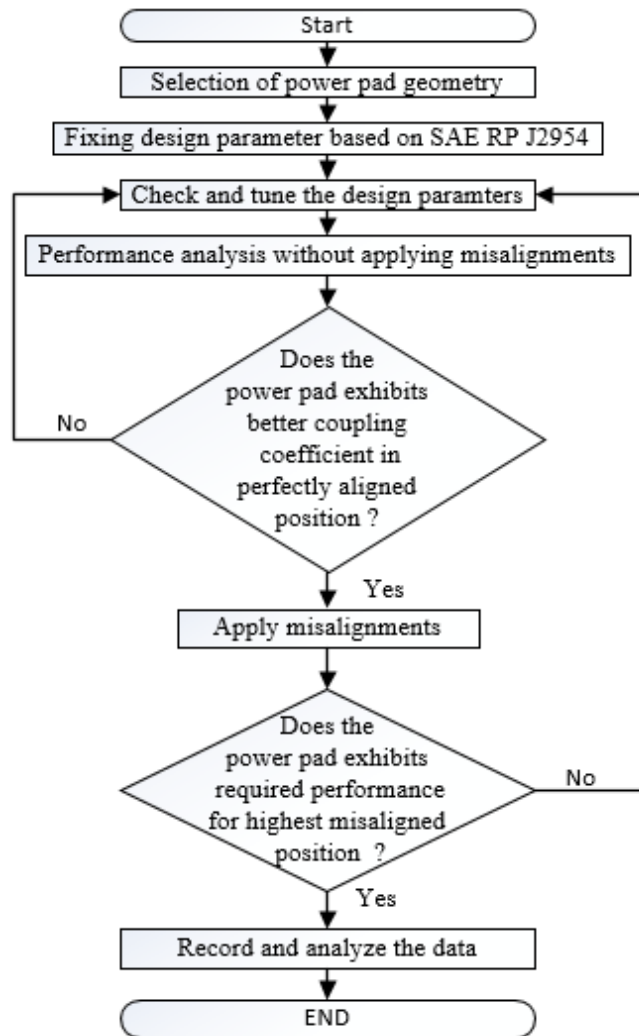


Figure 3.4: Flow chart of performance evaluation procedure for power pads.

### 3.3 Modeling and Simulation of power Pads

In this section, the simulation is conducted for both DD and circular power pads using models built in Figure 3.3. Figure 3.5 represents the variation of coupling coefficient for both types of power pads with the vertical displacement ranging from 15 mm to 150 mm between GA and VA. The value of the coupling coefficient indicates the condition of flux linkage between transmitting and receiving power pads. A greater value of coupling coefficient indicates stronger coupling

between transmitting and receiving sides of power pads, which is very crucial for EV wireless charging systems.

For DD power pads, when the vertical displacement distance is 15 mm, the coupling coefficient is the highest, equal to 0.5760. The coupling coefficient gradually decreases with the increase of vertical displacement. At the vertical displacement equal to 150 mm, the coupling coefficient is dropped to 0.1189. For circular power pads, the coupling coefficient at the smallest vertical displacement of 15 mm is 0.4870. Similar to DD power pads, the values decrease with the increment of the air-gap between transmitting and receiving power pads. For the displacement of 50 mm, 100 mm, and 150, the coupling coefficient is 0.1875, 0.0628 and 0.000037, respectively.

It is found that DD power pads show higher coupling coefficient than circular power pads, the difference is much pronounced for larger vertical displacements. Especially at 150 mm, the coupling coefficient of circular power pads becomes zero, but the coupling coefficient of DD power pads is 0.1189, i.e., the coupling remains strong for DD power pads.

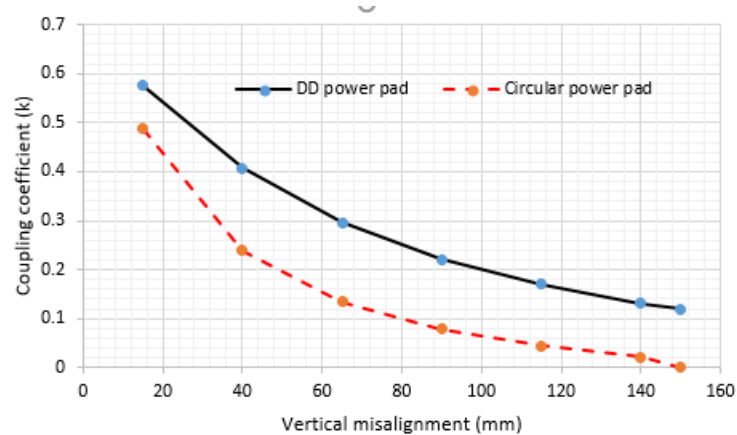


Figure 3.5: Variation of coupling coefficient vs vertical misalignment between VA and GA for DD and circular power pads.

Similarly, Figure 3.6 represents the variation of mutual inductance for DD and circular power pads with the vertical misalignment ranging from 15 mm to 150 mm between the transmitting and receiving sides. Mutual inductance indicates the strength of common magnetic flux between two magnetically connected power pads. For DD power pads, the mutual inductance is 22.50  $\mu\text{H}$  when the vertical misalignment is 15 mm, and is reduced to 4.87  $\mu\text{H}$  when the vertical misalignment is increased to 150 mm. For circular power pads, the mutual inductance values for 15 mm, 50 mm, 100 mm and 150 mm are 16.0156  $\mu\text{H}$ , 8.1523  $\mu\text{H}$ , 2.7331  $\mu\text{H}$ , and 0.000005  $\mu\text{H}$ , respectively.

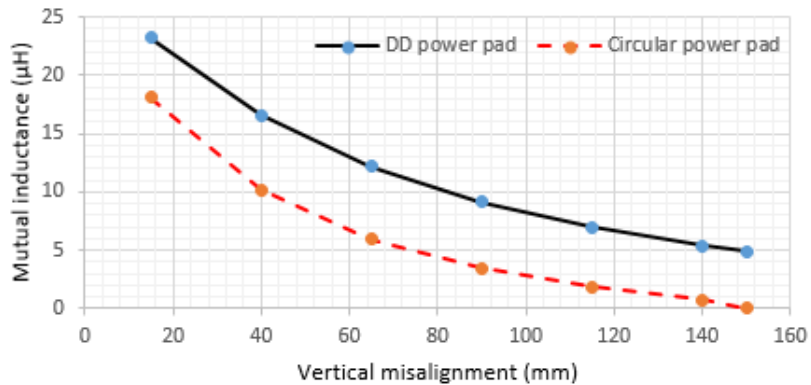


Figure 3.6: Variation of mutual inductance vs vertical misalignment between VA and GA for DD and circular power pads.

Figure 3.7 represents coupling coefficients of DD power pads when both vertical and horizontal misalignment are applied. The green line indicates the change of coupling coefficient with respect to different vertical misalignment when the horizontal misalignment is kept constant at 15 mm. Similarly, the horizontal misalignment distances of 45 mm, 75 mm, 100 mm are applied, and the coupling coefficient with respect to different vertical misalignment at these cases are shown in the same figure. When the horizontal misalignment is 15 mm, the maximum value of coupling

coefficient is 0.5645. The maximum coupling coefficient value for 45 mm, 75 mm, 100 mm are 0.4953, 0.3837, and 0.2728, respectively. Therefore, the effect of horizontal misalignment is quite significant.

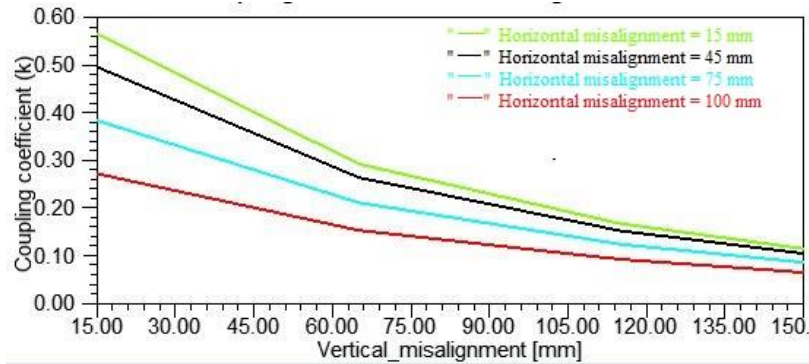
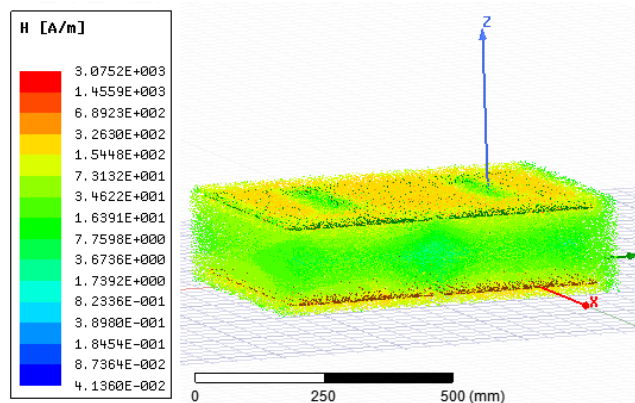
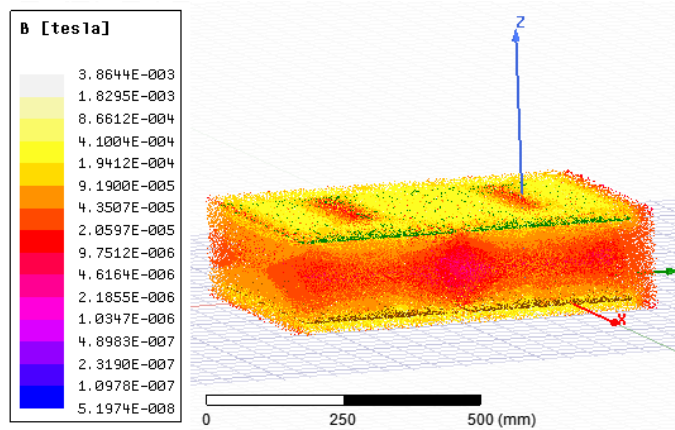


Figure 3.7: Variation of coupling coefficient when both vertical and horizontal misalignment are applied to DD power pads.

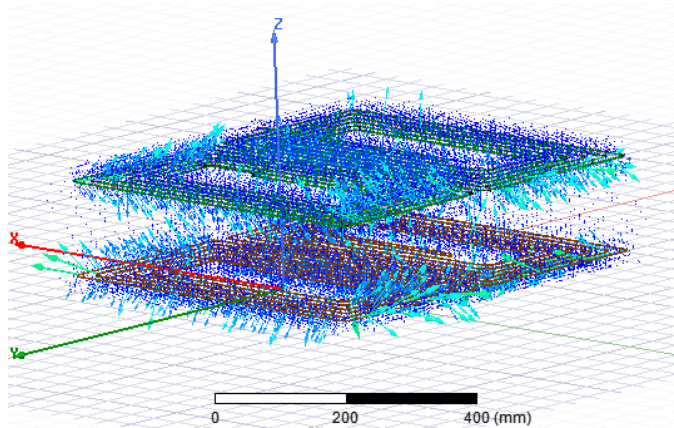
Figure 3.8 represents 3D plots of the magnetic field intensity (H), the magnetic flux density (B), and the magnetic flux for DD power pads at the vertical misalignment of 150 mm. The magnetic field intensity and magnetic flux density decrease with the increase in vertical misalignment, and they are minimum when the vertical distance is the maximum (150 mm).



(a)



(b)



(c)

Figure 3.8: Parameters variations (3D plots) for DD power pads at the vertical misalignment of 150 mm: (a) magnetic field intensity (H), (b) magnetic flux density (B), (c) magnetic flux lines.

Figure 3.9 represents coupling coefficients of circular power pads when both vertical and horizontal misalignment are applied. The green line indicates the change of coupling coefficient with respect to different vertical misalignment when the horizontal misalignment is kept constant

at 15 mm. Similarly, the horizontal misalignment distances of 45 mm, 75 mm, 100 mm are applied and the coupling coefficient with respect to different vertical misalignment for these cases are shown in the same figure.

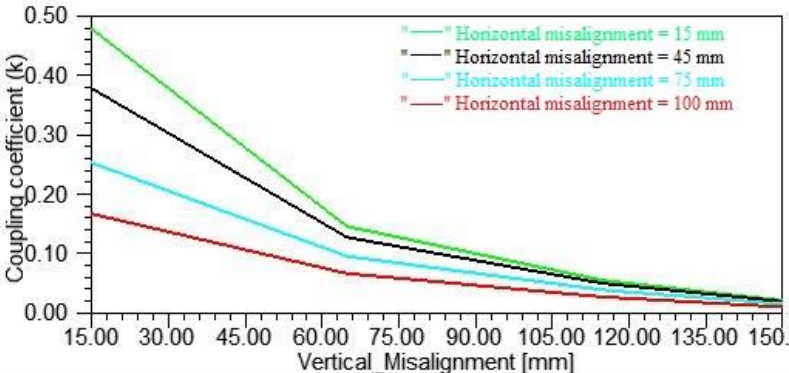
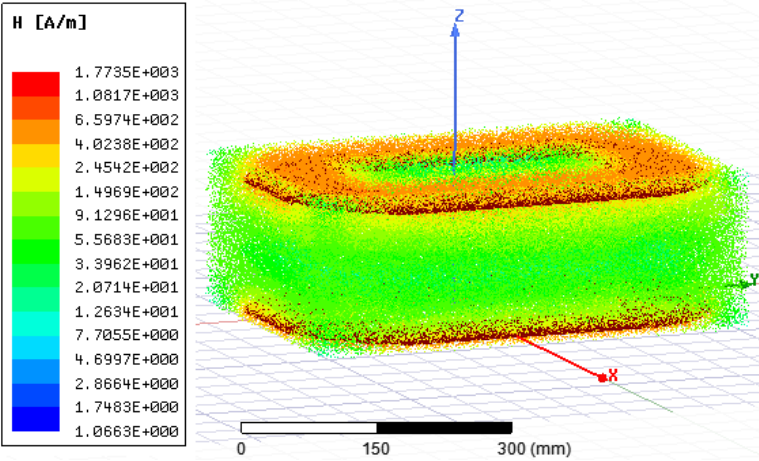
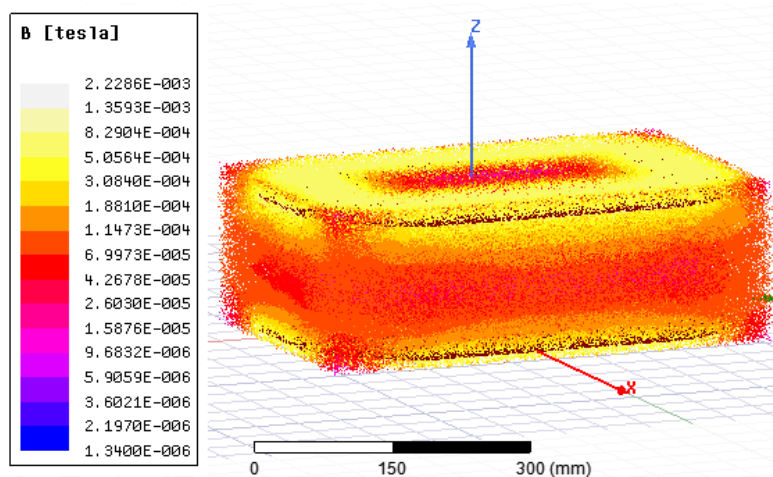


Figure 3.9: Variation of coupling coefficient when both vertical and horizontal misalignment are applied to circular power pads.

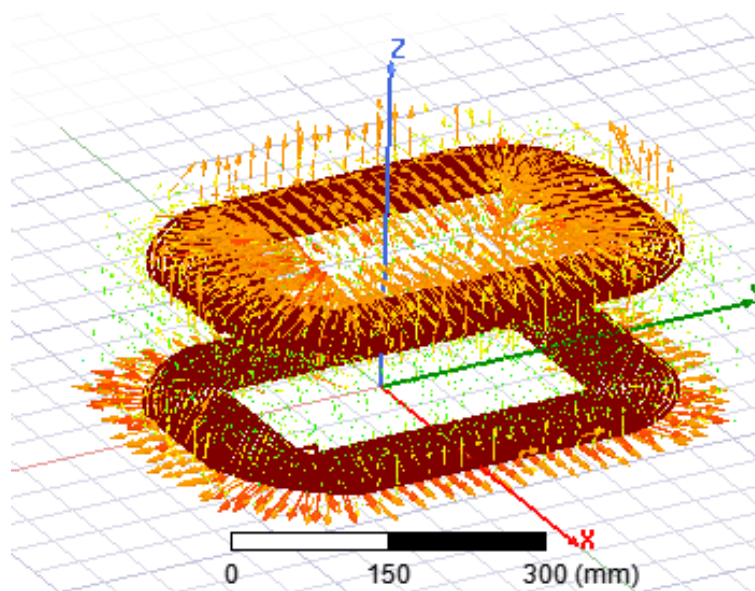
Figure 3.10 represents 3D plots of the magnetic field intensity (H), the magnetic flux density (B), and the magnetic flux, for circular power pads at the vertical misalignment of 150 mm.



(a)



(b)



(c)

Figure 3.10: Parameters variations (3D plots) for circular power pads at the vertical misalignment of 150 mm: (a) magnetic field intensity (H), (b) magnetic flux density (B), (c) magnetic flux lines.

In this paper, the simulation is carried out without considering the shielding effect and ferrite bars. Based on the values of coupling coefficient and mutual inductance, DD power pads exhibit better misalignment tolerance compared to circular power pads.

### **3.4. Conclusions**

In this paper, a comparative analysis is carried out between DD and circular power pads for EV's wireless power transfer systems. The physical models for both types of power pads are built using ANSYS Maxwell 3D based on the recommended physical dimensions in SAE J2954. For each type of power pads, the vertical misalignment between transmitting and receiving sides varies between 15 mm to 150 mm. Four horizontal misalignment at 15 mm, 45 mm, 75 mm and 100 mm are also applied. Parameters such as the coupling coefficient, mutual inductance, magnetic field intensity, magnetic flux density are investigated for both types of power pads. Simulation result indicates that DD power pads exhibit high potential for their use in EV wireless charging systems.

## References

- [1] G. d. F. Lima and R. B. Godoy, "Modeling and prototype of a dynamic wireless charging system using LSPS compensation topology," *IEEE Trans. Ind. Appl.*, vol. 55, no.1, January/February 2019.
- [2] S. Jeong, Y. J. Jang, and D. Kum, "Economic analysis of the dynamic charging electric vehicle," *IEEE Trans. Power Electron*, vol. 30, no. 11, pp. 6368-6377, November 2015
- [3] R. Xiong, J. Cao, Q. Yu, H. He, and F. Sun, "Critical review on the battery state of charge estimation methods for electric vehicles," *IEEE Access*, vol. 6, pp. 1832-1843, 2018.
- [4] D. Vilathgamuwa and J. Sampath, "Wireless power transfer (WPT) for electric vehicles (EVS) - Present and future trends," in *Plug in electric vehicles in smart grids*, ed: Springer, pp. 33-60, 2015.
- [5] S. Chopra and P. Bauer, "Driving range extension of EV with on-road contactless power transfer-a case study," *IEEE Trans. Ind. Electron.*, vol. 60, no. 1, pp. 329-338, January 2013.
- [6] W. Zhong and S. Hui, "Maximum energy efficiency tracking for wireless power transfer systems," *IEEE Trans. Power Electron*, vol. 30, pp. 4025-4034, 2015.
- [7] A. Tejada, C. Carretero, J. T. Boys, and G. A. Covic, "Ferrite-less circular pad with controlled flux cancelation for EV wireless charging," *IEEE Trans. Power Electron*, vol. 32, no. 11, pp. 8349-8359, November 2017.
- [8] M. G. S. Pearce, G. A. Covic, and J. T. Boys, "Robust ferrite-less double D topology for roadway IPT applications," *IEEE Trans. Power Electron* (early access), DOI: 10.1109/TPEL.2018.2883129, 2018.

- [9] U. Pratik, B. J. Varghese, A. Azad, and Z. Pantic, "Optimum design of decoupled concentric coils for operation in double-receiver wireless power transfer systems," *IEEE Journal of Emerging and Selected Topics in Power Electronics* (early access), DOI: 10.1109/JESTPE.2018.2871150, 2018.
- [10] D. Patil, M. K. McDonough, J. M. Miller, B. Fahimi, and P. T. Balsara, "Wireless Power Transfer for Vehicular Applications: Overview and Challenges," *IEEE Transactions on Transportation Electrification*, vol. 4, no.1, pp. 3-37, March 2018.
- [11] M. Budhia, G. A. Covic, and J. T. Boys, "Design and optimization of circular magnetic structures for lumped inductive power transfer systems," *IEEE Trans. Power Electron*, vol. 26, no. 11, pp. 3096-3108, November 2011.
- [12] M. Budhia, J. T. Boys, G. A. Covic, and C.-Y. Huang, "Development of a single-sided flux magnetic coupler for electric vehicle IPT charging systems," *IEEE Trans. Ind. Electron.*, vol. 60, no. 1, pp. 318-328, January 2013.
- [13] A. Zaheer, G. A. Covic, and D. Kacprzak, "A bipolar pad in a 10-kHz 300-W distributed IPT system for AGV applications," *IEEE Trans. Ind. Electron.*, vol. 61, no. 7, pp. 3288-3301, July 2014.
- [14] S. Kim, G. A. Covic, and J. T. Boys, "Tripolar pad for inductive power transfer systems for EV charging," *IEEE Trans. Power Electron*, vol. 32, no. 7, pp. 5045-5057, July 2017.
- [15] SAE Recommended Practice J2954, "Wireless power transfer for light-duty plug-in/electric vehicles and alignment methodology," November 2017.
- [16] General discussion on coupling coefficient and mutual inductance can be accessed at: <https://www.electronics-tutorials.ws/inductor/mutual-inductance.html> [January 10, 2018].

## Chapter 4

### **Design of a Ferrite-Less Power Pad for Wireless Charging Systems of Electric Vehicles**

Muhammad Sifatul Alam Chowdhury, *Student Member, IEEE*, Xiaodong Liang, *Senior Member, IEEE*

Faculty of Engineering and Applied Science, Memorial University of Newfoundland, St. John's, Newfoundland, Canada.

A version of this chapter has been published in the proceedings of 2019 Canadian Conference of Electrical and Computer Engineering (CCECE). Muhammad Sifatul Alam Chowdhury developed this work under the supervision of Dr. Xiaodong Liang. Sifat's contributions to this paper are listed as follows:

- Performed review literature review required for the background information.
- Developed all the codes and performed analysis in ANSYS Maxwell.
- Analyzed the results.
- Wrote the paper.

Dr. Xiaodong Liang provided continuous technical guidance, checked the results, reviewed the manuscript, provided important suggestions to accomplish the work, and modified final version of the manuscript. In this chapter, the manuscript is presented with altered figure numbers, table

numbers and reference formats in order to match the thesis formatting guidelines set out by Memorial University of Newfoundland.

**Abstract-** Inductive power transfer (IPT) systems unleashed a new era for wireless charging systems of electric vehicles (EVs). EVs can be charged stationary or in motion through IPT systems. Different types of power pads are introduced to increase the efficiency of IPT systems, among them, the most commonly used power pads is circular structure, another type with good potential is double D (DD) structure as recommended in Society of Automotive Engineers (SAE) recommended practice J2954. In this paper, a new power pad structure is proposed by combining circular and DD power pads to further improve the performance. Physical models of circular and DD power pads are first built by using specifications in SAE J2954, these models are then combined to form the proposed power pad. The design and simulation of the proposed power pad are carried out using the Finite Element Analysis (FEA) simulation software, ANSYS Maxwell 3D. Simulation results indicate that the proposed power pad shows improved performance compared to circular and DD power pads.

**Keywords-** Wireless charging system, power pad, electric vehicles, Finite Element Analysis (FEA).

## 4.1 Introduction

Electric vehicles (EVs) have opened a new era in the field of electrified transportation. EVs are 30% more efficient than conventional vehicles [1]. To increase the driving range of EVs, various energy harvesting technologies are introduced in research. Different variations of EVs are introduced to mitigate the range limitation. At present, plug-in charging system is widely used for charging electric vehicles [2][3]. Wireless charging systems of EVs exhibits numerous advantages, and requirements of such systems are discussed in SAE J2954 [4]. Power pads play a key role in transferring power to an EV. Different electromagnetic characteristics of power pads, such as coupling coefficient, self- and mutual- inductance under different misaligned positions, highly affect the overall efficiency of the entire charging system [5][6].

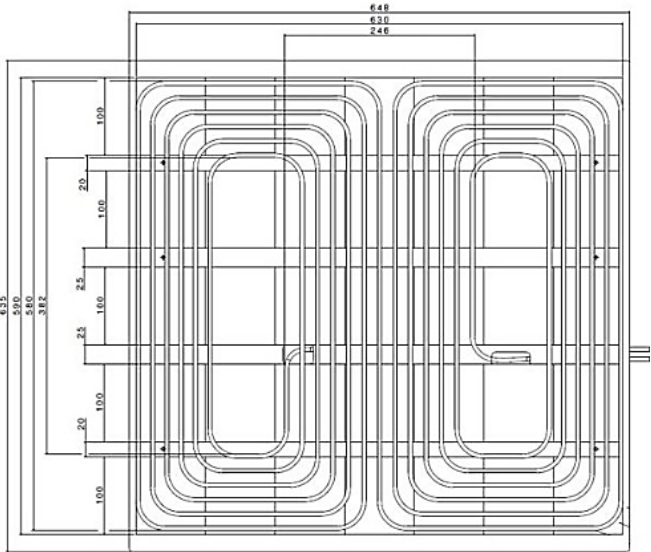
EVs can be charged either stationary or in motion through wireless charging systems. Various wireless charging topologies are discussed in [7][8]. An EV wireless charging system consists of two parts: ground assembly (GA) and vehicle assembly (VA). Power electronic devices and power pads are required in each part [4]. Power pads used for EV wireless charging include circular, double D (DD), double D quadrature (DDQ) power pads [9]-[11]. Circular power pads are most widely used, but DD and DDQ power pads exhibit better coupling in misaligned positions. In case of DDQ power pads, a quadrature pad is added to the existing DD power pad, which creates a three times larger power zone compared to a circular power pad and results in better performance at different misaligned positions [9]. In this paper, inspired by DDQ power pads, a new power pad structure by combining circular and DD power pads is proposed to obtain improved performance. Depending on the configuration, the cost of stationary wireless charging systems ranges between

USD 40,000 and USD 60,000, whereas the cost of dynamic charging systems ranges between USD 50,000 and USD 60,000 [12].

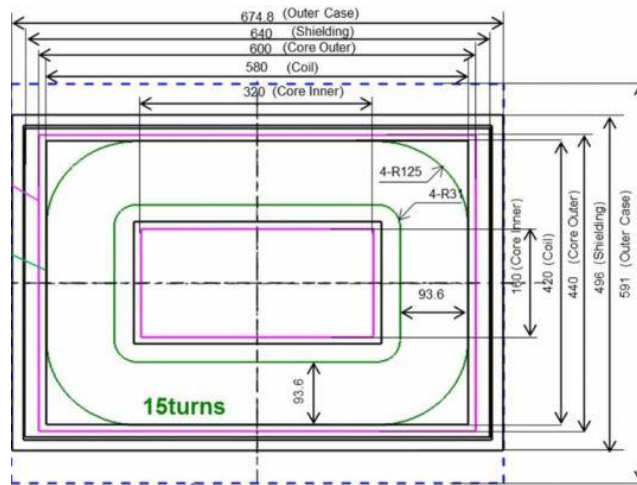
The paper is organized as follows: Section 4.2 discusses the design of the proposed power pad; Section 4.3 shows simulation results for different misaligned positions of the proposed power pad; A comparison is made among the proposed power pad, circular and DD power pads through the parameters of coupling coefficient and mutual-inductance in Section 4.4; Conclusions are drawn in Section 4.5.

### 4.2 Design of the Proposed Power Pad

Although much research on various design of power pads has been reported in literature, only circular and DD power pads with physical dimensions are provided in SAE recommended practice J2954 as shown in Figure 4.1.



(a)



(b)

Figure 4.1: Physical dimensions recommended in SAE J2954 for power pads: (a) DD, (b) Circular [4].

In this paper, SAE J2954's recommended physical dimensions for circular and DD power pads is followed to design the proposed power pad. Firstly, both circular and DD power pads are designed separately using SAE J2954's physical dimensions. The two power pads are then combined using finite element analysis tool, ANSYS Maxwell 3D, to create the proposed power pad at the power level up to 3.7 kW. The dimensions of the proposed power pad are kept the same on both GA and VA. Figure 4.2 shows the final design of the proposed power pad. The circular coil is in purple, and the DD coil is in green. In physical construction of the power pad, the circular coil is placed above the DD coil with a distance of 1 mm in this design, there should be an insulation between the two coils. The two coils are connected in parallel electrically, sharing the same pair of power leads.

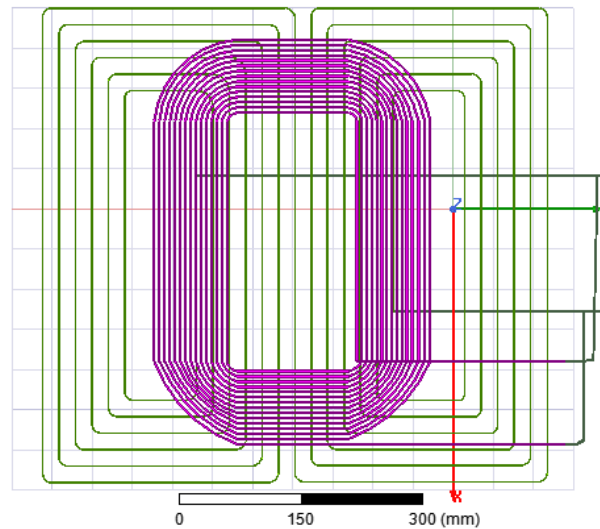


Figure 4.2: The proposed power pad designed using ANSYS Maxwell 3D.

For WPT1/Z1 class wireless charging systems (The Z classification is based on the expected maximum VA coil ground clearance [4]) defined in SAE J2954, the vertical distance between the two power pads on GA and VA can be in the range from 15 mm to 150 mm. To evaluate the performance of the proposed power pad, both vertical and horizontal misalignments can be applied. The procedure for a comprehensive evaluation for the designed power pad is shown in Figure 4.3. Figure 4.4 represents different stages of the power pad design using the software.

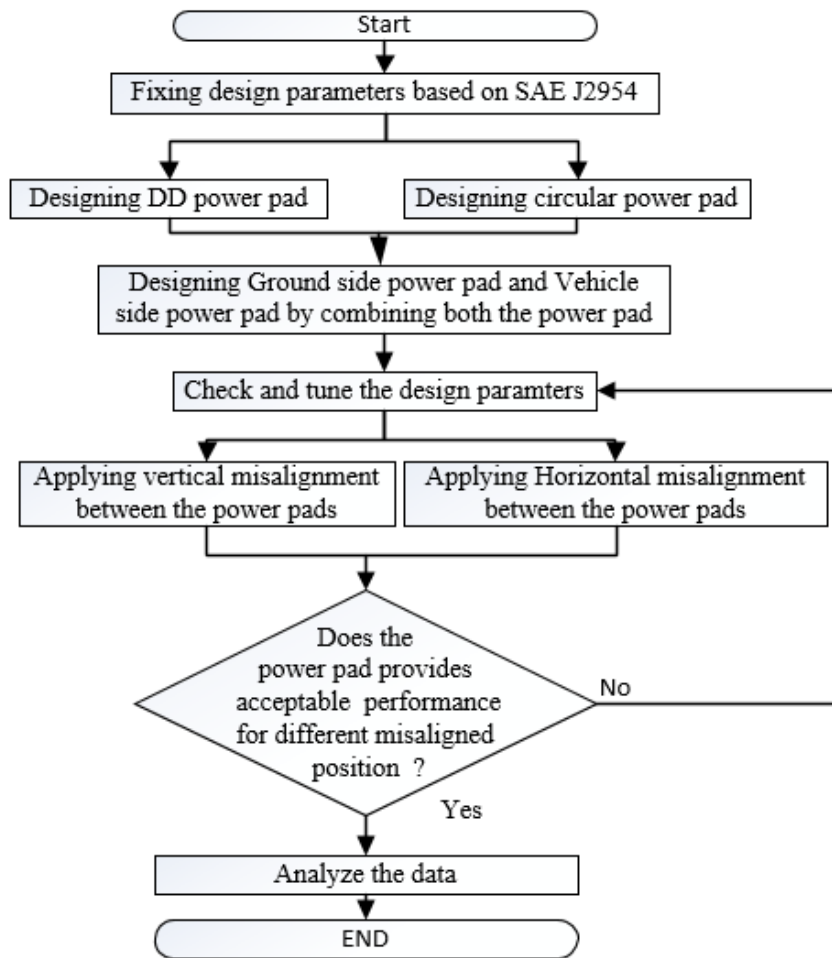
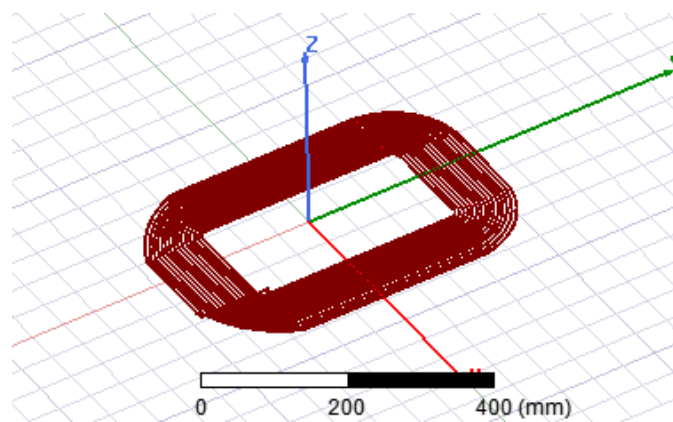
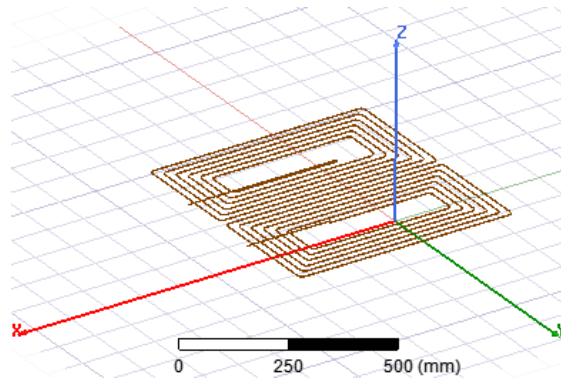


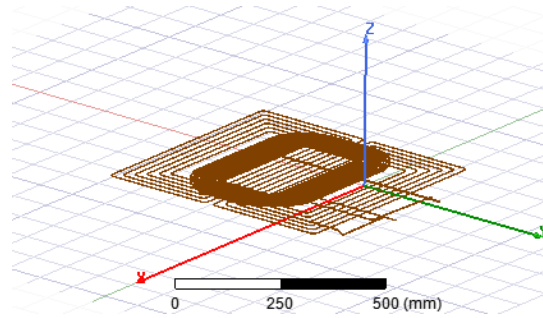
Figure 4.3: A comprehensive evaluation procedure for a power pad design.



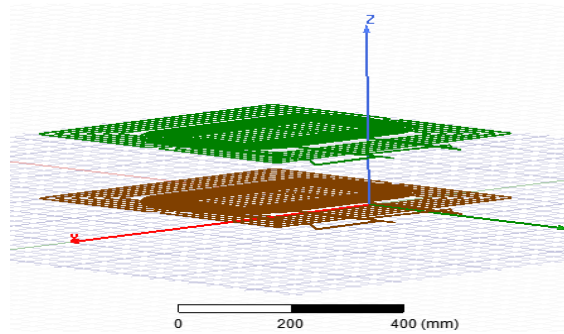
(a)



(b)



(c)



(d)

Figure 4.4: Different stages of the proposed power pad design using software: (a) create a circular power pad model; (b) create a DD power pad model; (c) create a proposed power pad model; (d) create both transmitting and receiving ends of power pads.

### 4.3 Simulation Results

Electromagnetic characteristics of the proposed power pad are the best when both vertical and horizontal misalignments are minimum. Eq. (1) is used in ANSYS Maxwell 3D to solve the magnetostatics problem for power pads [13].

$$J_z(x,y) = \nabla \times ( 1/(\mu_0\mu_r) (\nabla \times A_z(x,y))) \quad (1)$$

Where,  $\mu_0$  is the permeability in vacuum,  $\mu_r$  is the relative permeability,  $J_z(x,y)$  is the DC current density at z-axis,  $A_z(x,y)$  is the z-axis magnetic vector potential. The magnetic flux density (B) and the magnetic field intensity (H) can be calculated as follows:

$$B = \nabla \times A \quad (2)$$

$$H = B / (\mu_0\mu_r) \quad (3)$$

#### 4.3.1 Vertical Misalignment

For the proposed power pad, the minimum and maximum vertical misalignment between GA and VA are 15 mm and 150 mm, respectively. For the minimum vertical misalignment of 15 mm, the coupling coefficient k is equal to 0.7126. Figure 4.5 shows the coupling coefficient k vs. vertical misalignment. It is found that k decreases with the increment of vertical misalignment. k is equal to 0.1049 at 150 mm vertical misalignment.

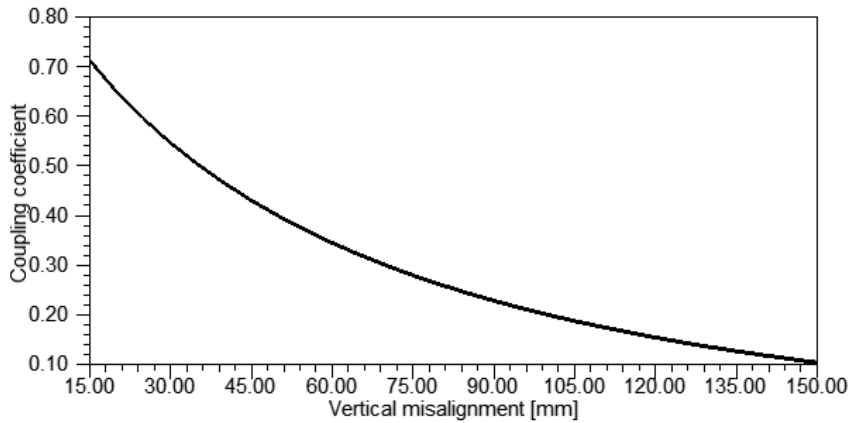


Figure 4.5: Coupling coefficient  $k$  vs. vertical misalignment between power pads.

The mutual inductance of the power pads between GA and VA follows the same pattern as the coupling coefficient as shown in Figure 4.6. The mutual inductance decreases with the increment of vertical misalignment between the power pads. At 15 mm vertical misalignment, the mutual inductance is the maximum, equal to  $36.4139 \mu\text{H}$ ; whereas at 150 mm vertical misalignment, the mutual inductance is the minimum, equal to  $5.6389 \mu\text{H}$ .

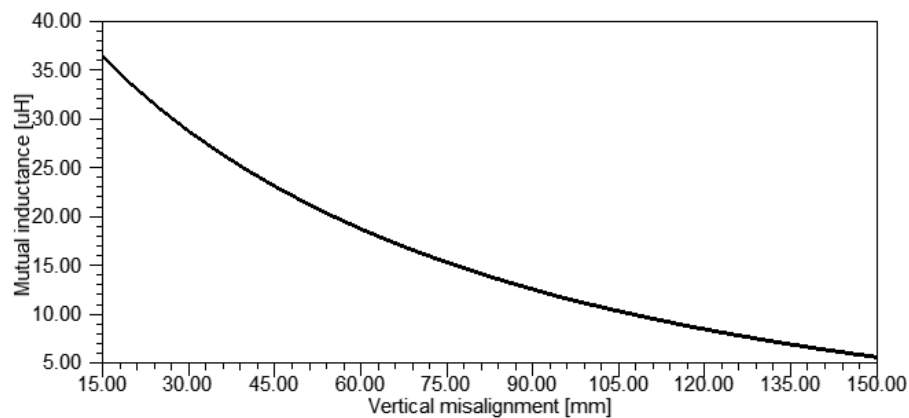
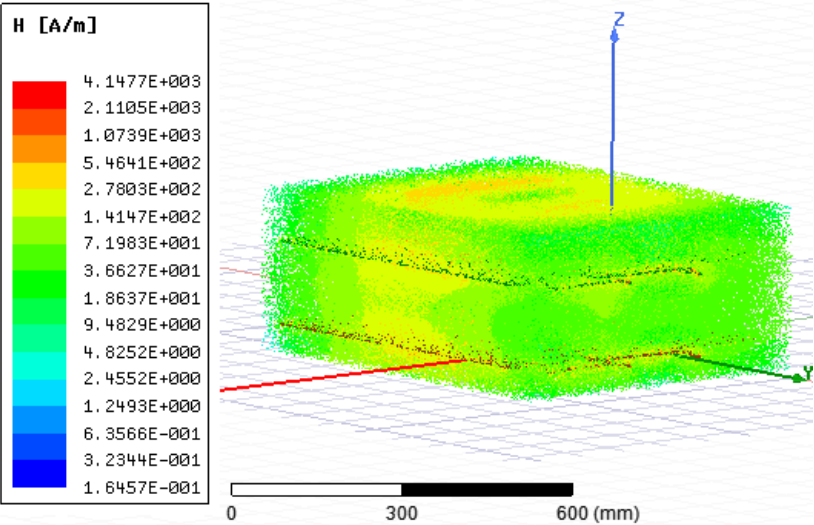


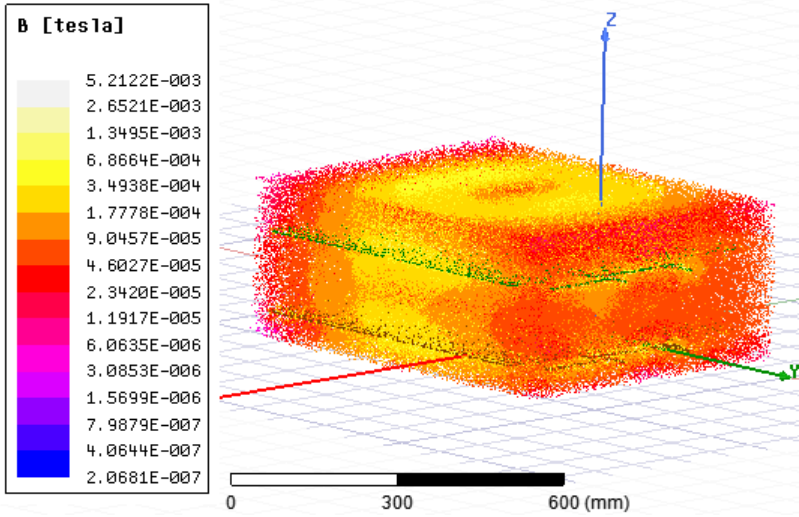
Figure 4.6: Mutual inductance vs. vertical misalignment between power pads.

The magnetic field intensity  $H$ , magnetic flux density  $B$ , and magnetic flux lines of the power pads for the case with 150 mm vertical misalignment are shown in Figure 4.7. Note, all simulation

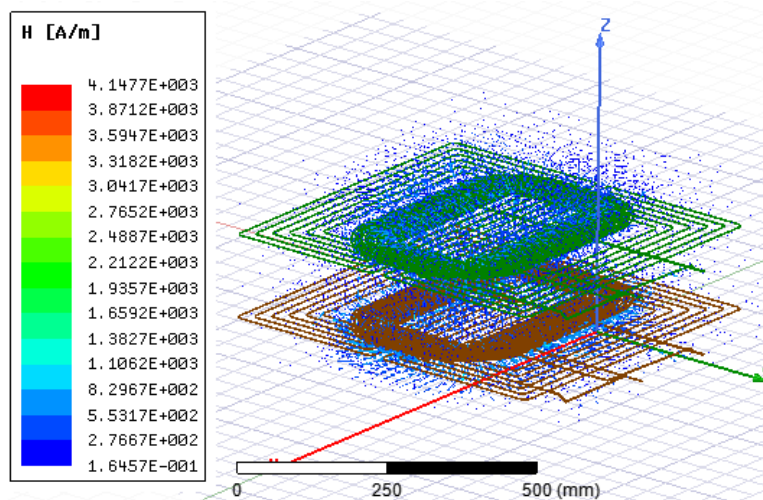
conducted in Figure 4.5-4.7 considered only vertical misalignment, i.e., the horizontal misalignment between the power pads is zero.



(a)



(b)



(c)

Figure 4.7: Simulation results at 150 mm vertical misalignment: (a) magnetic field intensity  $H$ ; (b) magnetic flux density  $B$ ; (c) magnetic flux lines.

### 4.3.2 Vertical and Horizontal Misalignment

Figure 4.8 represents the coupling coefficient vs. vertical misalignment for different horizontal misalignment values. For example, when both horizontal and vertical misalignments between GA and VA are 15 mm, the coupling coefficient is maximum, equal to 0.7034. For the same 15 mm horizontal misalignment, the coupling coefficient is only 0.108 at 150 mm vertical misalignment. If the horizontal displacement increases, the coupling coefficient will decrease. Compared to the 15 mm horizontal misalignment, if 50 mm horizontal misalignment is chosen instead, the coupling coefficient is 0.6203 and 0.104 for 15 mm and 150 mm vertical misalignment, respectively. A minimum coupling coefficient is 0.0726 when both vertical and horizontal misalignments are 150 mm. The mutual inductance of power pads between GA and VA follows the similar pattern as shown in Figure 4.9, although the shape is slightly different. When the power pads are 15 mm

horizontally misaligned, the mutual inductance values for the vertical misalignment of 15 mm, 50 mm, 85 mm, 120 mm and 150 mm are 36.2307  $\mu\text{H}$ , 21.7870  $\mu\text{H}$ , 13.7605  $\mu\text{H}$ , 8.020  $\mu\text{H}$  and 5.898  $\mu\text{H}$ , respectively. The magnetic field intensity  $H$ , magnetic flux density  $B$ , and magnetic flux lines of the power pads are shown in Figure 4.10 for the case when both horizontal and vertical misalignments are 150 mm.

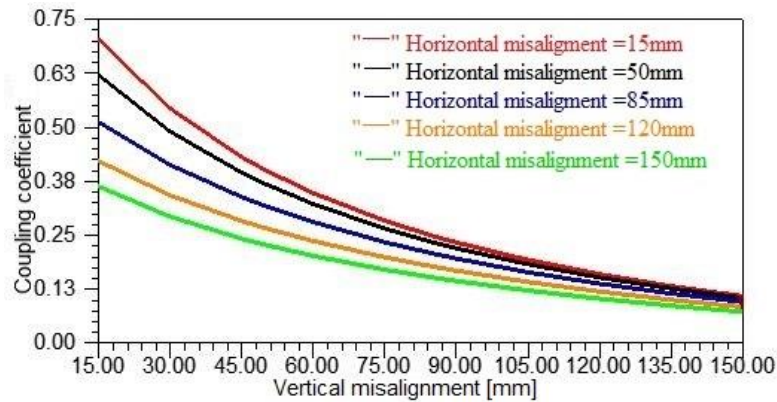


Figure 4.8: Coupling coefficient vs. vertical misalignments for different horizontal misalignments.

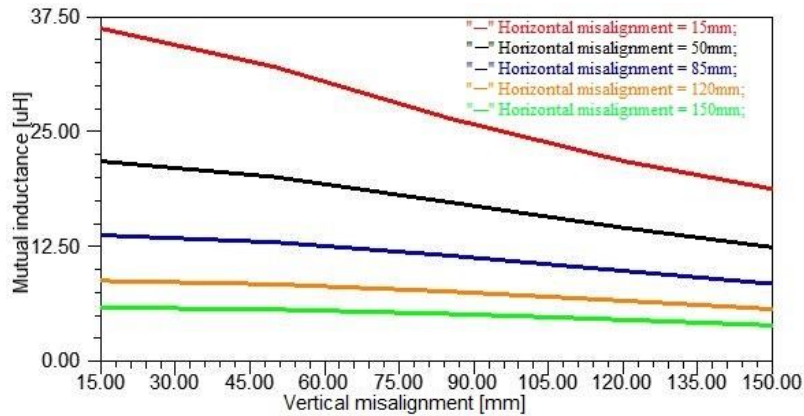
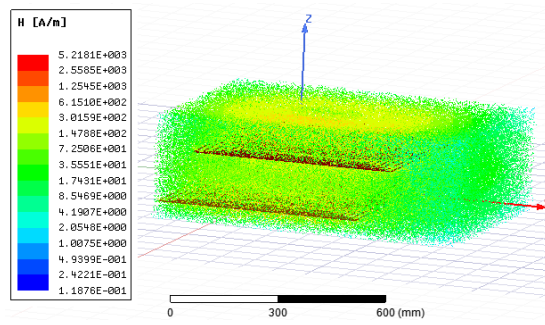
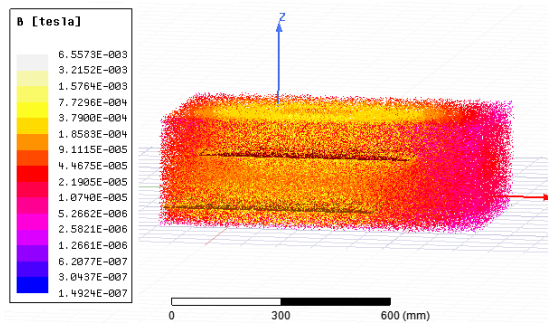


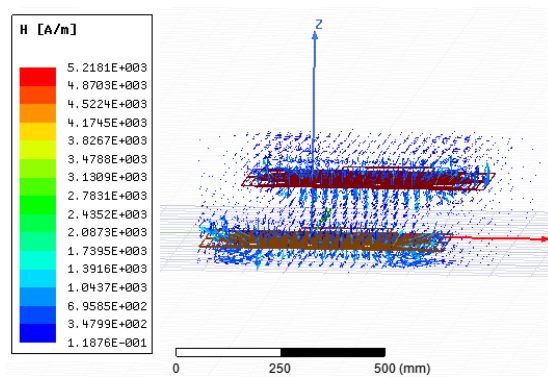
Figure 4.9: Mutual inductance vs. vertical misalignments for different horizontal misalignments.



(a)



(b)



(c)

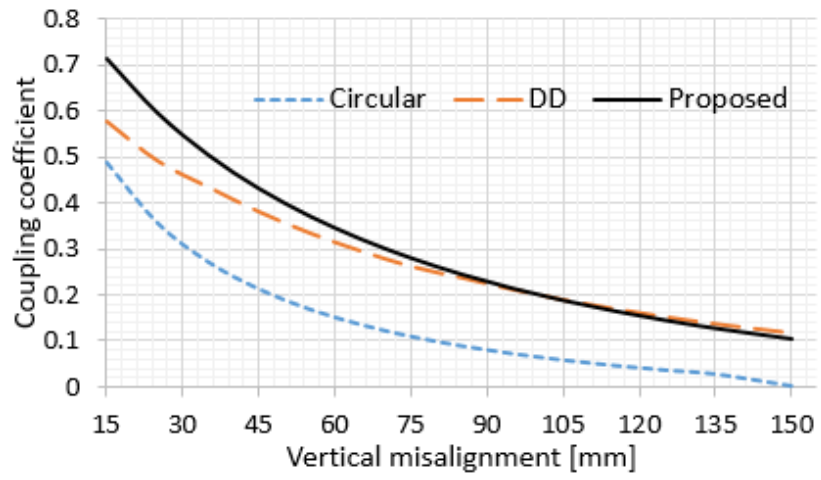
Figure 4.10: Simulation results when both horizontal and vertical misalignments between the power pads are 150 mm: (a) magnetic field intensity  $H$ ; (b) magnetic flux density  $B$ ; (c) magnetic flux lines.

## 4.4 Comparison with Other Power Pads

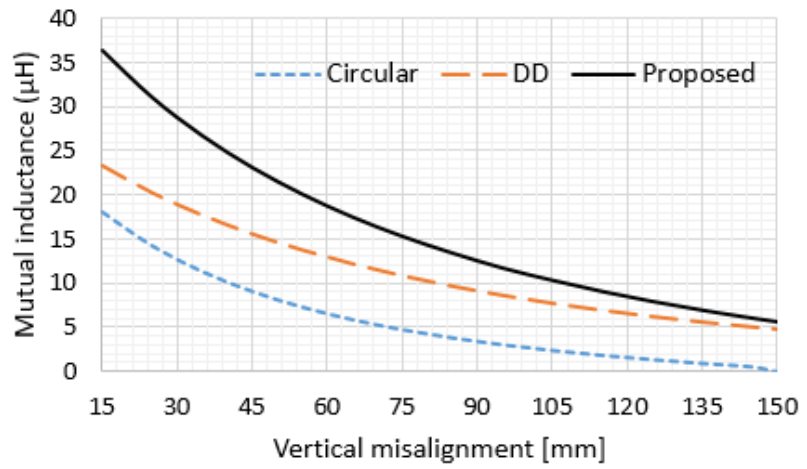
The performance of the proposed power pad is compared to circular and DD power pads as shown in Figure 4.11. The coupling coefficient and mutual inductance of the power pads considering vertical or horizontal misalignment for the three types of power pads are evaluated.

For a perfect horizontal alignment (the horizontal misalignment is zero), Figure 4.11 (a) and (b) show the coupling coefficient and mutual inductance between power pads vary with various vertical misalignments. It is found that the proposed power pad exhibits better magnetic coupling than circular and DD power pads. At 15 mm vertical displacement, the coupling coefficient is 0.712 for the proposed power pad, 0.576 for DD power pad, and 0.487 for circular power pad. A higher coupling coefficient significantly reduces the overall system complexity and configuration cost. Circular power pads require a higher current rating than the proposed power pad to overcome a lower coupling coefficient.

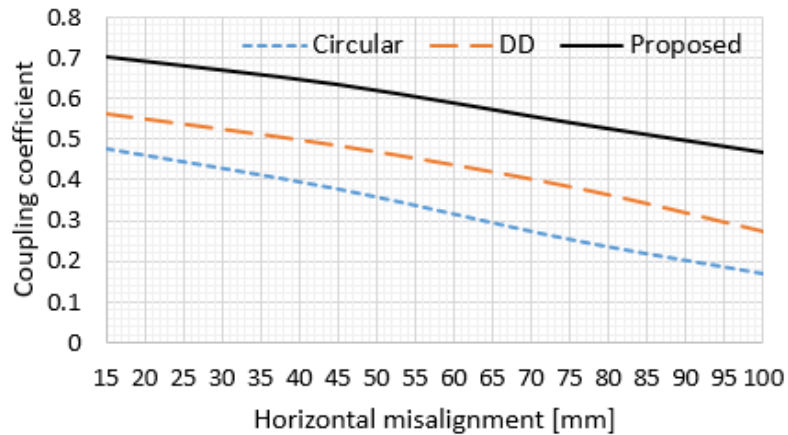
In Figure 4.11(c), a comparison of the coupling coefficient  $k$  vs. horizontal misalignments is made among the proposed power pad, circular and DD power pads. The vertical misalignment between the power pads is kept constant at 15 mm. The proposed power pad exhibits much higher coupling coefficient for different horizontal misalignments than circular and DD power pads in this case.



(a)



(b)



(c)

Figure 4.11: The proposed power pad compared to circular and DD power pads: (a) coupling coefficient vs. vertical misalignment; (b) mutual inductance vs. vertical misalignment; (c) coupling coefficient vs. horizontal misalignment (the vertical misalignment is equal to 15 mm).

## 4.5 Conclusion

A ferrite-less power pad for EV wireless charging system is proposed in this paper. The new design is constructed by combining a circular power pad and a DD power pad. The physical dimensions of the circular and DD power pads used in the design follow the recommended dimensions in SAE recommended practice J2954. The circular coil is placed above the DD coil with a distance of 1 mm in this design with the insulation in between. The circular and DD coils are connected in parallel, sharing the same pair of power leads. The model of the proposed power pad is built using ANSYS Maxwell 3D, the performance of the power pad is simulated using this model. By comparing the coupling coefficient and mutual inductance of the designed power pad

with circular and DD power pads considering vertical and horizontal misalignments, it is found that the proposed power pad exhibits much improved performance.

## References

- [1] G. de Freitas Lima and R. Godoy, "Modeling and Prototype of a Dynamic Wireless Charging System Using LSPS Compensation Topology", *IEEE Trans. Ind. Appl.*, vol. 55, no. 1, pp. 786-793, January/February 2019.
- [2] A. Ahmad, M. S. Alam, and R. Chabaan, "A comprehensive review of wireless charging technologies for electric vehicles," *IEEE Trans. Transportation Electrification*, vol. 4, no. 1, pp. 38-63, March 2018.
- [3] X. Liang and M. S. A. Chowdhury, "Emerging Wireless Charging Systems for Electric Vehicles-Achieving High Power Transfer Efficiency: A Review," *Proceedings of 2018 IEEE Industry Applications Society Annual Meeting (IAS)*, pp. 1-14, 2018.
- [4] SAE Recommended Practice J2954, "Wireless power transfer for light-duty plug-in/electric vehicles and alignment methodology," November 2017.
- [5] J. M. Miller, O. C. Onar, and M. Chinthavali, "Primary-side power flow control of wireless power transfer for electric vehicle charging," *IEEE Journal of Emerging and Selected Topics in Power Electronics*, vol. 3, no. 1, pp. 147-162, March 2015.
- [6] D. Patil, M. K. McDonough, J. M. Miller, B. Fahimi, and P. T. Balsara, "Wireless Power Transfer for Vehicular Applications: Overview and Challenges," *IEEE Trans. Transportation Electrification*, vol. 4, no. 1, pp. 3-37, March 2018.
- [7] S. Choi, J. Huh, W. Lee, and C. Rim, "Asymmetric coil sets for wireless stationary EV chargers with large lateral tolerance by dominant field analysis," *IEEE Trans. Power Electron.*, vol. 29, no. 12, pp. 6406–6420, December 2014.

- [8] M. Yilmaz and P. T. Krein, "Review of battery charger topologies, charging power levels, and infrastructure for plug-in electric and hybrid vehicles," *IEEE Trans. Power Electron.*, vol. 28, no. 5, pp. 2151–2169, May 2013.
- [9] G. A. Covic and J. T. Boys, "Modern trends in inductive power transfer for transportation applications," *IEEE Journal of Emerging and Selected topics in power electronics*, vol. 1, no. 1, pp. 28-41, March 2013.
- [10] M. Budhia, G. A. Covic, and J. T. Boys, "Design and optimization of circular magnetic structures for lumped inductive power transfer systems," *IEEE Trans. Power Electron.*, vol. 26, no. 11, pp. 3096-3108, November 2011.
- [11] R. Bosshard and J. W. Kolar, "Inductive Power Transfer for Electric Vehicle Charging," *IEEE Power Electronics Magazine*, pp. 22-30, september 2016.
- [12] Y. Jang, S. Jeong, and M. Lee, "Initial Energy Logistics Cost Analysis for Stationary, Quasi-Dynamic, and Dynamic Wireless Charging Public Transportation Systems," *Energies*, vol. 9, no. 7, p. 483, June 2016.
- [13] Mathematical expression used to solve magnetostatic problem can be found at : <https://ansyshelp.ansys.com/account/secured?returnurl=/Views/Secured/Electronics/v180/home.html> [December 24, 2018].

## Chapter 5

# Power Transfer Efficiency Evaluation of Different Power Pads for Electric Vehicle's Wireless Charging Systems

Muhammad Sifatul Alam Chowdhury, *Student Member, IEEE*, Xiaodong Liang, *Senior Member, IEEE*

Faculty of Engineering and Applied Science, Memorial University of Newfoundland, St. John's, Newfoundland, Canada.

A version of this chapter has been published in the proceedings of 2019 Canadian Conference of Electrical and Computer Engineering (CCECE). Muhammad Sifatul Alam Chowdhury developed this work under the supervision of Dr. Xiaodong Liang. Sifat's contributions to this paper are listed as follows:

- Performed literature review required for the background information.
- Developed all the codes and performed analysis in ANSYS Maxwell.
- Analyzed the results.
- Wrote the paper.

Dr. Xiaodong Liang provided continuous technical guidance, checked the results, reviewed the manuscript, provided important suggestions to accomplish the work, and modified final version of the manuscript. In this chapter, the manuscript is presented with altered figure numbers, table

numbers and reference formats in order to match the thesis formatting guidelines set out by Memorial University of Newfoundland.

**Abstract-** Introduction of wireless charging systems for electric vehicles (EVs) is a revolutionary step in the field of electrified transportation. Misalignments between transmitting and receiving power pads significantly affect the overall power transfer efficiency of EV wireless charging systems. In this paper, three power pads are evaluated for power transfer efficiency in wireless charging systems with respect to various vertical and horizontal misalignments. They are circular power pads, double D (DD) power pads, and a new power pad designed in this research named as double D circular (DDC). Circular and DD power pads are designed following the Society of Automotive Engineers (SAE) recommended practice J2954 using the software, ANSYS Maxwell 3D. The new DDC power pad is designed by combining a circular power pad and a DD power pad. The power transfer efficiency among the three types of power pads is compared in the paper. The new DDC power pad has 14.48% and 18.03% improved performance compared to the circular power pad at 150mm vertical misalignment and 115mm horizontal misalignment, respectively.

**Keywords-** Electric vehicle, Finite Element Analysis, power transfer efficiency, wireless charging system.

## 5.1 Introduction

Plug-in chargers are conventionally used to charge the electric vehicles (EV). EV's wireless charging systems have received consumers' increasing attraction recently due to its enhanced safety features and user-friendly operational designs [1]. Wireless chargers do not have physical connections between the charging system and the vehicle. Wireless charging can be classified into two classes: a) stationary charging; b) dynamic charging [2]. A vehicle must be parked when using the stationary wireless charging technology; while a dynamic charging system enables the charging when the vehicle is in motion and reduces the initial high cost of the energy storage system [3]. As the vehicle can be recharged while cruising, a high energy storage capacity requirement can be reduced [4]-[6].

Wireless charging systems of EVs are developed mainly based on inductive power transfer (IPT) system where the power is transferred through electromagnetic induction [7]. Power transfer through IPT has exhibited impressive efficiency for a shorter ground clearance of a vehicle. The entire IPT system is a combination of power electronic devices and power pads. The power pads (one installed on the ground side, another one installed on the vehicle side) play a key role to transfer power. Power pads with different shapes are introduced in research to obtain the maximum power transfer efficiency [8]-[10]. Although circular power pad is widely used for EV wireless charging, the double D (DD) topology also exhibits a promising power transfer efficiency. SAE J2954 provides a comprehensive specification for EV wireless charging system focusing on light duty electric vehicle [11], where circular and DD power pads are discussed.

In this paper, three types of power pads are considered in wireless charging systems to evaluate the overall system power transfer efficiency. They are circular power pads, DD power pads, and a new power pad developed by the authors in this study. Circular and DD power pads are designed following the SAE J2954's recommended physical dimensions, and the new power pad is designed by combining a circular power pad and a DD power pad named as double D circular (DDC) power pads. The electromagnetic analysis tool, ANSYS Maxwell 3D, is used in power pad design. To evaluate power transfer efficiency of power pads, a reduced order model [12] is prepared using ANSYS Simplorer.

The paper is arranged as follows: A generic power transfer efficiency analysis procedure for power pads are discussed in Section 5.2. The power transfer efficiency analysis of circular, DD and DDC power pads and their comparison are discussed in Section 5.3. Conclusions are drawn in Section 5.5.

## **5.2 Power Transfer Efficiency Evaluation Methodology**

To evaluate the power transfer efficiency, the design of circular and DD power pads based on SAE J2954 [11] is shown in Figure 1. Inspired by double D quadrature (DDQ) power pads, a new DDC power pad is designed in this research by combining circular and DD power pads as shown in Figure 5.1. To analyze the power transfer efficiency for all three power pads, a generic evaluation method is proposed as shown in Figure 5.2. The procedure of the evaluation is explained in the following two steps:

**Step 1:** Designing power pads using ANSYS Maxwell 3D. Because an IPT system transfers power through electromagnetic induction, it is crucial to analyze the electromagnetic properties of

power pads, such as the coupling coefficient  $k$ , mutual inductance, self-inductance, magnetic flux density  $B$ , magnetic field intensity  $H$ , magnetic flux lines etc. The power transferred to the vehicle side largely depends on the coupling coefficient  $k$ , which varies between 0 and 1.

**Step 2:** Calculating power transfer efficiency of power pads. Parameters obtained by ANSYS Maxwell 3D are imported to ANSYS Simplorer. A reduced order simulation model is prepared using ANSYS Simplorer to simulate and analyze the power transfer efficiency of power pads. The power transfer efficiency is evaluated considering two cases: 1) applying vertical misalignments; 2) applying horizontal misalignments. In this research, a vertical misalignment

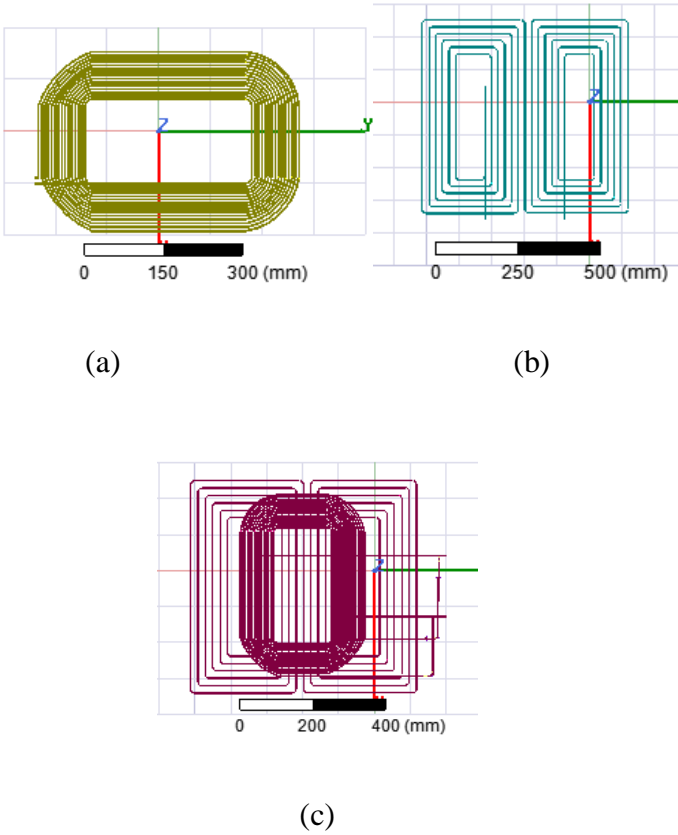


Figure 5.1: Power pad designed using ANSYS Maxwell 3D: (a) Circular power pads; (b) DD power pads; (c) DDC power pads.

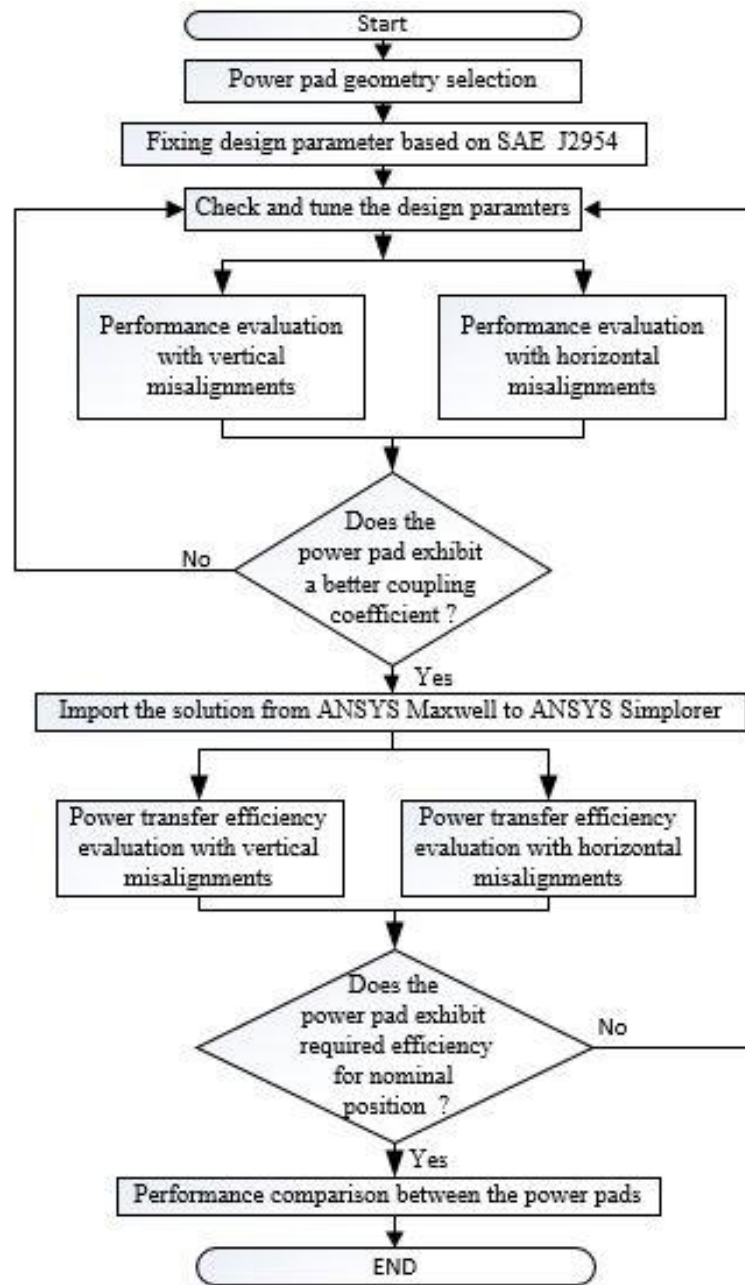


Figure 5.2: The proposed power transfer efficiency evaluation method for power pads.

between 15 mm and 150 mm and a horizontal misalignment between 15 mm and 115 mm are considered between power pads installed on the ground and vehicle sides. If the calculated efficiency reaches the required value, 85% based on SAE J2954's recommendation [11], then the

efficiency calculation for this specific power pad is finished, otherwise, go back to Step 1 to fine tune the design parameters.

## 5.3 Efficiency Analysis of Power Pads

### 5.3.1 Circular Power Pads

Circular power pads are widely used in EV wireless charging systems due to its compact design and installation flexibility. Figure 5.3 represents the magnetic field intensity  $H$  at a vertical misalignment/air-gap of 150 mm between the two power pads installed at the ground and vehicle sides. In this research, the ferrite material and shielding effect is not considered. The addition of ferrite material and shielding can significantly improve the overall power transfer efficiency of power pads.

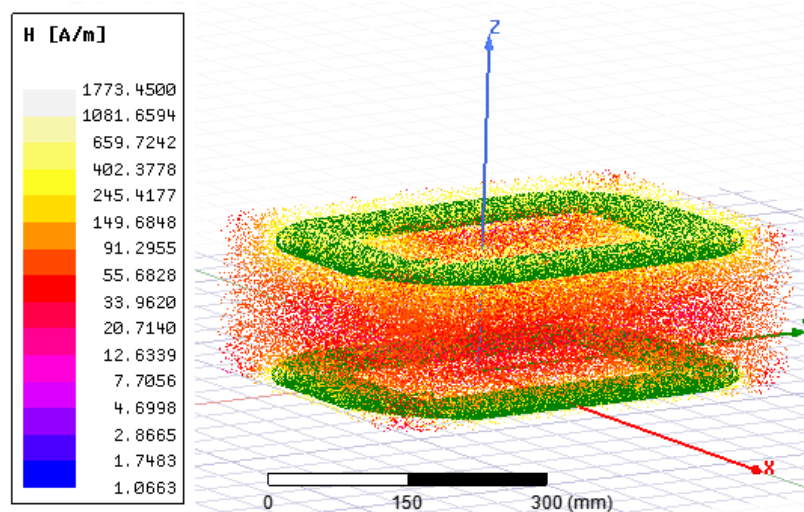


Figure 5.3: The magnetic field intensity for circular power pads at 150 mm vertical misalignment.

Figure 5.4 shows the power transfer efficiency of the circular power pads vs. the inverter operating frequency considering five different vertical misalignments (15 mm, 55 mm, 95 mm, 115 mm and 150 mm) and without horizontal misalignments. The power transfer efficiency is measured by the ratio of the transmitting power and the receiving power through the frequency sweep with the frequency between 10 kHz and 200 kHz. When the vertical misalignment is 15 mm, the peak efficiency of 99.94% is observed at 85 kHz. The peak efficiency is 93.76% for a 55 mm vertical misalignment at 90 kHz. Increasing vertical misalignment will lead to a decreased peak efficiency. It can be observed in Figure 5.4, the peak efficiency point for 95 mm, 115 mm and 150 mm vertical misalignments is all located at 90 kHz.

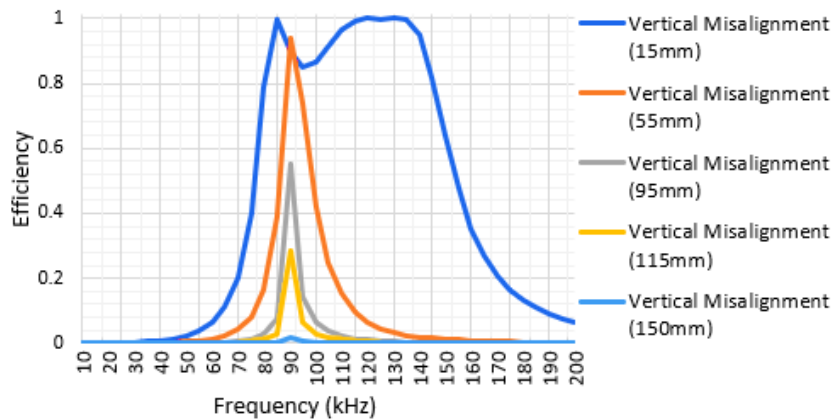


Figure 5.4: The power transfer efficiency vs. the inverter operating frequency for different vertical misalignments (circular power pads).

Figure 5.5 shows the power transfer efficiency of the circular power pads vs. the inverter operating frequency considering four different horizontal misalignments (15 mm, 55 mm, 95 mm and 115 mm) while the vertical misalignment is 100 mm. The peak efficiency of 84.59 % is observed at 90 kHz for the 15 mm horizontal misalignment. With the increase of the horizontal

misalignment, the peak efficiency decreases. When the horizontal misalignment is 95 mm, the peak efficiency is dropped to 69.07 % at 90 kHz. For different horizontal misalignment, the corresponding frequency at the peak efficiency remains at 90 kHz. Therefore, it can be concluded that for circular power pads, the optimal inverter operating frequency is 90 kHz to obtain the highest efficiency considering both vertical and horizontal misalignments.

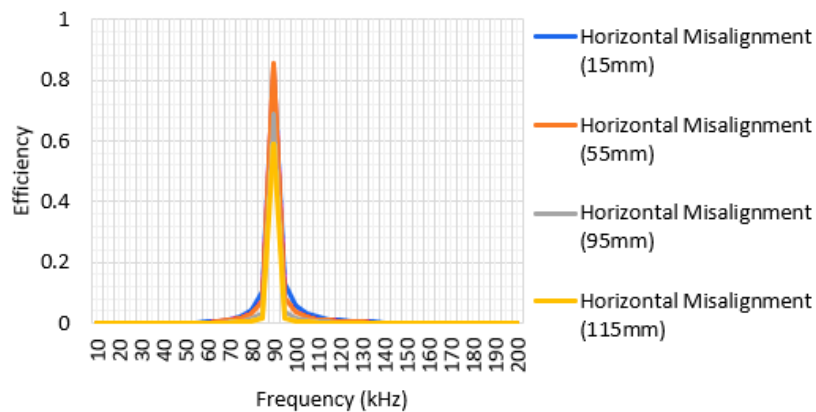


Figure 5.5: The power transfer efficiency vs. the inverter operating frequency for different horizontal misalignments (circular power pads).

### 5.3.2 DD Power Pads

DD power pads exhibit good performance. For the similar size power pads, the flux path height of DD power pads is doubled compared to circular power pads. The improved flux path height can significantly reduce the leakage flux and result in a higher coupling coefficient. The magnetic field intensity of the DD power pads is illustrated in Figure 5.6 for a 150 mm vertical misalignment between the ground and vehicle sides.

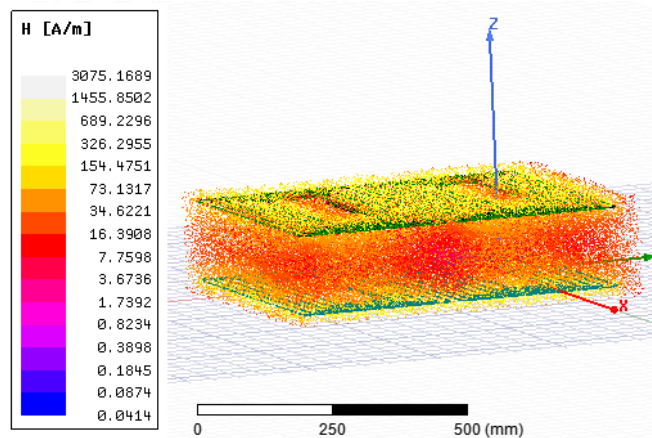


Figure 5.6: The magnetic field intensity for DD power pads at 150 mm vertical misalignment.

Figure 5.7 shows the power transfer efficiency of the DD power pads vs. the inverter operating frequency considering five different vertical misalignments (15 mm, 55 mm, 95 mm, 115 mm and 150 mm) without horizontal misalignments. For a vertical misalignment of 15 mm, the first peak efficiency is 90.14% at 70 kHz, and the second peak efficiency is 99.91% at 135 kHz. For the 55 mm vertical misalignment, the peak efficiency is 88.63% at 75 kHz. It is found that the power transfer efficiency decreases gradually with the increase of vertical misalignments for DD power pads. For vertical misalignments at 95 mm, 115 mm, and 150 mm, the peak efficiency is all located at 75 kHz.

Figure 5.8 shows the power transfer efficiency of the DD power pads vs. the inverter operating frequency considering four different horizontal misalignments (15 mm, 55 mm, 95 mm and 115 mm) while the vertical misalignment is 100 mm. The peak efficiency of 81.72 % is observed at 75 kHz for the 15 mm horizontal misalignment. When the horizontal misalignment is increased to 95 mm, the peak efficiency is dropped to 27.87%. The inverter operating frequency corresponding to the peak efficiency at all four horizontal misalignments is 75 kHz. Therefore, it can be concluded

that for DD power pads, the optimal inverter operating frequency is 75 kHz to obtain the highest efficiency considering both vertical and horizontal misalignments.

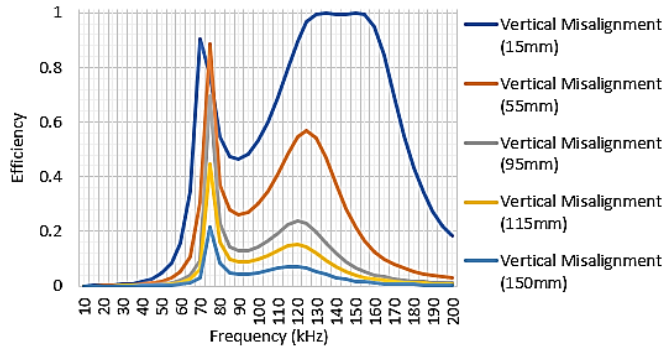


Figure 5.7: The power transfer efficiency vs. the inverter operating frequency for different vertical misalignments (DD power pads).

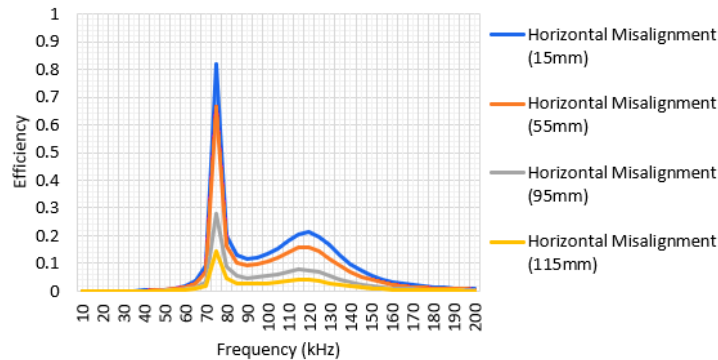


Figure 5.8: The power transfer efficiency vs. the inverter operating frequency for different horizontal misalignments (DD power pads).

### 5.3.3 DDC Power Pads

The DDC power pad is designed in this paper by combining circular and DD power pads inspired by double D quadrature (DDQ) power pads. The circular and DD power pads used in the DDC power pad design follow physical dimensions recommended in SAE J2954. Figure 5.9

represents the magnetic field intensity of the DDC power pads for a 150 mm vertical misalignment between the ground and vehicle sides.

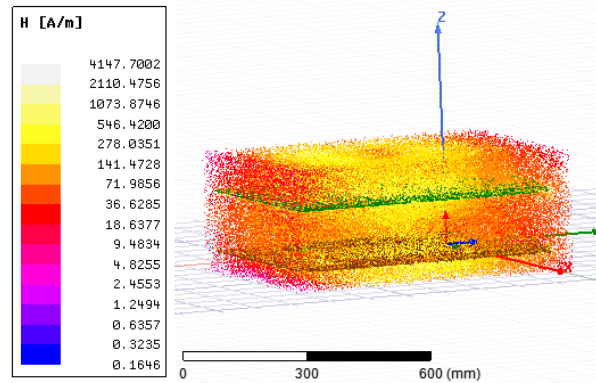


Figure 5.9: The magnetic field intensity for DDC power pads at 150 mm vertical misalignment.

Figure 5.10 shows the power transfer efficiency of the DDC power pads vs. the inverter operating frequency considering five different vertical misalignments (15 mm, 55 mm, 95 mm, 115 mm and 150 mm) without horizontal misalignments. For a vertical misalignment of 15 mm, the first peak efficiency is 94.36% at 65 kHz, the second peak efficiency is 99.98% at 110 kHz, and the third peak efficiency is 99.64% at 165 kHz. The peak efficiency is 83.63% for a 55 mm vertical misalignment at 65 kHz. The peak efficiency gradually drops with the increment of vertical misalignment. The peak efficiencies for 95 mm, 115 mm and 150 mm vertical misalignment are all located at 70 kHz.

Figure 5.11 shows the power transfer efficiency of the DDC power pads vs. the inverter operating frequency considering four different horizontal misalignments (15 mm, 55 mm, 95 mm and 115 mm) while the vertical misalignment is 100 mm. The peak efficiency for the 15 mm

horizontal misalignment is 78.90% at 60 kHz. For the 55mm horizontal misalignment, the peak efficiency is 91.01% at 60 kHz. The peak efficiencies decreases with the increase of horizontal misalignments. The inverter operating frequency corresponding to peak efficiencies at the four horizontal misalignments are all 60 kHz. Therefore, it can be concluded that for DDC power pads, the optimal inverter operating frequency is around 65 kHz to obtain the highest efficiency considering both vertical and horizontal misalignments.

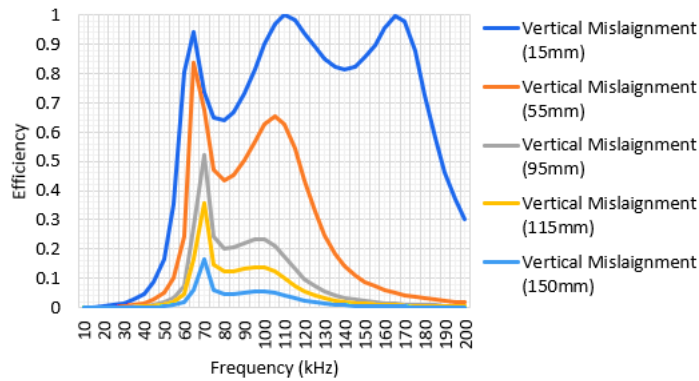


Figure 5.10: The power transfer efficiency vs. the inverter operating frequency for different vertical misalignments (DDC power pads).

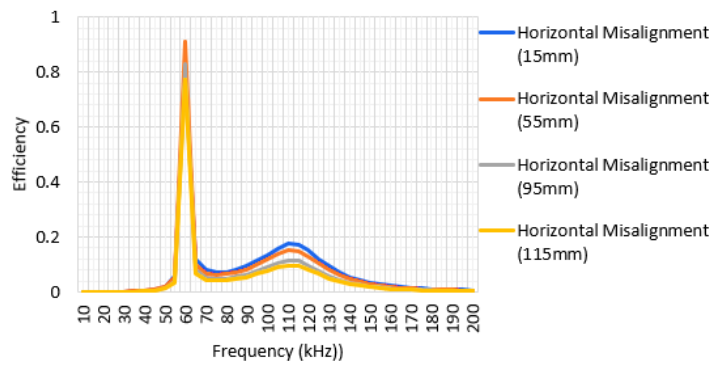
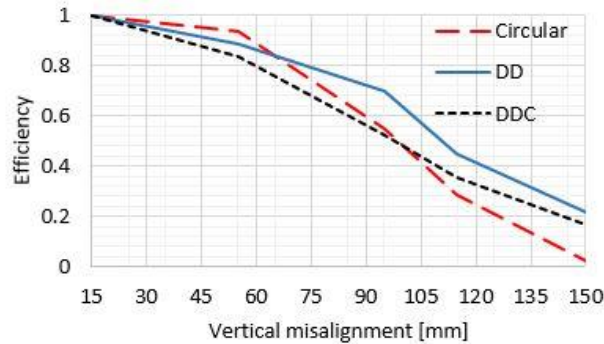


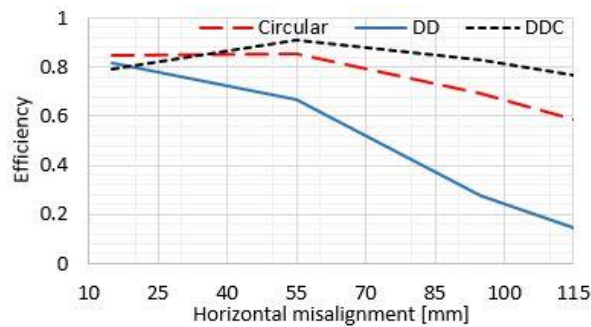
Figure 5.11: The power transfer efficiency vs. the inverter operating frequency for different horizontal misalignments (DDC power pads).

## 5.4 Comparison of the Three Types of Power Pads

The power transfer efficiencies of the three types of power pads, circular, DD and DDC power pads, are compared in Figure 5.12.



(a)



(b)

Figure 5.12: Comparison of power transfer efficiencies among circular, DD and DDC power pads: (a) vertical misalignments; (b) horizontal misalignment

When considering vertical misalignment in Figure 5.12 (a), DDC power pads have comparable efficiency to circular and DD power pads. The DDC power pads' efficiency performance is in between circular and DD power pads, and DD power pads have the highest efficiency at a vertical

misalignment larger than 60 mm. For the 15 mm vertical misalignment, the efficiency is 99.98%, 99.91%, and 99.94% for DDC, DD and circular power pads, respectively. With the increase of vertical misalignment, the efficiency pattern changes. For the 115 mm vertical misalignment, the efficiency is 35.57%, 44.62%, and 28.54%, for DDC, DD and circular power pads, respectively. When considering horizontal misalignment in Figure 5.12 (b), the DDC power pads show superior performance compared to circular and DD power pads. At a smaller horizontal misalignment less than 40 mm, the efficiency for the three types power pads are comparable, but when the horizontal misalignment is larger than 40 mm, DDC power pads show much higher efficiency values. For the 115 mm horizontal misalignment, the efficiency is 77%, 14.50%, and 58.96% for DDC, DD and circular power pads, respectively. DDC power pads should perform well especially for dynamic charging systems.

## **5.5 Conclusion**

In this paper, the power transfer efficiency evaluation of circular, DD and DDC power pads is carried out. A generic procedure to evaluate efficiency is proposed. The efficiency for each type of power pads is determined considering different vertical and horizontal misalignment, the efficiency vs. the inverter operating frequency is displayed. The optimal inverter operating frequency for the designed power pads can thus be determined to obtain the highest efficiency, which is 90 kHz for circular power pads, 75 kHz for DD power pads, and 65 kHz for DDC power pads. The new DDC power pads proposed in this study show the best efficiency performance considering horizontal misalignment, which can serve as suitable power pads for EV's dynamic charging systems.

## References

- [1] V.-B. Vu, D.-H. Tran, and W. Choi, "Implementation of the constant current and constant voltage charge of inductive power transfer systems with the double-sided lcc compensation topology for electric vehicle battery charge applications," *IEEE Trans. Power Electron.*, vol. 33, no. 9, pp. 7398-7410, September 2018.
- [2] S. Jeong, Y. J. Jang, and D. Kum, "Economic analysis of the dynamic charging electric vehicle," *IEEE Trans. Power Electron.*, vol. 30, no. 11, pp. 6368-6377, November 2015.
- [3] S. Lukic and Z. Pantic, "Cutting the cord: Static and dynamic inductive wireless charging of electric vehicles," *IEEE Electrification Magazine*, vol. 1, no. 1, pp. 57-64, September 2013.
- [4] D. Vilathgamuwa and J. Sampath, "Wireless power transfer (WPT) for electric vehicles (EVS)—Present and future trends," in *Plug in electric vehicles in smart grids*, ed: Springer, 2015, pp. 33-60.
- [5] S. Chopra and P. Bauer, "Driving range extension of EV with on-road contactless power transfer—a case study," *IEEE Trans. Ind. Electron.*, vol. 60, no. 1, pp. 329-338, January 2013.
- [6] W. Zhong and S. Hui, "Maximum energy efficiency tracking for wireless power transfer systems," *IEEE Trans. Power Electron.*, vol. 30, no. 7, pp. 4025-4034, July 2015.
- [7] K. A. Kalwar, M. Aamir, and S. Mekhilef, "Inductively coupled power transfer (ICPT) for electric vehicle charging—A review," *Renewable and Sustainable Energy Reviews*, vol. 47, pp. 462-475, July 2015.

- [8] A. Tejada, C. Carretero, J. T. Boys, and G. A. Covic, "Ferrite-less circular pad with controlled flux cancelation for EV wireless charging," *IEEE Trans. Power Electron.*, vol. 32, no. 11, pp. 8349-8359, November 2017.
- [9] M. G. S. Pearce, G. A. Covic, and J. T. Boys, "Robust Ferrite-less Double D Topology for Roadway IPT Applications," *IEEE Trans. Power Electron.*, 2018 (Early access).
- [10] U. Pratik, B. J. Varghese, A. Azad, and Z. Pantic, "Optimum Design of Decoupled Concentric Coils for Operation in Double-Receiver Wireless Power Transfer Systems," *IEEE Journal of Emerging and Selected Topics in Power Electronics*, 2018(Early access).
- [11] SAE Recommended Practice J2954, "Wireless power transfer for light-duty plug-in/electric vehicles and alignment methodology," November 2017.
- [12] Z. Tang, M. Christini, and T. Koga, "Wireless Power Transfer using Maxwell and Simplorer," in *Automotive Simulation-World Congress*, 2012.

## **Chapter 6**

### **Conclusion**

This chapter consists of a summary of the main contributions of this thesis, followed by an outlook on future work.

#### **6.1 Summary**

The main objective of this thesis is to design and develop an advanced power pad with improved power transfer efficiency for EV's wireless charging systems. A new DDC power pad is proposed in this thesis, and its performance is compared with two existing power pads (circular and DD power pads). It is found that the proposed DDC power pads are effective for EV's wireless charging systems.

In Chapter 1, the importance of the electrified transportation system based on the wireless charging system is explained. Advantages and challenges of EV's wireless charging systems are discussed. Limitations of EV's wireless charging with the related system deployment challenges are discussed and the ways to overcome those challenges are briefly outlined. Different system configurations and power pads considered for EV wireless charging systems are introduced.

In Chapter 2, an advanced charging mechanism for EV's wireless charging systems is introduced which is considered to be an attractive method to reduce the range anxiety of EV's. Recent literature is reviewed to gain a comprehensive knowledge about various power pads for EVs wireless charging systems. The review of existing power pad structures is essential before

making further efforts for designing a new power pad. Moreover, some state-of-the-art techniques for wireless charging systems are reviewed in a review paper.

In Chapter 3, a comparative analysis is carried out between circular and DD power pads for EV's wireless charging systems. The physical models for both types of power pads are built using ANSYS Maxwell 3D based on the recommended physical dimensions in SAE J2954. For each type of power pad, the vertical misalignment between transmitting and receiving sides varies between 15 mm to 150 mm. Four horizontal misalignments at 15 mm, 45 mm, 75 mm and 100 mm are also applied. Simulation results indicate that DD power pads exhibit good potential for EV's wireless charging system design. The work reported in this chapter can facilitate better understanding of power pad structures and their performance, and thus assist a better selection and design of power pads.

In Chapter 4, a ferrite-less power pad for EV's wireless charging systems named DDC power pad is proposed. The new design is constructed by combining a circular power pad and a DD power pad. The physical dimensions of the circular and DD power pads used in the design follow the recommended dimensions in SAE recommended practice J2954. The circular coil is placed above the DD coil with a distance of 1 mm in this design with the insulation in between. The circular and DD coils are connected in parallel, sharing the same pair of power leads. The model of the proposed power pad is built using ANSYS Maxwell 3D and the performance of the power pads is simulated using this model. The proposed DDC power pad can transfer power to the vehicle with higher efficiency compared to existing power pads. The coupling coefficient and mutual inductance of the proposed DDC power pad are compared to that of existing circular and DD

power pads by considering vertical and horizontal misalignments. It is found that the proposed DDC power pad exhibits much improved performance.

In Chapter 5, the power transfer efficiency evaluation of circular, DD and DDC power pads is carried out. A generic procedure to evaluate efficiency is proposed in this chapter. Power transfer efficiency is evaluated by applying vertical and horizontal misalignments. The efficiency for each type of power pad is determined considering different vertical and horizontal misalignments; the efficiency vs. the inverter operating frequency is displayed in this paper. The optimal inverter operating frequency for the designed power pads can be determined to obtain the highest efficiency, which is 90 kHz for circular power pads, 75 kHz for DD power pads, and 65 kHz for DDC power pads. The new DDC power pads proposed in this thesis show the best efficiency performance considering horizontal misalignment, which can serve as suitable power pads for EV's dynamic charging systems.

## **6.2 Future Works**

- Performance analysis of power pads carried out in this thesis are only a part of entire EVs wireless charging systems. Reduced order model of wireless charging systems is used to determine the power transfer efficiency. A complete circuit consisting of individual power electronic devices from the grid to the vehicle can also be studied in the future.
- Performance of the proposed DDC power pad in this thesis is compared with that of circular and DD power pads. In the future, a performance comparison can be carried out

between the proposed DDC power pad and the existing DDQ. Application of both the power pads for stationary and dynamic wireless charging can be evaluated.

- Experimental validation of the proposed DDC power pad can be conducted in the future to validate its performance.

## **List of Publications**

### **Refereed Journal Papers**

- [1] Muhammad Sifatul Alam Chowdhury\*, and Xiaodong Liang, "Design and Performance Evaluation for A New Power Pad in Electric Vehicles Wireless Charging Systems", submitted to IEEE Canadian Journal of Electrical and Computer Engineering (under review).
- [2] Md Nasmus Sakib Khan Shabbir\*, Muhammad Sifatul Alam Chowdhury\*, and Xiaodong Liang, "A Guideline of Feasibility Analysis and Design for Concentrated Solar Power Plants", IEEE Canadian Journal of Electrical and Computer Engineering, vol. 41, no. 4, pp. 203 - 217, Fall 2018.
- [3] Md Nasmus Sakib Khan Shabbir\*, Mohammad Zawad Ali\*, Xiaodong Liang, and Muhammad Sifatul Alam Chowdhury\*, "A Probabilistic Approach Considering Contingency Parameters for Peak Load Demand Forecasting", IEEE Canadian Journal of Electrical and Computer Engineering, vol. 41, no. 4, pp. 224 - 233, Fall 2018.

### **Refereed Conference Papers**

- [4] Muhammad Sifatul Alam Chowdhury\*, and Xiaodong Liang, "Comparative Characteristic Analysis of Circular and Double D Power Pads for Electric Vehicle Wireless Charging Systems," Proceedings of IEEE Canadian Conference of Electrical and Computer Engineering (CCECE) 2019, Edmonton, AB, Canada, May 5-8, 2019.
- [5] Muhammad Sifatul Alam Chowdhury\*, and Xiaodong Liang, "Design of a Ferrite-Less Power Pad for Wireless Charging Systems of Electric Vehicles," Proceedings of IEEE

Canadian Conference of Electrical and Computer Engineering (CCECE) 2019, Edmonton, AB, Canada, May 5-8, 2019.

- [6] Muhammad Sifatul Alam Chowdhury\*, and Xiaodong Liang, "Power Transfer Efficiency Evaluation of Different Power Pads for Electric Vehicle's Wireless Charging Systems", Proceedings of IEEE Canadian Conference of Electrical and Computer Engineering (CCECE) 2019, Edmonton, AB, Canada, May 5-8, 2019.
- [7] Xiaodong Liang, and Muhammad Sifatul Alam Chowdhury\*, "Emerging Wireless Charging Systems for Electric Vehicles – Achieving High Power Transfer Efficiency: A Review", Proceedings of 2018 IEEE Industry Applications Society (IAS) Annual Meeting, pp. 1-14, Portland, OR, USA, September 23 - 27, 2018.
- [8] Mohammad Zawad Ali\*, Md Nasmus Sakib Khan Shabbir\*, Muhammad Sifatul Alam Chowdhury\*, Arko Ghosh, and Xiaodong Liang, "Regression Models of Critical Parameters Affecting Peak Load Demand Forecasting", Proceedings of the 31st Annual IEEE Canadian Conference on Electrical and Computer Engineering (CCECE 2018), pp. 1-4, Québec City, Québec, Canada, May 13-16, 2018.
- [9] Md Nasmus Sakib Khan Shabbir\*, Mohammad Zawad Ali\*, Muhammad Sifatul Alam Chowdhury\*, and Xiaodong Liang, "A Probabilistic Approach for Peak Load Demand Forecasting", Proceedings of the 31st Annual IEEE Canadian Conference on Electrical and Computer Engineering (CCECE 2018), pp. 1-4, Québec City, Québec, Canada, May 13-16, 2018.
- [10] Muhammad Sifatul Alam Chowdhury\*, Md. Arman Uddin, Khandakar Abdulla Al Mamun, Xiaodong Liang, and Amir Ahadi\*, "Concentrated Solar Power Generation in A

Remote Island”, Proceedings of the 31st Annual IEEE Canadian Conference on Electrical and Computer Engineering (CCECE 2018), pp. 1-4, Québec City, Québec, Canada, May 13-16, 2018.

### **Non-Refereed Local IEEE Conference Papers**

[11] Muhammad Sifatul Alam Chowdhury\*, and Xiaodong Liang, "A Comparative Approach to Select Power Pad for Electric Vehicle Wireless Charging System", 2018 Annual IEEE Newfoundland Electrical and Computer Engineering Conference (NECEC), pp. 1-5, St. John's, Canada, November 2018.

[12] Muhammad Sifatul Alam Chowdhury\*, and Xiaodong Liang, "Prospect of Concentrated Solar Power to Mitigate Power Crisis in Islands of Bangladesh", 2017 Annual IEEE Newfoundland Electrical and Computer Engineering Conference (NECEC), pp. 1-5, St. John's, Canada, November 2017.